VOLTAGE-DEPENDENT REGULATION OF INTRACELLULAR SIGNALING BY ETHER À GO-GO K^+ CHANNELS

by

Andrew Peter Hegle

A dissertation submitted in partial fulfillment
of the requirements for the degree of
Doctor of Philosophy
(Molecular, Cellular and Developmental Biology)
in The University of Michigan
2007

Doctoral Committee:

Assistant Professor Gisela Wilson, Co-Chair
Professor Richard I. Hume, Co-Chair
Associate Professor Cunming Duan
Associate Professor Lori L. Isom
Assistant Professor Mohammed Akaaboune

To my extraordinary sister Alicia,
in memory of our father
Terry Dean Hegle

ACKNOWLEDGEMENTS

More than anyone, I would like to thank Angelique Pilon, my dearest love and best friend. I can't imagine what these years would have been like without her in my life.

I sincerely thank Gisela Wilson for her encouragement, patience and inspiration as a mentor. Her scientific insights and boundless optimism, as well as our conversations of politics, music and life will be greatly missed. I also thank the members of my thesis committee for their tremendous support and guidance, particularly Rich Hume, who has contributed immeasurably to my experience here. In addition, I owe a great deal of thanks to Laura Olsen, Jesse Hay and Rolf Bodmer for believing in me during my undergraduate years, and for motivating me to pursue a career in scientific research. I also thank Mary Carr, Diane Durfy and the rest of the MCDB administrative staff, whose incredible support and wonderful sense of humor have been essential to my graduate career.

I wish to extend special thanks to my lab partner and colleague Dan Marble, who has been there with me every step of the way, and to all the others who have worked in the Wilson lab, including Eric Snyder II, Sarah Telfer, Katherine MacNair and Divya Sharma. I also thank Dylan Clyne, Louis Saint-Amant, David Parker, Tanya Johnson and Aaron Wyman for their sage advice and keen insights into graduate life over the years, and the rest of my fantastic third floor colleagues, in no particular order; Peter Schleuter,

Sean Low, Mark Miller, Emile Bruneau, Eric Horstick, Shlomo Dellal, Rachel Tittle and Dani Brennan, for everything. Special thanks is also due to Jonathan Pan, who persuaded me long ago to sit in front, pay attention and believe in myself.

Outside of MCDB, the rest of my family and friends have contributed greatly to my graduate experience. I especially thank my mother Janis and my sister Alicia for their unwavering love and support of all my endeavors. I am also indebted to the trust and guidance of my late father Terry, whose remarkable spirit I carry with me always, and to my late grandfather Alton Conklin, who taught me more during childhood than I ever realized. I also thank the Bosleys, Taglauers, Molyneauxs, and the rest of my incredible family for their patience, love and respect.

Finally, I want to thank the friends that have been with me, through thick and thin, from the Batcave and beyond, who have made these years unforgettable: Seth Gordon, Chris Goretski, Eric Dyer, Alison Melnick, Sarah Shotwell, Dan Kruse, Jon Kraus, Jeremy Mogtader, Mike DeYounker, Jack Van Dyke, Bill Bon, Andy Harrington, Steve Gertz, Mike Kuhn, Jon Goldstein, James Olzmann, and so many others without which my life would not be the same. A special thanks is also due to my oldest friends, Ryan Norton, Eric Ososki and Mike Paulus, whose influences remain an essential element of my character.

PREFACE

Some data presented in this thesis have been previously published or are in preparation for publication at the time of this writing. Chapter II was published in 2006 in the Proceedings of the National Academy of Sciences of the United States of America (PNAS 103.8:2886-2891). Chapter III is in preparation for submission to Nature. These chapters were written collaboratively with my thesis advisor, Gisela F. Wilson. Although I performed most of the data analysis and writing, Gisela contributed to the physiological characterization of EAG mutant channels presented in these chapters, and was also very helpful in the editing of the entire thesis. Dan Marble generated the *Drosophila* transgenics and several of the EAG point mutants, with assistance from an exceptional undergraduate student, Katherine MacNair. Dan also characterized the larval mutant phenotypes and contributed to the editing of Chapters II and III. I am immensely appreciative of Dan and Gisela's considerable contributions to this work, which would not have been possible without their efforts.

The Appendix was published in 2005 in the Journal of Neuroscience (J. Neurosci. 25.20:4898-4907). I performed the immunocytochemical experiments and analysis presented in Figures A.3 and A.6, and also assisted with the editing of the paper, which was primarily written by Dan and Gisela. Eric Snyder, Spiros Dimitratos and Peter J. Bryant also contributed to the experimental results, and I thank them for their work.

TABLE OF CONTENTS

APPENDIX

LIST OF FIGURES

ABSTRACT

Voltage-gated ion channels play a key role in neuronal function by regulating ion flux. My research has shown that the *Drosophila* Ether à-go-go (EAG) potassium channel has a distinct conductance-independent role as an upstream activator of intracellular signaling pathways. Heterologous expression of EAG in NIH 3T3 fibroblasts results in increased proliferation and p38 mitogen-activated protein kinase activity, an effect that occurs even when the channel is rendered non-conducting by mutation of the selectivity filter. Importantly, analysis of mutations that shift the voltage-dependence of channel gating reveals that EAG signaling activity is regulated by the voltage sensor. Targeted mutation of key residues in the intracellular EAG carboxyl terminus shows that signaling requires an intact calcium/calmodulin-dependent protein kinase II (CaMKII) binding domain, and biochemical assays confirm that the activity of membrane-associated CaMKII is modulated by voltage-dependent conformations of EAG. Conductance-independent, CaMKII-mediated EAG signaling activity is also observed with the mammalian isoform of EAG. Finally, in recordings at the *Drosophila* larval neuromuscular junction, EAG channels with mutations in the CaMKII binding domain largely failed to rescue the high levels of spontaneous activity characteristic of *eag* mutants, whereas non-conducting EAG channels rescued spontaneous activity with an efficiency nearly overlapping that observed for the wild type channel. These results suggest that voltage-dependent,

conductance-independent EAG signaling activity plays a role in synaptic homeostasis *in vivo* and implicate EAG signaling as a novel mechanism for linking neuronal activity to the state of intracellular messenger pathways. EAG signaling activity may contribute to the learning defects observed in *Drosophila eag* mutants, as well as to the oncogenic effects observed following abnormal expression of human EAG.

CHAPTER I

INTRODUCTION

A. OVERVIEW

The Ether à-go-go (EAG) potassium (K^+) channel is a truly distinctive biological molecule. As a voltage-gated ion channel, EAG selectively facilitates the flux of K^+ ions through its central pore and across the plasma membrane of cells. This hyperpolarizing function contributes to setting the resting membrane potential, and in excitable cells, repolarizes the membrane during action potentials to limit repetitive firing. EAG is different from other K^+ channels in that it possesses unusually long intracellular domains that associate with proteins involved in key signaling pathways, including the calcium-(Ca^{2+})-binding protein calmodulin (CaM), Ca^{2+}/CaM-dependent protein kinase II (CaMKII), and protein kinase A (PKA). The intracellular termini also include sequences required for association with scaffolding and adapter proteins, including membrane-associated guanylate kinases (MAGUKs) and other Src-homology 3 (SH3) proteins, allowing EAG to potentially assemble large protein complexes at the plasma membrane. The ability of enzymes and second messenger systems to assemble with a voltage-gated ion channel opens up the possibility of translating changes in membrane potential into biological signals.

While the modulation of ion channel activity via intracellular signals (e.g., phosphorylation) is well-characterized, this thesis proposes that EAG directly activates signaling pathways in a manner *independent* of its role as an ion channel. My research suggests that EAG stimulates signaling even when the channel pore is mutated to prevent ion flux. Most importantly, the voltage sensor of EAG - which does not require channel conductance to respond to changes in membrane potential - appears to be a "switch" for signal activation. I present evidence for voltage-dependent, conductance-independent EAG signaling in Chapter II of this thesis, and evidence that EAG signaling is mediated via voltage-dependent regulation of CaMKII in Chapter III.

The first suggestion that *Drosophila* EAG (dEAG) may be acting in a capacity beyond that of a K^+ channel came from early experiments done during my rotation in the Wilson lab. Following heterologous expression of dEAG in mammalian NIH-3T3 fibroblasts, there was a dramatic increase in cell density compared with vector-transfected controls. Subsequent experiments using the proliferation marker 5-bromo-2-deoxyuridine (BrdU), found that EAG-transfected coverslips exhibit higher BrdU incorporation than controls, suggesting that EAG stimulates proliferation. Because human EAG has been implicated in cell cycle progression and oncogenesis (Pardo et al., 1999), this was not an entirely unexpected result. However, proliferation also was increased in coverslips transfected with non-conducting EAG mutants - an exciting and crucial finding suggesting that the increases in proliferation were independent of any effect of EAG conductance on membrane potential, which could itself influence Ca^{2+}-dependent signaling via the activation of voltage-gated Ca^{2+} channels.

These initial observations set the stage for further investigations into the mechanism of EAG-stimulated proliferation, which have now implicated the downstream activation of key regulatory proteins including CaMKII and p38 mitogen-activated protein kinase (MAPK). Although this signaling activity results in the proliferation of NIH-3T3 cells *in vitro*, it is important to emphasize that cell growth is not necessarily the physiological role of EAG-mediated signaling *in vivo*. Nevertheless, much of the evidence presented here for EAG signaling relies on assays of proliferation in mammalian cell culture during transient transfection of *Drosophila eag* constructs. While this heterologous system may not at first seem physiologically relevant for the fly channel, it has provided a reliable system in which to test specific physical and mechanistic aspects of EAG signaling. Importantly, most of these results and conclusions have been duplicated in parallel studies using the mammalian ortholog of EAG, which suggests that this signaling function has been conserved throughout channel evolution. Furthermore, *in vivo* experiments done by other members of the Wilson lab provide evidence that EAG-mediated signaling underlies spontaneous activity at the larval neuromuscular junction, a well-characterized phenotype of *eag* mutants.

The aim of this thesis is to investigate the mechanisms by which EAG K^+ channels activate intracellular signaling pathways. Although the multifunctionality of EAG is unusual for an ion channel, the idea of channels with secondary roles is not without precedent. In fact, there are now reports of channels and their associated proteins involved in transcription regulation, protein phosphorylation, vesicle fusion, and numerous other intracellular mechanisms not commonly associated with ion channels. In this introduction chapter, I present a brief background of voltage-gated K^+ channels,

followed by a review of known multifunctional ion channel activity. This begins with a general discussion of ion channels correlated with proliferation, oncogenesis and apoptosis. I then focus on individual examples of channels with physiological functions that are independent of conductance, emphasizing channels that influence intracellular signaling pathways. Following is a discussion of channel auxiliary subunits and the signaling activity of multiprotein channel complexes. Finally, I summarize the structural and physiological attributes of the EAG channel and its association with key regulatory proteins, in order to make the case for EAG as an upstream regulator of intracellular signaling.

B. BACKGROUND & SIGNIFICANCE OF VOLTAGE-GATED K^+ CHANNELS

Voltage-gated K^+ channels comprise a large and diverse class of membrane proteins that are found in almost all living organisms, including animals, plants, fungi and bacteria. These proteins are largely responsible for regulating K^+ permeability in response to a variety of signals. In neurons, K^+ channels facilitate action potential repolarization, limit the rate of repetitive action potential firing, and maintain a negative (hyperpolarized) membrane potential when cells are at rest. This resting potential effectively acts as a "battery" to provide the driving force for ionic movement that underlies the action potential. However, the functions of K^+ channels are not limited to excitable cells in the nervous system. In addition to their role in membrane excitability and neurotransmitter release, K^+ channels mediate heart rate, smooth muscle contraction, insulin secretion, epithelial transport and other diverse cellular processes (Shieh et al., 2000). Correspondingly, the loss or disruption of K^+ channel activity has been implicated

in a range of diseases, including epilepsy, deafness, schizophrenia, Alzheimer's disease, episodic ataxia, diabetes and cardiac arrhythmias such as long Q-T syndrome (Shieh et al., 2000).

The idea of a selective K^+ conductance in excitable cells was first proposed in 1902 by Julius Bernstein (Bernstein, 1902), but the process by which membrane potential could be regulated by ions was not established until pioneering experiments on the squid giant axon were done by Alan Hodgkin, Andrew Huxley, Bernard Katz, Kenneth Cole, Howard Curtis and others during the mid-twentieth century (Cole and Curtis, 1939; Curtis and Cole, 1942; Fatt and Katz, 1953a,b; Hodgkin and Huxley, 1945; Hodgkin and Huxley, 1952a-d; Hodgkin et al., 1952; Hodgkin and Katz, 1949). Without knowledge of ion channel proteins, these experimenters formulated an empirical model of the kinetics of membrane excitability that remains largely sound to this day. As the modern era of cloning and molecular biology dawned, researchers began to realize that the proteins regulating ion permeation were far more diverse and functionally intricate than could have been envisioned by early biophysicists. This especially holds true for K^+ channels, which in most genomes far outnumber their sodium (Na^+) and Ca^{2+} counterparts. In the human genome, for example, there are 40 genes encoding voltage-gated K^+ channel α-subunits, whereas Na^+ and Ca^{2+} channel α-subunits are represented by 10 genes each (Yu and Catterall, 2004). This enormous diversity allows cells to express virtually unlimited combinations of different K^+ channel subtypes, fine-tuning the electrical properties of their membranes to an exceptional degree.

K^+ channels are historically classified by the type of current they produce. However, it is useful to consider topology when discussing the various classes. In general, K^+

channels are grouped by amino acid sequence relationships, separated into six-transmembrane (6TM), four-transmembrane (4TM) and two-transmembrane (2TM) families. These can then be further classified by their mechanism of activation or current properties. The largest group, 6TM channels, includes voltage-gated delayed-rectifier (Kv) channels, Ca^{2+}-activated K^+ channels, hyperpolarization- and cyclic-nucleotide gated channels, and slow delayed rectifiers. With a few exceptions, these channels form tetramers and generally produce outward K^+ current upon activation. Members of the 2TM subfamily are tetrameric inward rectifying K^+ channels, and include ATP-sensitive and G-protein coupled channels. Finally, 4TM channels contain two pore domains per subunit and are thought to form dimers. These channels are responsible for the so-called K^+ leak current (Goldstein et al., 2001). Due to the variable nomenclature that has resulted in many channels having more than one name, I refer to most human and mammalian channels throughout this thesis with names derived from the IUPHAR Compendium of Voltage-Gated Ion Channels (Gutman et al., 2003). For *Drosophila* ion channels, including EAG and Shaker (the ortholog of mammalian Kv1 channels), I use the original phenotype-derived names.

All Kv channel subunits have 6TM topology, with a "P-loop" region between the fifth and sixth transmembrane domains that forms the K^+ selectivity filter when four subunits assemble as a functional channel (Doyle et al., 1998; Heginbotham et al., 1994). In addition, positively-charged residues in the fourth transmembrane segment constitute the voltage sensor, a domain that couples changes in membrane potential to conformational shifts in the channel pore, thereby controlling ion permeation (Liman et al., 1991; Papazian et al., 1991). However, the biophysical mechanism by which the voltage sensor

moves charge within the membrane has been a subject of vigorous debate. Based on numerous accessibility studies, sequence analyses and mutagenesis screens, most models proposed for voltage sensor movement prior to 2003 envisioned an axial translation or rotation of the positively charged helix within a gating canal formed by the other transmembrane domains (Gandhi and Isacoff, 2002). The groundbreaking x-ray crystallization of the KvAP channel by Roderick MacKinnon and colleagues suggested that the voltage sensors are "paddles" extending outward from the channel core into the lipid bilayer (Jiang et al., 2003a,b). More recent investigations using electron paramagnetic resonance to measure the position of individual KvAP voltage sensor residues in a native environment have called this model into question (Cuello et al., 2004). In contrast to the crystal structure, these studies found that the positively-charged residues of the fourth transmembrane domain do not extend into the membrane, but rather lie near the protein/lipid interface, shielded by the other domains. Despite being partially protected from the membrane, these residues do not, however, appear to be enclosed within a gating canal, as proposed in classical models. Together with accessibility studies of the Shaker voltage sensor (Gandhi et al., 2003), these results suggest that the actual mechanism may lie somewhere between the axial translation and paddle models. Although the debate is far from being resolved, the voltage sensor of ion channels is arguably one of the most important protein structures in all of biology.

Voltage-gated channels serve as the interface between biochemical and electrical signals, routinely interacting with second messenger systems, regulatory enzymes and adapter proteins to modulate ion flux in direct response to intracellular signals (Levitan, 2006). These interactions provide a sensitive mechanism by which a host of biochemical

events can adjust the electrical properties of a cell, shaping the firing patterns that transmit sensory and motor information in the nervous system. Although channel modulation by signaling molecules has traditionally been viewed as a one-way process, a growing body of evidence suggests that some channels may, in turn, be able to influence cellular behavior and interact with signaling pathways in ways that are independent of the downstream effects of ion flux. Channel proteins with secondary roles have now been identified within all the major classes of cation channels, including K^+, Na^+, Ca^{2+} and transient receptor potential (TRP) channels (Dolmetsch et al., 2001; Gomez-Ospina et al., 2006; Kaczmarek, 2006; MacLean et al., 2003; Malhotra et al., 2000; Runnels et al., 2001). Several studies have shown that such channels affect cellular behavior, including proliferation and differentiation, oncogenesis, apoptosis, and homeostasis. Many channels also associate with auxiliary proteins, and it has become increasingly apparent that some channel-protein complexes permit direct interaction with biochemical pathways via second messengers, cytoskeletal components and regulatory enzymes. A few even have intrinsic enzymatic activity or undergo proteolytic cleavage to become transcription factors. Remarkably, many of these effects are observed even when the channel pores have been altered to prevent conduction or blocked with specific inhibitors. Here I discuss the known secondary functions of ion channels, before focusing on the signaling activity of the EAG K^+ channel and its associated proteins.

C. ION CHANNELS THAT INFLUENCE THE CELL CYCLE

Although several classes of ion channel have been implicated in cell proliferation (Allen et al., 1997; Cahalan et al., 2001; Kaczmarek, 2006), K^+ channels are by far the

most well-characterized as having key regulatory roles in the cell cycle progression of both normally proliferating (e.g., lymphocytes, Schwann cells and glia) and abnormally proliferating (cancerous) cell types (Chandy et al., 2004; Pardo, 2004; Vautier et al., 2004; Wilson and Chiu, 1993). Inhibition of Kv channels, through the use of peptide and small molecule blockers, potently and effectively decreases proliferation in immune cells as well as that of various types of tumors (Wonderlin and Strobl, 1996). However, only certain classes of Kv channel appear to be involved in proliferation.

In human T-lymphocytes, the activity of Kv1.3 is responsible for the initiation of cell cycle progression in response to antigen presentation (Freedman et al., 1992; Lin et al., 1993; Price et al., 1989). Although other types of K^+ channel are involved in sustaining lymphocyte proliferation, Kv1.3 is by far the most abundantly expressed voltage-gated channel in these cells, and its activation is considered a key step in the immune response (Chandy et al., 2004; Lewis and Cahalan, 1995). In tumors, examples of K^+ channel-associated proliferation are more numerous. The two-pore domain channel K2p9.1 has been shown to be expressed in approximately 40% of breast cancers (Mu et al., 2003), Kv10.1 is expressed in neuroblastoma, melanoma, breast carcinoma and cervical cancer cells (Farias et al., 2004; Meyer and Heinemann, 1998; Meyer et al., 1999; Pardo et al., 1999), and Kv11.1 is found in endometrial tumors, leukemias, and colon cancer, among others (Cherubini et al., 2000; Lastraioli et al., 2004; Pillozzi et al., 2002). Intriguingly, Kv11.1 also has been shown to play a role in apoptosis (Wang et al., 2002a). Other classes of ion channel, including the Na^+ channels Nav1.5 and Nav1.7 (Brackenbury and Djamgoz, 2006; Fraser et al., 2005) and the TRP family member TRPV6 (Schwarz et al., 2006), are also associated with tumor proliferation. In this section, I discuss the specific

roles of each of these channels, beginning with the best-understood example: Kv1.3 in lymphocytes.

C.1. Channel-mediated proliferation in the immune system

The role of voltage-gated K^+ channels in immune cell proliferation was first recognized in pioneering experiments done by the Cahalan group in 1984. Applying the whole-cell patch clamp technique to human T-lymphocytes, these researchers identified a delayed-rectifying K^+ conductance, the activation kinetics of which could be increased by introducing phytohaemagglutinin (PHA), a known stimulator of lymphocyte mitogenesis (DeCoursey et al., 1984). Using ^{3}H-thymidine incorporation as a marker for DNA synthesis, they found that PHA-stimulated proliferation was inhibited in a dose-dependent manner by the organic K^+ channel blockers tetraethylammonium (TEA), 4-aminopyridine (4-AP) and quinine, suggesting that K^+ channel activity is associated with lymphocyte mitogenesis (DeCoursey et al., 1984). In a subsequent study, this effect was further characterized using ^{3}H-lysine, providing evidence that the block of K^+ channels with 4-AP also reduces protein synthesis, including the production of the cytokine interleukin-2 (IL-2), a protein known to play a major role in lymphocyte proliferation (Chandy et al., 1984). The reintroduction of IL-2 in the presence of 4-AP only weakly rescued the mitogenic inhibition, and had no effect at high 4-AP concentrations, suggesting that K^+ channel activity is crucial for the synthesis of proteins involved in lymphocyte proliferation (Chandy et al., 1984).

These experiments laid the groundwork for subsequent investigations of K^+ channel-regulated proliferation in the immune system, including further studies of human T-

lymphocytes (e.g., Sidell and Schlichter, 1986), peripheral blood mononuclear cells (Price et al., 1989) and murine B-lymphocytes (Amigorena et al., 1990), which gave support to the conclusion that K^+ channel inhibition correlates with reduced proliferation. However, the underlying mechanism remained elusive, and due to the cell-permeability of the organic inhibitors, there was uncertainty as to whether the observed reductions in proliferation were the direct result of K^+ channel inhibition or nonspecific effects of the small molecules on other cellular processes.

To more precisely investigate the role of K^+ channel activity in lymphocyte mitogenesis, several groups used high-affinity, membrane impermeable peptides to block K^+ channels during lymphocyte activation. Charybdotoxin (CTX), a scorpion venom-derived blocker of both inactivating Kv channels and Ca^{2+}-activated K^+ channels, inhibits both lymphocyte proliferation and IL-2 production following PHA stimulation (Freedman et al., 1992; Price et al., 1989), consistent with results obtained using the less-specific organic inhibitors. Experiments using CTX in combination with margatoxin (MgTX), a selective Kv channel blocker, proved that the voltage-gated current is important for lymphocyte activation (Lin et al., 1993).

IL-2 expression is essential for G1 phase progression during the cell cycle in lymphocytes, strongly suggesting that the Kv channel promotes G1 entry (Wonderlin and Strobl, 1996). In mitogen-stimulated murine B lymphocytes exposed to K^+ channel inhibitors, Amigorena and colleagues detected early G1 markers such as Ia and FcγRII, but no expression of transferrin receptor, a marker of late G1 phase (Amigorena et al., 1990). Moreover, experiments with CHX show the peak effectiveness of the toxin on proliferation to be within 4 hours of mitogen stimulation (Lin et al., 1993; Price et al.,

1989). Together with reports of G1 cell cycle arrest in MCF-7 human breast cancer cells by K^+ channel antagonists (Woodfork et al., 1995), these data suggest that the voltage-gated channel may be essential for directing the transition from quiescence into the G1 phase of the cell cycle.

Kv1.3 is the most abundant K^+ channel in lymphocytes and underlies the previously characterized *n* type delayed rectifier K^+ current (Lewis and Cahalan, 1995). However, the exact role of this channel in proliferation has remained somewhat unclear. Most theories suggest that membrane hyperpolarization following Kv1.3 opening provides the increased driving force on Ca^{2+} required for lymphocyte activation, and facilitates the generation of IP3 following antigen presentation. In turn, the IP3-stimulated release of Ca^{2+} from intracellular stores is thought to open both Ca^{2+}-activated K^+ channels and Ca^{2+} release-activated (CRAC) Ca^{2+} channels, which together sustain the high intracellular Ca^{2+} concentrations ($[Ca^{2+}]_i$) required for initiating signaling cascades leading to proliferation (Chandy et al., 2004).

An alternative hypothesis is that K^+ efflux during channel activation may contribute to cell cycle progression via the regulation of cell volume. One study demonstrates that an osmotically-induced 25% increase in neuroblastoma cell volume inhibits proliferation by 82%, an effect that can be mimicked by K^+ channel block with TEA and 4-AP. Conversely, the reduction of cell volume stimulates increases in proliferation (Rouzaire-Dubois and Dubois, 1998). Despite these observations, the relative contributions of membrane hyperpolarization and changes in cell volume on proliferation remain elusive, as the two processes are certainly intertwined. It is nevertheless established that changes in membrane potential and cell volume are both required for cell cycle progression

(Pardo, 2004) and that Kv1.3 plays a crucial role in lymphocyte proliferation, most likely via the regulation of IP-2-induced G1 progression (Wonderlin and Strobl, 1996).

C.2. The role of K^+ channels in cancer

In addition to its role in lymphocyte activation, Kv1.3 is expressed in a variety of tumors, including colon, prostate and breast cancers (Abdul and Hoosein, 2002a; Abdul et al., 2003; Yao and Kwan, 1999) as well as in melanoma and glioma cells (Artym and Petty, 2002; Preussat et al., 2003). Because of the extensive research that has been done in lymphocytes, it has been proposed that Kv1.3 influences tumor growth via a similar mechanism, i.e., the regulation of Ca^{2+} pathways. Using a combination of K^+ channel antagonists and Ca^{2+} imaging in proliferating colorectal adenocarcinoma cells, Yao and Kwan were among the first to show that inhibitors of Kv1.3 at concentrations that reduce proliferation also decrease Ca^{2+} entry (Yao and Kwan, 1999). Another role for Kv1.3 in tumors is suggested from fluorescence resonance energy transfer (FRET) experiments in melanoma cells. These studies showed that Kv1.3 physically interacts with β-integrins on the membrane, implying that the effects of channel blockers on tumor cell behavior may be due to disruption of integrin-containing membrane structures, known to be involved in metastatic processes (Artym and Petty, 2002).

In addition to contributing to lymphocyte proliferation and oncogenesis, Kv1.3 and other Kv1 (Shaker-type) isoforms, including Kv1.4 and Kv1.5, are involved in the differentiation of astrocytes and oligodendrocytes (MacFarlane and Sontheimer, 2000; Vautier et al., 2004), and enhance the ability of activated microglia to kill hippocampal neurons (Fordyce et al., 2005). Interestingly, Kv1.3 knockout mice have much smaller,

but more numerous, olfactory glomeruli than wild type mice, resulting in a significantly decreased threshold for odorant detection (Fadool et al., 2004). These mice also have elevated expression of several K^+ channel-associated signaling and adapter proteins, including Src kinase, tyrosine kinase receptor B (TrkB), 14-3-3 and PSD-95, compared to wild type mice, suggesting that the function of Kv1.3 during development and differentiation may extend beyond ion conduction.

Another type of K^+ channel, the two-pore domain K2p9.1, has been shown to have oncogenic properties. The gene encoding K2p9.1 (KCNK9) was isolated in a genomic screen of several DNA probes isolated from a novel human breast cancer amplicon, and was subsequently found to be overexpressed between 5- and 100-fold in 28 of 64 breast cancers (Mu et al., 2003). Furthermore, K2p9.1 promotes tumor formation when overexpressed in cells implanted into athymic mice, and confers serum-independence on C8 cells in culture (Mu et al., 2003). However, the tumor-promoting ability of K2p9.1 depends on K^+ flux, because a point mutation introduced into the selectivity filter renders the channel non-conducting and abolishes any oncogenic effects (Pei et al., 2003).

Perhaps the most well-characterized K^+ channels in tumorogenesis are Kv10.1 (EAG) and the related channel Kv11.1 (human EAG-related gene, hERG). EAG was first shown to be involved in cell cycle progression during heterologous expression studies in *Xenopus* oocytes, which are physiologically arrested in G2 during the first meiotic division. Subsequent activation of mitosis-promoting factor (MPF) relieves this arrest, but also dramatically reverses the rectification properties of heterologously expressed EAG: at more positive membrane potentials, EAG current is seen to decrease, rather than increase (Bruggemann et al., 1997). This curious effect was found to be a result of

intracellular Na^+ block of the channel pore, and similar to an effect on current that occurs during the M phase in mammalian cells (Pardo et al., 1998). Although the relevance of these findings for cell cycle regulation by EAG are yet to be fully understood, it has been suggested that interactions with cytoskeletal elements during the M phase may underlie EAG's involvement in proliferation (Pardo et al., 2005). This theory is supported by the observation that the application of nocodazole or colchecine, drugs that disrupt microtubules, similarly affect the rectification of EAG in inside-out patches (Camacho et al., 2000).

Despite being preferentially expressed in the nervous system (Ludwig et al., 1994), EAG mRNA has been observed in many human somatic cancers, but absent from the corresponding healthy tissues. These include breast carcinoma lines (MCF7, EFM-19 and BT-474), cervical carcinoma (HeLa) and neuroblastomas (Pardo et al., 1999), melanomas (Meyer et al., 1999), and gliomas (Patt et al., 2004). When heterologously overexpressed in mammalian cell lines, human EAG (hEAG) confers oncogenic properties such as increased proliferation, loss of contact inhibition and substrate independence, effects that can be reversed with hEAG-specific antisense oligonucleotides that down-regulate hEAG expression (Pardo et al., 1999). In addition, CHO cells transfected with *eag* stimulate tumor growth when transplanted into immune-suppressed mice. These findings have made EAG a promising target for novel cancer drugs, as well as a potential marker for early tumor detection and diagnosis (Pardo et al., 2005).

HERG is a K^+ channel related to EAG that exhibits gating typical of EAG and other outwardly rectifying channels, yet has a fast inactivation mechanism that confers inward rectification properties (Smith and Yellen, 2002; Trudeau et al., 1995). For this reason,

hERG function is thought to be similar to that of pacemaker channels, and mutations in the channel have been well-characterized as the basis of some forms of long Q-T syndrome in humans (Curran et al., 1995). HERG was first suggested to be involved in the cell cycle with observations that shifts in its voltage-dependence of activation correlate with changes in the resting potential of cycling neuroblastoma cells (Arcangeli et al., 1995). Subsequent investigations have found hERG overexpressed in primary cultures of myeloid leukemia, endometrial tumors and colon cancer cells (Cherubini et al., 2000; Lastraioli et al., 2004; Pillozzi et al., 2002), and hERG current is detected in a variety of tumor cell lines from human and murine sources, including neuroblastoma, adenocarcinoma, pituitary tumors, monoblastic leukemia and insulinoma β-cells (Bianchi et al., 1998). Furthermore, the inhibition of hERG decreases proliferation of neuroblastoma cells (Crociani et al., 2003). One proposed mechanism for hERG in mediating oncogenesis is that by maintaining hyperpolarized resting potentials, tumor cells expressing hERG have a selective advantage in surviving the ischemic environment that is typical of tumors (Bianchi et al., 1998). Another study suggests that hERG affects tumor growth by promoting the membrane surface expression of tumor necrosis factor receptor 1 (TNFR1), which enhances TNFα-stimulated tumor proliferation (Wang et al., 2002a)

Further evidence implicating hERG in proliferation includes known interactions between hERG and cell cycle-related proteins, such as Src kinase (Cayabyab and Schlichter, 2002) and 14-3-3 signaling adapter proteins (Kagan et al., 2002), as well as the finding that hERG and a splice-variant isoform lacking the N-terminus are expressed in a cell-cycle dependent manner (Crociani et al., 2003). In that study, the truncated

isoform (HERG1B) was upregulated during S-phase, while expression of the full-length channel (HERG1) increased during G1 (Crociani et al., 2003). HERG1B lacks the N-terminal PAS domain, which is conserved in the EAG channel family and is postulated to serve as an oxygen sensor (Morais Cabral et al., 1998). As tumor progression often involves hypoxia (Guillemin and Krasnow, 1997), the PAS domain of HERG1 may sense environmental oxygen during hypoxic events by altering the heterotetrameric ratio of HERG1B to HERG1, thereby shifting the channel's activation curve to limit K^+ loss (Crociani et al., 2003).

Von-Hippel-Lindau (VHL), a tumor-suppresor protein implicated in the hypoxic response, has been shown to induce the differentiation of neuroblastoma cells into functional neurons. Neuroblastomas overexpressing VHL show increased expression of neuronal markers such as neuropeptide Y, grow neurite-like processes and exhibit a secretory response to depolarization or cholinergic stimulation (Murata et al., 2002). Intriguingly, the activation of EAG channel activity in these cells is also diminished, and can be restored with VHL inhibition, suggesting that the PAS domain of EAG may also serve a functional oxygen-sensing role (Crociani et al., 2003). To date, hypoxia is the only cellular response known to modulate the activity of all four of the tumor-associated K^+ channels discussed here: Kv1.3, K2p9.1, Kv10.1 and Kv11.1 (Pardo, 2004).

C.3. Other channels involved in oncogenesis

Although the role of voltage-gated ion channels in cell cycle progression and tumor growth has mainly focused on the expression and activity of K^+ channels, other classes of channel are associated with oncogenesis, including some voltage-dependent Na^+ channels

and at least one TRP channel. High expression levels of Na^+ channels, especially Nav1.5 and Nav1.7, are detected in human prostate and breast cancers *in vivo* (Abdul and Hoosein, 2002b; Fraser et al., 2005), and are found in melanoma, lymphoma and small cell lung cancer cell lines (Allen et al., 1997; Fraser et al., 2004; Onganer and Djamgoz, 2005). These studies show that, in general, pharmacological Na^+ channel block decreases tumor proliferation, as is observed for K^+ channels.

Na^+ channels in tumor cells are thought to contribute to metastatic cellular behavior. This hypothesis was recently tested in the MDA-MB-231 breast cancer line using assays of motility, endocytosis and invasion, all of which were significantly reduced following treatment with the Na^+ channel blocker tetrodotoxin (TTX) (Fraser et al., 2005). Three channel isoforms were isolated from these cells: Nav1.6 and Nav1.7, which are TTX-sensitive in the nanomolar range, and Nav1.5, which requires higher (micromolar) TTX concentrations for inhibition. Using RT-PCR, Nav1.5 was detected as the predominant isoform in human breast cancer biopsy sections (Fraser et al., 2005). Nav1.5 is also the most prevalent Na^+ channel in Jurkat cells, a human T-cell leukemia line, in which channel activity was found to be essential for lymphocyte invasiveness (Fraser et al., 2004). Furthermore, a recent study of Nav1.7 in Mat-LyLu rat prostate cancer cells found that TTX inhibition reduces cell migration in Transwell assays, indicating that this isoform may also be important for conferring metastatic potential (Brackenbury and Djamgoz, 2006).

Although Na^+ channels are thought to regulate cell proliferation through the effects of Na^+ flux on cell volume (Soroceanu et al., 1999), they have been shown to contribute to other cellular behaviors associated with oncogenic invasiveness, including motility

(Fraser et al., 2003), secretion (Mycielska et al., 2003) and cell adhesion (Malhotra et al., 2000). The specific interactions between Na^+ channel β-subunits with cell adhesion molecules such as ankyrin is explored in detail below.

Another ion channel with an established involvement in oncogenesis is TRPV6, a highly selective Ca^{2+} channel likely to be involved in endothelial Ca^{2+} reuptake (Hoenderop et al., 2005). *In situ* hybridization of prostate cancer biopsy sections show that transcription of the TRPV6 is significantly upregulated compared to benign prostate tissues (Fixemer et al., 2003). A recent study indicates that overexpression of TRPV6 in HEK-293 cells increases proliferation in a Ca^{2+}-dependent manner (Schwarz et al., 2006), suggesting that the channel may exert oncogenic effects via the stimulation of Ca^{2+} pathways, as in the case of lymphocyte activation (Cahalan et al., 2001).

C.4. Channel-mediated apoptosis and tumor suppression

In addition to having roles in the stimulation of proliferation and oncogenesis, some ion channels have been shown to mediate apoptotic events or the suppression of tumor growth. Remarkably, several of these are the same K^+ channel subtypes that are associated with proliferation, including Kv1.3, K2p1.9 and Kv11.1. Here I discuss several studies that implicate ion channel involvement in apoptosis and tumor suppression.

As discussed in C1 above, Kv1.3 channels play an essential role in lymphocyte proliferation following antigen presentation, a process that requires K^+ conductance through the channel (Lewis and Cahalan, 1995). In addition, however, cell shrinkage due to K^+ effux has been identified as being crucial for apoptosis in lymphocytes (Bortner et

al., 1997) as well as in neurons (Yu et al., 1997). Could Kv1.3 mediate both processes? Experiments in Jurkat T-lymphocytes show that activation of Fas receptors to initiate the apoptosis signaling cascade doubles Kv1.3 current amplitude (Storey et al., 2003). This effect was found to depend on the expression of the Fas-associated death domain protein (FADD), as well as the activation of caspase 8, both key components of the apoptotic signaling pathway. However, blocking Kv1.3 activity does not prevent apoptotic decreases in cell volume, suggesting that K^+ flux through other channels may contribute to apoptosis in these cells (Storey et al., 2003).

In fact, another K^+ channel has been shown to promote cell shrinkage: K2p9.1. In addition to its involvement in breast cancer cell proliferation (Mu et al., 2003), K2p9.1 activity regulates apoptotic volume decreases in mouse embryos (Trimarchi et al., 2002). These authors showed that pharmacological K^+ channel blockers such as quinine prevent cell shrinkage following exposure to H_2O_2, a known apoptotic stimulus. Currents similar to K2p9.1 were identified as the source of the K^+ efflux from these cells, suggesting that apoptotic cell shrinkage involves the recruitment of channels (such as K2p9.1) that regulate cytoplasmic volume (Trimarchi et al., 2002).

In neurons, apoptosis may be regulated by Kv2.1 channels. Primary cultures of cortical neurons expressing dominant negative Kv2.1 are resistant to the apoptosis-related enhancement of K^+ current observed in control cells, and are also protected from oxidant-induced apoptosis, as measured by luciferase assays of viability (Pal et al., 2003). Confirming its specific role in promoting cell death, CHO cells expressing Kv2.1 also exhibit enhanced apoptosis, an effect that does not occur in Kv1.4-expressing controls (Pal et al., 2003).

Kv11.1 (hERG) has been shown to regulate apoptosis in various tumor cell lines, including human SK-BR-3 breast cancer cells, SH-SY5Y neuroblastomas and HL-1 rat atrial tumor cells (Wang et al., 2002a). In fluorescent labeling assays of DNA fragmentation, a hallmark of apoptosis, these cell lines show substantially increased apoptosis upon H_2O_2 exposure compared to tumor cells not expressing hERG. This increase can be eliminated by applying a specific hERG inhibitor, Dof, which has no effect on control cell apoptosis (Wang et al., 2002a). Other experiments using *herg*-transfected HEK cells show that hERG expression confers apoptotic sensitivity to H_2O_2, an effect that is not observed using a non-conducting mutant (Wang et al., 2002a). These results suggest that the function of hERG in promoting apoptosis may be related to changes in cell volume accompanying K^+ flux, similar to that of other K^+ channels described above.

TRP channels are also involved in apoptosis and the inhibition of tumor growth. TRPM1 is a Ca^{2+}-selective channel whose expression appears inversely correlated with metastasic behavior in B16 murine melanomas: TRPM1 mRNA is substantially decreased in more aggressively metastatic cells, despite being expressed at much higher levels in weakly metastatic cell variants (Duncan et al., 1998). The related channel isoform TRPM2 is permeable to Na^+ and K^+, as well as Ca^{2+}, and has been implicated in the stimulation of apoptosis in monocytic leukemia cells (Zhang et al., 2006). In these cells, functional TRPM2 channel expression confers an enhanced susceptibility to oxidative stress or TNFα-induced apoptosis, which correlates with increased $[Ca^{2+}]_i$. Furthermore, biochemical analysis of downstream cell death signaling molecules show that TRPM2 activation results in the cleavage of procaspase-8, -9, -3 and -7, as well as

the inactivation of PARP, indicating that TRPM2 expression activates both intrinsic and extrinsic apoptotic pathways (Zhang et al., 2006).

Lastly, two other TRP family members, TRPP1 and TRPP2, are shown to suppress cell proliferation. Also known as polycystin-1 and -2, these proteins are typically found in renal tubules, where they are thought to be involved in fluid sensing (Huang, 2004). While not functional channels individually, TRPP1 and TRPP2 subunits coassemble to form a functional, Ca^{2+}-permeable channel (Hanaoka et al., 2000). However, mutation or loss of either protein results in the formation of cysts due to overproliferation of epithelial cells in renal tubule walls (Wilson and Falkenstein, 1995). As one piece of evidence explaining this negative regulation, TRPP1 has been shown to induce cell cycle arrest in MDCK kidney cell lines via stimulation of the JAK-STAT signaling pathway, an effect that requires TRPP2 expression (Bhunia et al., 2002). In addition, a recent study by the Caplan group shows that TRPP2-expressing kidney cells exhibit reduced proliferation and diminished tubule branching morphology compared to control cells. This effect occurs independently of the presence of serum, and is correlated with nuclear exclusion of phosphorylated extracellular signal-regulated kinase (ERK), a known component of proliferation pathways (Grimm et al., 2006).

D. NON-CONDUCTING FUNCTIONS OF ION CHANNEL PROTEINS

So far, I have discussed numerous cases in which certain ion channels encompass a nontraditional role, acting outside the nervous system to affect cell proliferation and apoptosis. In many of these situations, the proposed mechanisms require ion movement through the channel pore, and therefore it could be argued that these channels are not

truly "multifunctional". However, it is important to recognize that many of the effects on proliferation or apoptosis by these channels cannot be explained solely by a changing membrane potential, nor replicated when other channels with similar current properties are substituted (Kaczmarek, 2006). Here, I focus on several examples of channels that have physiological functions wholly independent from their roles as ion conductors. These include the enzymatic activity of TRPM channels, homeostatic regulation of channel expression by Kv4 (Shal) channels, modulation of synaptic facilitation by HCN channels and the coupling of Ca^{2+} channel gating to muscle contraction and synaptic vesicle fusion. A discussion of non-conducting channel functions that are mediated via auxiliary subunits is presented in part E.

D.1. TRP channels have intrinsic enzymatic activity

Perhaps the most striking examples of ion channels operating independently of ion conduction are certain members of the TRP superfamily that have intrinsic enzymatic functions. TRP channels, first discovered in *Drosophila* phototransduction studies (Cosens and Manning, 1969), are cation-selective channels formed by the association of four six-transmembrane domain α-subunits with intracellular N- and C-terminal domains. While topologically similar to voltage-gated K^+, Na^+ and Ca^+ channels, TRP channels lack the complete set of positive S4 residues responsible for voltage sensing (Huang, 2004). TRP channels are grouped into six families based on amino acid sequence similarity (TRP-C, -V, -M, -P, -ML and -N), and have a diverse range of functions, including heat, cold and taste sensation, epithelial Ca^+ transport, ciliary mechano-sensation, and vesicle sorting (Huang, 2004). I have already discussed the role of TRPV6 in proliferation (Fixemer et al., 2003; Schwarz et al., 2006), the regulation of tumor

suppression by TRPP1/2 (Grimm et al., 2006; Wilson and Falkenstein, 1995) and apoptotic stimulation via TRPM2 (Zhang et al., 2006).

TRPM subfamily members have a high degree of amino acid sequence conservation, including several conserved N-terminal subdomains and a C-terminal coiled-coil domain. In addition, the C-terminal sequences of TRPM6 and TRPM7 contain a zinc-finger domain with strong homology to α-kinases, suggesting that these proteins may function as both ion channels and protein kinases (Runnels et al., 2001; Schmitz et al., 2004). TRPM7 (TRP-PLIK) was first characterized by the Clapham group, which found that TRPM7 expresion in CHO cells produces a steep outwardly rectifying current carried by magnesium (Mg^{2+}) and Ca^{+} ions (Runnels et al., 2001). Using radiolabeled ATP assays of kinase activity, they also found that TRPM7 can phosphorylate itself as well as other substrates such as myelin basic protein (MBP). This kinase activity appears to be essential for channel activity; removal of ATP from the pipette solution or mutation of putative ATP-binding and catalytic residues substantially reduces both outward and inward current in TRPM7-expressing cells (Runnels et al., 2001). Subsequent investigation of TRPM7 has characterized it as a serine/threonine kinase and shows that Mg^{2+}, which permeates the channel, also modulates kinase activity *in vivo* (Ryazanova et al., 2004). In contrast to TRPM7, the kinase activity of TRPM6 has not been well-characterized, in part due to difficulties with functional expression (Schmitz et al., 2004). Some evidence exists that the isolated kinase domain exhibits phosphotransferase activity, and can even phosphorylate TRPM7, but not vice versa (Riazanova et al., 2001; Schmitz et al., 2005).

Although the physiological roles of TRPM6 and TRPM7 remain unclear, a growing body of evidence suggests that these channel kinases are important for Mg^{2+} homeostasis (Schmitz et al., 2004). Autosomal-recessive hypomagnesemia, in which patients are unable to absorb Mg^{2+} in the distal tubule of the kidney, is associated with mutations in TRPM6. TRPM6 maps to the genomic disease locus and is expressed primarily in regions known to be involved in Mg^{2+} absorbtion (Schlingmann et al., 2002). Furthermore, TRPM7-deficient B-lymphocytes exhibit Mg^{2+} deficiency and die within 48 hours, but can be restored to wild type growth with Mg^{2+}-supplemented media, in analogy to hypomagnesemia patients who can live healthily with a Mg^{2+}-supplemented diet (Schmitz et al., 2003). However, expression of TRPM6 in these cells cannot rescue the Mg^{2+} deficiency caused by TRPM7 deletion, indicating that the channels have nonredundant functions in Mg^{2+} regulation, even though they can modulate each other (Schmitz et al., 2005). While much is yet to be learned about the effect of intrinsic Mg^{2+}-sensitive kinase activity on TRPM6/7 channel activation, it is tempting to speculate that the kinase portions of the channels respond to Mg^{2+} levels by modulating current density to facilitate Mg^{2+} reuptake.

Finally, one other TRPM family member is shown to have intrinsic enzymatic activity: TRPM2. Also called LTRPC2, TRPM2 is a Ca^{2+}-permeable channel containing a C-terminal region with a high degree of sequence homology to ADP-ribose pyrophosphatases. Perraud and colleagues showed that this enzymatic domain is not only able to cleave the ribose-5-phosphate from ATP-ribose, but that the remaining bound ADP-ribose enhances channel activation (Perraud et al., 2001). TRPM2 can also bind nicotinamide adenine dinucleotide (NAD^{+}), which activates the channel and stimulates

Ca^{2+} influx into monocytes (Sano et al., 2001). As discussed above, TRPM2 also contributes to immune cell death by stimulating the pro-apoptotic caspase signaling pathways (Zhang et al., 2006). Thus, although the function of these channels is still unclear, the pyrophosphatase activity of TRPM2 may serve to integrate information from nucleotide signaling molecules in the regulation of Ca^{2+} influx in the immune system.

D.2. K^+ channels regulate homeostatic channel expression

Shal is a member of the Shaker family of K^+ channels, and the invertebrate ortholog of the mammalian Kv4 channel, which underlies the rapidly-inactivating A-type K^+ current, I_A. These channels are predominantly inactivated at rest, but during prolonged bursts of activity the inhibition is removed, allowing I_A to slow the rate of action potential firing (Hille, 2001). Several recent studies have shown that Shal may coordinate neuronal excitability in the lobster stromatogastric ganglion (STG) via the upregulation of HCN channels. In the STG neuronal network, pyloric dilator (PD) neurons provide pacemaking activity that generates rhythmic muscle contraction in the stomach (Ayali and Harris-Warrick, 1999). This is accomplished via the coordination of slowly oscillating membrane potentials and action potentials bursts within the circuit, which relies on the proper arrangement of synaptic inputs as well as the combination of ion channels expressed (Selverston and Moulins, 1985). In the STG, the I_A current provided by Shal is essential for maintaining rhythmic activity.

Surprisingly, the Harris-Warrick group recently found that overexpressing Shal in PD neurons does not change the rhythmic firing of action potentials, despite providing a significant increase in I_A (MacLean et al., 2003). Upon further examination, they

observed an increase in the hyperpolarization-activated current, I_h, which acts to counterbalance the enhancement of I_A following Shal overexpression, an effect not seen when overexpressing Shaker. Conversely, overexpression of HCN channels in PD neurons increases I_h without affecting I_A, suggesting that the homeostatic compensation is unique to Shal (Zhang et al., 2003). In addition, pharmacological block of I_h uncovers the increased latency and interspike interval that are characteristic effects of I_A (MacLean et al., 2003). These results suggest that Shal increases the expression of hyperpolarization-activated cyclic nucleotide-gated (HCN) channels, which conduct I_h to offset the enhanced I_A, thereby maintaining rhythmic firing patterns. Subsequent mathematical modeling studies confirmed that increased I_h via HCN upregulation can sufficiently compensate for increases in I_A in the STG circuit, ruling out the alternative explanation that I_A is somehow mislocalized to electrically isolated cellular compartments (MacLean et al., 2005).

Importantly, the Shal-induced increase in I_h is still observed when using a non-conducting mutant channel, indicating that the mechanism underlying the effect does not itself depend on I_A (MacLean et al., 2003). Shal therefore provides a conductance-independent intracellular signal to influence HCN expression. Because the Shal-mediated increase in I_h is not affected by blockers of transcription (MacLean et al., 2003), this mechanism likely involves the regulation of HCN channel translation, localization or activation by Shal. However, because the increase in I_h is approximately 20-fold, recruitment of an existing pool of HCN channels does not adequately explain the enhancement. It seems more likely that Shal and HCN channels are co-translated or co-assembled prior to membrane insertion, or that Shal reduces the steady-state removal of

HCN channels from the membrane (MacLean et al., 2003). Regardless, it is clear that the activity-independent role of Shal in regulating HCN channel expression is an important homeostatic mechanism in the STG. It remains to be seen whether this type of compensatory expression is mediated by ion channels in other oscillating neuronal circuits.

D.3. HCN channels contribute to synaptic facilitation

As well as being the target for Shal-mediated homeostasis in the STG, HCN channels may have a secondary function of their own. As discussed above, HCN channels conduct the hyperpolarization-activated K^+ current, I_h (Hille, 2001). These channels are modulated in response to elevations of intracellular cyclic adenosine monophosphate (cAMP), which shifts the voltage-dependence of activation in a positive direction upon binding, permitting channel activation at more depolarized potentials. This effect of cAMP is thought to occur via the displacement of a C-terminal linker region that partially inhibits the channel in the absence of cAMP (Accili et al., 2002).

Studies by the Zucker group have shown that cAMP stimulation of presynaptic HCN channels affects synaptic facilitation at the crayfish neuromuscular junction in a manner not obviously related to membrane potential changes. Application of seratonin or forskolin to presynaptic crayfish motor neurons stimulates adenylyl cyclase to produce cAMP, and causes a significant and sustained increase in excitatory junctional potentials (EJPs) recorded from the postsynaptic muscle fiber (Beaumont and Zucker, 2000). A similar EJP enhancement is seen following high-frequency tetanic stimulation of the presynaptic cell, which elicits a brief hyperpolarization via the increased activity of

Na^+/K^+ ATPase (Beaumont et al., 2002). In both cases, the onset of the enhancement is mediated by HCN channels, because specific HCN channel blockers prevent the effect if present during stimulation. However, HCN channels are not required for sustaining the increased neurotransmitter release, because application of HCN blockers after the initial enhancement has no effect (Beaumont et al., 2002).

Other experiments show that HCN involvement in initiating facilitation is a result of interactions with the cytoskeleton. Application of actin depolymerizers blocks synaptic enhancement by HCN channels induced by tetanic stimulation, but not by cAMP, suggesting that a second cAMP-stimulated pathway may be a component of the long-lasting phase of facilitation (Beaumont et al., 2002). This phenomenon, by which previous stimulation of HCN channels renders subsequent cAMP stimulation of facilitation HCN- and actin-independent, is known as "synaptic tagging" and may be an important form of synaptic plasticity (Zhong and Zucker, 2004).

Together these results suggest that the effects of HCN channels in synaptic tagging may be independent of changes in the membrane potential. Serotonin-stimulated HCN activation only results in a 10 mV depolarization, yet induces EJP enhancement; this amount of depolarization in the absence of cAMP has no effect (Beaumont and Zucker, 2000). Moreover, although increases in cAMP following serotonin application cause a rise in $[Ca^{2+}]_i$ through HCN channels, chelation of Ca^{2+} with BAPTA does not prevent the enhancement of transmitter release, and HCN-mediated depolarization is insufficient to open voltage-gated Ca^{2+} channels (Zhong et al., 2004). Whether activation of HCN channels results in voltage-dependent signaling that is independent of channel conductance remains to be determined, and the mechanism by which this could occur is

far from clear. However, experiments showing that actin polymerizers can substitute for HCN activation in the induction of synaptic enhancement suggest that channel activity may lead to cytoskeletal rearrangements crucial for the delivery of vesicles to the synaptic terminal (Zhong and Zucker, 2004).

D.4. Ca^{2+} channels regulate muscle contraction and vesicle fusion

In the immune system, Ca^{2+} release from the sarcoplasmic reticulum and influx via the activation of CRAC channels stimulates pathways leading to proliferation and T-lymphocyte activation (Chandy et al., 2004). I have already discussed how K^+ channel activation sustains the driving force for Ca^{2+} entry in these cells; however, the molecular identity of CRAC channels has remained elusive until recently. No voltage-gated Ca^{2+} channels are expressed at significant levels in T-lymphocytes (Lewis and Cahalan, 1995), but expressed sequence tags encoding a TRPC channel were isolated from human B-cells and mouse T-cells, initially suggesting that CRACs are Ca^{2+}-permeable TRPC channels (Cahalan et al., 2001). Recent investigations have disproved this hypothesis, finding instead that the 4TM *Drosophila* protein Orai forms the pore subunit of the channel mediating the CRAC current (Prakriya et al., 2006; Yeromin et al., 2006).

Regardless of their molecular identity, the function of CRAC channels in the immune system implicitly depends on the ability to conduct Ca^{2+}, which initiates the wide array of Ca^{2+}-dependent signaling pathways involved in T-cell proliferation. In contrast, voltage-gated Ca^{2+} (Cav) channels were probably the earliest recognized channel with a function that does not require ion flux. In skeletal muscle, Cav1 (L-type) channels mediate excitation-contraction (E-C) coupling, in which the depolarization of transverse (T)

tubules by motor neurons induces the release of Ca^{2+} from intracellular stores, thereby activating the contractile actin/myosin machinery underlying muscle contraction (Berchtold et al., 2000; Schneider, 1981). Initiating this process are Cav1 channels on the T-tubule membrane, called dihydropyridine receptors (DHPRs), that are physically linked to ryanodine-sensitive Ca^{2+} release channels (RyRs) controlling Ca^{2+} release from the sarcoplasmic reticulum (Berchtold et al., 2000). These junctions, or Ca^{2+}-release units (CRUs), exist both in skeletal and cardiac muscle. However, whereas EC coupling in cardiac tissue requires a large Ca^{2+} current through DHPRs, skeletal muscle CRUs can operate in the absence of extracellular Ca^{2+}, implying that DHPRs there act solely as a voltage sensor for RyR opening (Flucher and Franzini-Armstrong, 1996).

The idea of a voltage-dependent interaction between DHPRs and $[Ca^{2+}]_i$ was first proposed in a pioneering 1973 study that characterized the charge movement across the membrane of frog muscle fibers using a three-electrode voltage clamp technique (Schneider and Chandler, 1973). Although the researchers did not know at the time that the small current they detected was the gating of a Ca^{2+} channel itself, they speculated that it could be associated with a molecule extending from the T-tubule to the sarcoplasmic reticulum, translating voltage changes into intracellular Ca^{2+} release (Schneider and Chandler, 1973). Further investigations revealed that DHPRs are the source of the charge movement, and can pass a slow Ca^{2+} current themselves (Rios and Brum, 1987; Tanabe et al., 1988). Bidirectional interaction between DHPRs and RyRs was subsequently confirmed in studies showing that DHPRs control RyR channel gating (Grabner et al., 1999) and that RyRs, in turn, enhance the slow Ca^{2+} current through DHPR channels (Nakai et al., 1996). However, this slow current is not necessary for

depolarization-induced Ca^{2+} release by RyRs, which consistently occurs in skeletal muscle following removal of Ca^{2+} from extracellular solutions (Rios and Pizarro, 1991).

Recently, conformational coupling between the two channels has been physically demonstrated using freeze-fracture to examine the relative position of DHPRs bound to RyR channels. Within the CRU, four DHPR molecules bind to a single RyR channel, forming a "tetrad" of DHPRs that can be easily identified using electron microscopy. Treatment with ryanodine, which inactivates RyR channels by locking them in a non-conducting conformation, results in a ~2 nm uniform shift in DHPR spacing compared with untreated tetrads, providing strong evidence for a conformational link between the two channels (Paolini et al., 2004).

Neuronal Cav2 (N-type) channels have also been shown to link their voltage-sensing ability to a cellular function, namely neurotransmitter release, independently of Ca^{2+} flux. Presynaptic Cav2 channels interact directly with the soluble NSF attachment receptor (SNARE) proteins syntaxin and SNAP-25, via an intracellular loop called the synprint domain (Rettig et al., 1996). The synprint domain also binds to synaptotagmin on the vesicle membrane (Sheng et al., 1997). These interactions are regulated via phosphorylation by protein kinase C (PKC) and CaMKII (Yokoyama et al., 1997) and likely allow docked vesicles to be positioned near Ca^{2+} channels at synaptic terminals to facilitate rapid Ca^{2+}-mediated exocytosis (Catterall, 2000).

Although activity-dependent neurotransmitter release is typically triggered by a local increase in $[Ca^{2+}]_i$, neurotranmitter release also can occur in the absence of a Ca^{2+} signal. For example, in superior cervical ganglion (SCG) neurons, synaptic vesicle fusion can be induced by sucrose solutions in the presence of the Ca^{2+}-chelater BAPTA, and recorded

as miniature excitatory post-synaptic potentials (mEPSPs) (Mochida et al., 1998). Tetanic stimulation of the presynaptic cell enhances this Ca^{2+}-independent neurotransmitter release, as indicated by increases in mEPSP frequency that are proportional to the frequency of the stimulation. This enhancement is prevented by injection of a synprint peptide inhibitor, which disrupts the association between Ca^{2+} channels and SNARE proteins (Mochida et al., 1998), suggesting that gating of the channel may be linked to SNARE activity. Supporting this conclusion is a study in dorsal root ganglion neurons that used measurements of membrane capacitance to show that depolarization is sufficient to induce neurotransmitter secretion in the absence of Ca^{2+} (Zhang and Zhou, 2002). Together, these findings suggest that the physical association between Cav2 channels and SNAREs at synaptic terminals allows voltage-dependent changes in channel conformation to be directly translated to the activity of vesicle fusion machinery.

D.5. Other voltage-sensing proteins

In contrast to ion channels that have linked their voltage sensing ability to secondary functions, including enzymatic catalysis and the activation of intracellular signaling pathways, there are evolutionary instances of signaling proteins that have coupled their activity to voltage sensing domains. One example of this phenomenon was discovered in the ciliate *Paramecium tetraurelia*, which generates cAMP upon hyperpolarization of the plasma membrane (Schultz et al., 1992). This process is generated by an unusual adenylyl cyclase that, when purified from ciliary membranes and reconstituted in lipid bilayers, shows single-channel activity very similar to K^+ channels. Cyclic nucleotides

generated in response to hyperpolarization are thought to increase the Ca^{2+} influx that controls ciliary motility (Bernal and Ehrlich, 1993).

A more recently discovered example of voltage-sensing in non-channel proteins is the phosphoinositide phosphatase of the aquatic invertebrate *Ciona intestinalis*. This enzyme contains an intrinsic voltage-sensing domain, and was named *C. intestinalis* voltage-sensor-containing phosphatase (Ci-VSP). Initial examination of the Ci-VSP sequence revealed four transmembrane domains, including a region rich in positively charged residues that aligns well with the S4 voltage sensor of Kv1 channels. The transmembrane domains of Ci-VSP are followed by a phosphatase-like sequence instead of the more typical channel pore. When heterologously expressed in *Xenopus* oocytes, Ci-VSP, while lacking an ionic current, displays transient outward and inward currents very similar to the gating currents of voltage-gated channels, indicating that the voltage sensor of Ci-VSP is functional (Murata et al., 2005). In addition, phosphate release assays show that the protein is able to dephosphorylate phosphatidylinositol-3,4,5-trisphosphate ($PtdIns(3,4,5)P_3$) to form $PtdIns(4,5)P_2$, paralleling the activity of phosphate and tensin homologue (PTEN), with which Ci-VSP also shares sequence similarities. Mutation of a cysteine residue of Ci-VSP corresponding to the catalytic cysteine of PTEN disrupts the phosphatase activity, confirming that its catalytic mechanism is similar to that of PTEN (Murata et al., 2005).

Most relevant to studies of EAG signaling activity, the voltage sensor of Ci-VSP appears to modulate phosphatase activity. To investigate whether Ci-VSP phosphotase activity is voltage-dependent, Murata and colleagues coexpressed Ci-VSP in oocytes with inwardly rectifying K^+ channels, which are activated by phosphoinositides. In these

experiments, changes in a membrane potential resulted in a PtdIns(4,5)P_2-dependent enhancement of K^+ current that was not observed using catalytically-inactive Ci-VSP mutants (Murata et al., 2005). Because Vi-CSP is expressed primarily in *C. intestinalis* sperm tail, the coupling of a voltage-sensor to phosphotase activity is thought to regulate sperm motility in response to hyperpolarizing sperm-attracting steroid signals (Murata et al., 2005).

Human and mammalian orthologs of Ci-VSP have been identified, and appear to be functional proton channels. Both the human channel, Hv1, and the mouse voltage-sensor-only protein (mVSOP) have four transmembrane domains that include the voltage sensor, exhibit proton-selective outward current and are gated by pH and divalent metal ions (Ramsey et al., 2006; Sasaki et al., 2006). Hv1 channels are expressed in immune cells and likely mediate the phagocytotic oxidative burst response (Ramsey et al., 2006). However, the voltage-sensing domains of these channels do not appear to be structurally linked to any enzymatic activity, and likely function solely as proton channels. Future studies addressing the evolutionary roles of these proteins may reveal other examples of voltage-sensitive proteins and shed light on the emergence of voltage-gated ion channels.

E. AUXILIARY SUBUNITS AND ION CHANNEL SIGNALING

Most endogenous ion channels have one or more auxiliary subunits that associate with the channel core to form larger macromolecular complexes, and are often essential for normal channel function. These subunits typically contribute to the modulation of channel activity, but also facilitate interaction with cytoskeletal elements, enzymes and signaling pathway components, allowing channel function to be integrated into myriad

biochemical processes (Isom et al., 1994). Here I discuss several examples of proteins that confer unusual properties on the channel complexes they comprise, allowing the principal channel subunits to participate in functions not typically associated with ion channels themselves. This includes the cell adhesion properties of Na^+ channel β-subunits, the enzymatic functions of various K^+ channel subunits, and the role of calmodulin, the ubiquitous signaling pathway component that also associates with several ion channel complexes. Finally, I will discuss another mechanism by which ion channel complexes can interact with biochemical pathways: proteolytic cleavage of channel proteins or their subunits to yield free peptides with numerous roles.

E.1. Na^+ channel β subunits are cell adhesion proteins

Na^+ channels became the first known ion channel complexes with the discovery of the β1 and β2 subunits, which copurify with the channel in brain preparations (Hartshorne and Catterall, 1984). β1 and β2 are membrane-spanning proteins with long, glycosylated extracellular regions and short intracellular C-termini, and are physically attached to the Na^+ channel α-subunit; β2 is linked via disulfide bonds, while β1 associates noncovalently (Isom et al., 1994). These proteins regulate Na^+ channel expression and enhance activation kinetics, but are also members of the immunoglobin (Ig) family of cell adhesion molecules (CAMs), as they contain characteristic Ig domains in their extracellular N-termini. These regions mediate cell adhesion via homotypic interactions, demonstrated in experiments in which β1 or β2 overexpression induces cell aggregation, an effect not observed when expressing the α-subunit alone (Malhotra et al., 2000). Many studies have shown that the β1 and β2 subunits also participate in heterophilic

associations with other CAMs, including contactin, connexin-43, N-cadherin and neurofascins (Malhotra et al., 2004; McEwen and Isom, 2004; Ratcliffe et al., 2001). Intracellularly, the C-domains of β1 and β2 bind to the cytoskeletal protein ankyrin, promoting the recruitment of ankyrin to points of contact between cells (Malhotra et al., 2000).

The complex interactions between β-subunits, ankyrin and extracellular CAMs may help to coordinate extracellular matrix proteins and intracellular cytoskeletal components around Na^+ channel complexes, and provide a mechanism for the accumulation of Na^+ channels at nodes of Ranvier. An ankyrin-G binding motif in Na^+ α-subunits has been shown to be essential for targeting channels to axonal initial segments and nodes of Ranvier (Garrido et al., 2003), and a nearly identical motif is present in Kv7 channels, suggesting a convergence of ankyrin-based targeting mechanisms during axonal evolution (Pan et al., 2006). In addition, β1 subunits colocalize with neurofascin at nodes in sciatic nerve axons, and these proteins coimmunoprecipitate from rat brain lysates (Ratcliffe et al., 2001). β2 subunits contain sequences similar to contactin, a CAM that binds the oligodendrocyte molecules tenascin-C and tenascin-R, which have both fibronectin and epidermal growth factor (EGF)-like binding domains. β2 interacts strongly with the fibronectin domains, but not EGF domains (Srinivasan et al., 1998), resulting in a dynamic interplay during cell migration. Because β-subunits are expressed in neurons prior to myelination, this interaction may be important for repelling tenascin-secreting oligodendrocytes, thus maintaining nodes of Ranvier during myelin formation (Xiao et al., 1999). Together, these studies imply that β-subunits are essential for targeting Na^+ channels to electrically active axonal domains, not only by promoting

ankyrin recruitment to Na^+ channels, but also by associating extracellularly with neurofascins and repelling oligodendrocytes at nodes of Ranvier.

Finally, another role for β-subunits in development was suggested by the finding that β1 stimulates neurite outgrowth in dissociated cerebellar granule cells (Davis et al., 2004). In this study, neurons from wild type or β1 (-/-) mice were grown on a monolayer of support cells expressing β1. Compared to the wild type, neurite extension in the β1 knockout cells was significantly reduced, implying that homotypic β1-mediated adhesion promotes growth. Interestingly, β2-transfected monolayer cells inhibit wild type neurite extension and suggest that the two subunits have anagonistic influences during neuronal organization (Davis et al., 2004). In summary, these studies provide evidence that the cell adhesion properties of Na^+ channel β-subunits allow the channel complex to be involved in more than ion conduction. Certainly, the β-subunits may contribute to the localization of Na^+ channels into cellular domains where ion flux is needed; however, whether channel gating is linked to β-subunit function remains an open question. As discussed below, Na^+ channel β-subunits are also cleaved by certain secretases, yielding free peptides that can influence Na^+ channel expression and membrane excitability.

E.2. K^+ channel β-subunits have enzymatic activity

As the most diverse class of voltage-gated ion channels, K^+ channels correspondingly associate with a multitude of ancillary proteins, including signaling molecules, second messengers and scaffolding proteins. However, certain K^+ channels possess native auxiliary subunits that are considered essential channel components, contributing to voltage-dependence, kinetic properties and membrane localization (Kaczmarek, 2006).

Several of these β-subunits exhibit intrinsic enzymatic activity and signaling properties, suggesting that the non-conducting roles of K^+ channels in intracellular signaling pathways may be in part mediated through β-subunits. In addition, regulatory enzymes such as PKA, PKC, CaMKII and others frequently associate with K^+ channels and modulate channel activity in response to a variety of biochemical cues (Levitan, 2006). While not considered *bona fide* β-subunits, these are often important for the fine-tuning of K^+ channel complexes, and can also contribute to certain non-conducting signaling roles, as in the case of EAG and CaMKII.

Before exploring the secondary roles that individual K^+ channel β-subunits have in the activation of intracellular signaling, it will be useful to briefly discuss the association of kinases and phosphatases with ion channel complexes. Some initial evidence that channels interact with such enzymes came from the Levitan group, who found that large conductance Ca^{2+}-activated K^+ (BK) channels, when reconstituted in artificial lipid bilayers, exhibit increased open probability upon application of ATP (Chung et al., 1991). This observation, which can be reversed by the addition of protein phosphatase 1 (PP1), suggested that kinase activity is somehow associated with the channel. Subsequent experiments determined this activity to be similar to that of PKC, which itself mimics the effect when applied to the preparation. Moreover, microcystin and other phosphatase inhibitors enhance channel modulation by ATP, implying the presence of a PP1-like phosphatase (Reinhart and Levitan, 1995). These findings were consistent with other observations of the effects of ATP on purified channels, although it was not initially known whether the kinase and phosphatase activities were mediated by the channels

themselves or by tightly associated proteins that copurified with the channels (Levitan, 2006).

Numerous coimmunoprecipitation studies have since confirmed that K^+ channels commonly associate with protein kinases and phosphatases that affect channel activity and expression. For example, the tyrosine kinase Src associates with K^+ channels via short, proline-rich Src-homology 3 (SH3) domain binding motifs; in the case of Kv1.5, Src-mediated tyrosine phosphorylation suppresses current (Holmes et al., 1996). The overexpression of Kv1.3 in HEK 293 cells decreases endogenous tyrosine phosphorylation in a manner dependent on Kv1.3 conductance, providing evidence of a role for K^+ channels in Src-mediated signaling (Holmes et al., 1997). The *Drosophila Slowpoke* (dSlo) channel also binds Src, as well as the catalytic subunit of PKA, and both kinases phosphorylate tyrosine residues in dSlo to affect channel localization (Wang et al., 1999). PKA itself frequently associates with channels via A kinase anchoring proteins (AKAPs), which serve as scaffolding for the recruitment of PKA and other enzymes to channel complexes (Wong and Scott, 2004). One AKAP in particular, Yotiao, has been shown to enhance Kv7 current independently of PKA activity, suggesting a critical role for such adaptor proteins in K^+ channel complexes (Kurokawa et al., 2004).

Serine/threonine phosphorylation is another common mechanism of channel regulation. Small-conductance Ca^{2+}-activated K^+ (SK) channels, which mediate the slow afterhyperpolarization of action potentials, are regulated by protein kinase CK2 and protein phosphatase 2A. These bind in a complex with calmodulin (CaM), and alter the Ca^{2+} sensitivity of channel activation by regulating CaM phosphorylation (Bildl et al.,

2004). Another kinase, CaMKII, associates with EAG and enhances current via C-terminal threonine phosphorylation of the channel (Wang et al., 2002c). This EAG/ CaMKII interaction provides a striking example of K^+ channels as signaling complexes, because EAG also regulates the kinase activity of CaMKII (Sun et al., 2004). The consequences of this two-way communication are a central tenet of my thesis, and are examined in detail below.

These studies highlight the fact that K^+ channels can associate with a variety of promiscuous regulatory enzymes, providing a useful mechanism for the regulation of cellular excitability by signaling molecules. However, like Na^+ channels, K^+ channels also have endogenous auxiliary subunits that are critical for proper channel function. I now focus on several examples of K^+ channel β-subunits that have secondary roles, including enzymatic activity and transcription regulation.

One of the first K^+ channel β-subunits to be characterized, *Drosophila* Hyperkinetic (Hk), was identified on the basis of a mutant leg-shaking phenotype similar to that observed for *Shaker* and *eag* mutants (Kaplan and Trout, 1969). When coexpressed with *Shaker* in *Xenopus* oocytes, *Hk* shifted the voltage-dependence of activation and inactivation, and dramatically increased current amplitudes by approximately 2-fold (Chouinard et al., 1995). The mammalian ortholog, Kvβ1, was cloned from the rat nervous system and confers fast inactivation to some variants of the Kv1 family, the corresponding orthologs of *Drosophila* Shaker channels (Rettig et al., 1994). Deletion and substitution analyses showed that this effect occurs via an N-terminal structure that occludes the ion conduction pathway, similar to that seen in Shaker via its own C-terminal ball domain (Hoshi et al., 1990). Mutation of an oxidation-sensing cysteine

residue eliminates the inactivation by Kvβ1, implying that its effects are sensitive to the redox environment of the cytoplasm (Rettig et al., 1994). The x-ray crystal structure of Kvβ1 confirms that the subunit has structural similarities to aldo-keto reductases (AKRs), enzymes that convert aldehydes to alcohols using nicotinamide cofactors (Gulbis et al., 1999). This finding suggests that Kvβ1 can function as an enzyme coupled to the voltage-sensing α-subunit, perhaps modulating excitability in response to changes in redox potential.

Although enzymatic activity has not yet been established for Kvβ1, the structurally similar Kvβ2 has recently been shown to have AKR activity. Intriguingly, the effects of Kvβ2 on Kv1 channel function more closely parallel the effects previously observed for Hk on Shaker channels; UV absorption spectroscopy reveals that Kvβ2 converts bound NADPH to $NADP^+$ when presented with aldehyde substrates (Weng et al., 2006). Kvβ2-mediated oxidation occurs independently of the Kv1 α-subunit, but when expressed with the channel pore, the reaction has been shown to modulate channel current (Weng et al., 2006). These results demonstrate a functional link between channel gating and enzymatic activity mediated by a K^+ channel β-subunit, with the implication that Kv1 channels are modulated as a response to oxidative stress. However, this association also suggests the possibility that channel gating could in turn affect the oxidizing activity of the β-subunit, influencing redox pathways during prolonged depolarization.

Another example of a K^+ channel β-subunit with enzymatic function was discovered in the nematode *Caenorabditis elegans*. MPS-1 was identified in *C. elegans* as an ortholog of mammalian MinK-related peptides (MiRPs), which are β-subunits of the Kv3, Kv7 and Kv11 classes of channels (Kaczmarek, 2006). MPS-1 forms a complex

with the nematode voltage-gated channel KVS-1, and is critical for neuronal activity, because RNA interference of the MPS1 gene results in impaired chemotaxis and locomotion (Bianchi et al., 2003). Initial examination of the MPS-1 amino acid sequence revealed ATP-binding and catalytic domains characteristic of kinases, and radiolabeled ATP assays confirmed that MPS-1 is a serine/threonine kinase that can phosphorylate KVS-1 as well other substrates such as MBP (Cai et al., 2005). Moreover, MPS-1-mediated phosphorylation of KVS-1 modulates the channel by decreasing open channel probability, thereby contributing to inactivation of the whole-cell current in heterologous expression systems. Inactivation or deletion of the catalytic domain of MPS-1 does not completely abolish its effect on KVS-1 current properties, emphasizing its bifunctional role as both a functional kinase and a channel subunit (Cai et al., 2005). To date, MPS-1 is the only MiRP known to have such a role, as none of its mammalian orthologs exhibit kinase activity (Kaczmarek, 2006)

Slowpoke (dSlo), the *Drosophila* ortholog of SK channels, not only associates with Src kinase and the catalytic domain of PKA, but also has at least two β-subunits that modulate its activity. Slowpoke-interacting protein (Slip) was identified in a yeast two-hybrid screen and reduces dSlo current by affecting membrane trafficking of the channel complex (Xia et al., 1998a). The slowpoke-binding protein (Slob), also identified using yeast two-hybrid, increases channel activity (Schopperle et al., 1998) and is a protein kinase. *In vitro*, Slob weakly phosphorylates itself and histone substrates, but this activity is greatly enhanced when the protein is pretreated with the catalytic subunit of PKA (Zeng et al., 2004). Mutation of a candidate serine residue in Slob abolishes the effect, which can be restored by the introduction of a phospho-mimic aspartate residue,

suggesting that PKA phosphorylation regulates Slob kinase activity (Zeng et al., 2004). Slob also recruits the scaffolding protein 14-3-3 to the dSlo complex, which can itself modulate channel function in a manner dependent on the phosphorylation of Slob by CaMKII (Zhou et al., 1999).

This intricate regulation of dSlo activity by its associated proteins obviously speaks to the dynamic regulation of the channel complex *in vivo*. In the *Drosophila* CNS, dSlo modulation may have a role in circadian pathways. Slob expression in photoreceptors and pars intercerebralis (PI) neurons cycles in tandem with circadian-regulated proteins, a pattern not observed in clock gene mutants (Jaramillo et al., 2004). Another clue may come from the adaptor proteins in the dSlo complex. Because 14-3-3 also binds various nuclear signaling proteins, including Raf, a key component of mitogen-activated protein kinase (MAPK) signaling pathways (Fu et al., 1994), it is interesting to consider the potentially central role for the dSlo complex in stimulating these pathways in *Drosophila*. Slob also binds EAG (Schopperle et al., 1998), further suggesting the possibility that β-subunit-regulated phosphorylation is important for EAG/CaMKII-mediated intracellular signaling, discussed below.

A final example of bifunctional K^+ channel β-subunits is the K^+ channel-interacting protein (KChIP) family of proteins. The multifunctional nature of these proteins is hard to deny, as they have been independently discovered three times; first as a Ca^{2+}-binding protein that regulates presenilin, a protein involved in Alzheimer's disease (Buxbaum et al., 1998), then as a Ca^{2+}-mediated transcriptional repressor of nociception genes (Carrion et al., 1999), and finally as a β-subunit of the Kv4 family of K^+ channels (An et al., 2000). Each of the four known KChiP isoforms contains four characteristic EF-hand Ca^{2+}-

binding domains that allow them to serve as Ca^{2+} sensors in several capacities. As Kv4 β-subunits, KChIP1 and KChIP2 increase channel conductance and recovery from inactivation in a manner that depends on the presence of the EF-hand domain (An et al., 2000). KChIP3, also called calsenilin, binds and regulates the activity of presenilin, a component of the transmembrane γ-secretase complex that is implicated in early-onset Alzheimer's disease (Buxbaum et al., 1998). Calsenilin binding to presenilin has several effects, including the reduction of IP3-mediated Ca^{2+} release from intracellular stores, stimulation of apoptosis and the formation of amyloid β plaques (Buxbaum, 2004).

As a transcription factor, KChIP3 binds to downstream regulatory element (DRE) sequences to repress the transcription of various genes, including the human prodynorphin gene involved in memory acquisition and pain, and the early response gene *c-fos* (Carrion et al., 1999). The transcription repression function of KChIP3, also called DRE-agonist modulator (DREAM), is relieved after binding of Ca^{2+} to the EF hands, which disrupts binding to the DRE (Buxbaum, 2004). A similar role in transcriptional control has been found for KChIP2, which along with DREAM regulates proliferation and the expression of IL-2 and interleukin in T-lymphocytes (Savignac et al., 2005). Remarkably, DREAM knockout mice exhibit less sensitivity to pain, as measured by tail-flick and paw withdrawal assays (Cheng et al., 2002), and suggest that DREAM is an integral part of the modulation of pain signaling pathways. It is clear that KChIPs have diverse functions in addition to their role in Kv4 channel modulation. Because Kv4 is the mammalian ortholog of Shal, which regulates HCN channel expression in the lobster STG, it will be of interest to know whether KChIPs or their orthologs are involved in homeostatic compensation mechanisms.

E.3. Calmodulin-mediated channel signaling

While not traditionally considered an auxiliary ion channel subunit, the ubiquitously expressed Ca^{2+} sensor protein calmodulin (CaM) constitutively binds and modulates the functions of several voltage- and ligand-gated ion channels. These include some Ca^{2+}-sensitive K^+ and Na^+ channels, Cav channels, cyclic nucleotide-gated (CNG) channels and N-methyl-D-aspartate (NMDA) glutamate receptors (Levitan, 2006). CaM is a small protein that binds a maximum of four Ca^{2+} ions in two lobe-like pairs of EF-hand domains connected by an α-helix, which give CaM a dumbbell-like shape (Saimi and Kung, 2002). Typically, Ca^{2+} binding causes a conformational shift that opens each lobe, revealing hydrophobic stretches of amino acids that bind and activate target molecules. However, in the absence of Ca^{2+}, CaM can bind certain peptide sequences called isoleucine-glutamine (IQ) motifs, permitting the constitutive binding of CaM to some proteins, including ion channels (Saimi and Kung, 2002). This association allows Ca^{2+}-induced conformational shifts in CaM to modulate channel activity in response to changes in $[Ca^{2+}]_i$. CaM-associated channel complexes may, in turn, be able to influence the downstream activity of Ca^{2+}-mediated signaling pathways such as those mediated by MAPK (Dolmetsch et al., 2001). Here I describe the role of CaM as a regulator of voltage-gated channels, highlighting its ability to link channel activity and intracellular Ca^{2+} signaling.

One role of CaM as a voltage-gated channel regulatory subunit is in the activation of small (SK) and intermediate (IK) conductance Ca^{2+}-activated K^+ channels. SK channels are both voltage- and Ca^{2+}-dependent, and are thus able to modulate the membrane potential in response to changes in Ca^{2+}concentrations, a property that is essential for the

fine-tuning action potentials during the afterhyperpolarization (Hille, 2001). However, it was not initially known whether this sensitivity is conferred by direct binding of Ca^{2+} to the channel α-subunit, as in BK channels, or via another protein. Using yeast two-hybrid analysis and immunoprecipitation experiments, the Adelman group identified CaM as a binding partner of all three SK isoforms (Xia et al., 1998b). Surprisingly, this association is not mediated via the canonical IQ motif, but rather a novel domain consisting of four α-helices; mutations introduced into this region abolish Ca^{2+} gating of the channel. Also, CaM mutants with altered Ca^{2+}-binding affinity shifted the dose-response curves of SK Ca^{2+} gating, demonstrating the integral role of CaM as an SK subunit (Xia et al., 1998b). Subsequent experiments found that CaM regulates IK channels in a similar manner (Fanger et al., 1999).

In light of the phospho-dependent regulation of CaM by protein kinase CK2 and protein phosphatase 2A in SK protein complexes (Bildl et al., 2004), it is clear that CaM plays a pivotal role in SK activity. However, this role is not limited to functional modulation - CaM also affects SK assembly and trafficking. In SK4-transfected CHO cells, overexpression of a peptide containing the CaM-binding domain decreases the pool of CaM available to bind channels and prevents SK4 membrane expression (Joiner et al., 2001). This redistribution results in decreased whole-cell current, an effect that can be rescued by overexpression of CaM. Moreover, immunoprecipitation experiments showed that SK4 multimerization is regulated by the presence of CaM, implying that CaM-mediated subunit assembly may underlie the effects on channel trafficking (Joiner et al., 2001).

CaM also plays a fundamental role in the Ca^{2+}-dependent inactivation of Cav1 (L-type) Ca^{2+} channels. Initially, researchers believed that this type of inactivation was a result of Ca^{2+} itself, in part because the lack of perturbation by Ca^{2+} chelators suggests the site of inactivation is very close to the pore, and also due to the presence of a putative EF-hand motif on the α_{1C} pore-forming subunit (Levitan, 1999). However, several groups have since confirmed that CaM activity underlies inactivation of these channels, offering a model in which CaM is constitutively bound to the α_{1C} subunit via an IQ motif and influences gating via Ca^{2+}-mediated conformational shifts (Peterson et al., 1999; Pitt et al., 2001; Qin et al., 1999). CaM has also been reported to contribute to frequency-dependent facilitation of L-type Ca^{2+}current, suggesting that it exerts both positive and negative effects on Ca^{2+} channel gating (Zuhlke et al., 1999).

In addition to mediating Ca^{2+}-dependent inactivation, the association of CaM with Cav1 channels also appears to be able to stimulate transcription via Ca^{2+}-dependent signaling pathways. Evidence for this type of signaling was found by the Tsien group, who discovered that a brief burst of stimulation applied to hippocampal CA3/CA1 neurons causes nuclear translocation of CaM and the phosphorylation of cAMP response element-binding protein (CREB) (Deisseroth et al., 1998). This effect is specific to the activation of Cav1 channels, because antagonists of other voltage-gated Ca^{2+} channels have no effect on CaM mobilization or CREB activation. Subsequent experiments showed that the activation of CREB by Cav1 stimulates the transcription of a CRE-activated reporter gene, and that signaling is mediated via the activation of Ras and MAPK pathways (Dolmetsch et al., 2001). Furthermore, signaling requires the functional association of CaM with the Cav1 IQ motif, because mutation of this domain

or of CaM disrupts MAPK activation (Dolmetsch et al., 2001). These results imply that Ras/MAPK activators interact with the channel complex, where they are directly or indirectly stimulated by CaM in response to channel activation.

Lastly, it should be noted that CaM is crucial for other forms of channel-mediated signaling due to its role as an activator of the multifunctional Ca^{2+}/CaM-dependent protein kinase II (CaMKII). CaMKII activity is central to many Ca^{2+} signaling pathways, and is thus an essential component of numerous cellular functions, including carbohydrate and fatty acid metabolism, muscle contraction, neurotransmitter release and synaptic plasticity, among others (Braun and Schulman, 1995). As mentioned above, CaMKII also binds and phosphorylates EAG, which increases current in the presence of Ca^{2+}-bound CaM. Once Ca^{2+} levels decline, EAG-bound CaMKII retains catalytic activity (Sun et al., 2004). In addition, CaM can bind directly to the C-terminus of both *Drosophila* and mammalian EAG and inhibits channel activity in response to increases in $[Ca^{2+}]_i$ (Schonherr et al., 2000; Stansfeld et al., 1996). My results, discussed below and detailed in the following chapters, show that the interaction of EAG and CaMKII stimulates intracellular signaling pathways in response to fluctuations in the membrane potential. Taken together, these studies suggest that CaM is not only a dynamic regulator of ion channel activity, but also plays key roles in channel-mediated signaling to the nucleus.

E.4. Proteolysis of channels and subunits

To conclude my overview of multifunctional ion channel subunits, I now turn to one other mechanism by which channels and their associated proteins have been shown to

influence cellular functions: the proteolytic cleavage of intracellular domains to yield free cytoplasmic peptides. This type of regulation is well-characterized for the Notch/Delta signaling pathway during development. In that case, the binding of Delta ligand to Notch membrane receptors stimulates proteolytic cleavage of the Notch intracellular domain (NICD), which translocates to the nucleus and converts certain transcriptional repressors to activators, initiating the expression of developmental genes (Mumm and Kopan, 2000). Some ion channel proteins, including Cav1 channels, TRPP channels and Na^+ channel β-subunits, undergo proteolysis to generate signaling molecules. Here I will discuss the regulated cleavage of these proteins, which may underlie their ability to function outside their normal roles as ion channels or subunits.

As described above, Na^+ channel β-subunits can function as cell adhesion molecules, in addition to their role in channel modulation (McEwen and Isom, 2004). The β-subunits are also substrates for presenilin/γ-secretases, enzymes that contribute to the formation of amyloid β plaques in Alzheimer's disease via the sequential cleavage of β-amyloid precursor protein (APP) (Wong et al., 2005). Each β-subunit isoform has amino acid sequences similar to APP that allows them to undergo a comparable series of proteolytic events. In cortical neurons, the extracellular N-terminus of β2 is removed first by α-secretase, leaving only the short intracellular C-terminal region, which is then cleaved by γ-secretase to yield a free peptide of about 10 kD (Kim et al., 2005). This peptide has recently been shown to stimulate transcription and expression of Nav1.1, leading to increased surface expression in neuroblastoma cells (Kim et al., 2007). However, in transgenic mice overexpressing γ-secretase to mimic Alzheimer's, increased β2 cleavage decreases the overall channel surface expression and Na^+ current density in

neuroblastoma and hippocampal neurons. This finding is consistent with the altered Nav1 levels in human Alzheimers' patients, and suggests a mechanism by which membrane excitability may be regulated by proteolytic events (Kim et al., 2007). The inhibition of γ-secretase also inhibits cell adhesion and migration in several motility assays, implying that proteolysis is also important for cellular functions requiring β-subunits, such as neurite outgrowth (Davis et al., 2004).

TRPP and Cav1 channels also undergo proteolysis to yield molecules with signaling abilities. TRPP channels, as discussed above, are expressed in renal tubules, where they may function as ciliary mechanosensors (Huang, 2004). One study suggests that proteolysis of these channels influences intracellular signaling pathways. In kidney epithelial cells of mice overexpressing full length TRPP1, a C-terminal fragment is cleaved and accumulates in the nucleus, as observed with fluorescent tissue labeling and western blots of nuclear fractions (Chauvet et al., 2004). When TRPP1 is heterologously expressed in CHO cells, nuclear translocation corresponds to increased activation of the AP-1 and JNK signaling pathways, an effect that is eliminated when a putative nuclear localization signal (NLS) in the TRPP1 C-terminus is mutated. Moreover, the signaling activity of the TRPP1 fragment is regulated by the pore-forming TRPP2 subunit, because nuclear translocation and AP-1 signal activation are prevented when both subunits are coexpressed in CHO cells, and TRPP2 knockout mice exhibit higher nuclear TPP1 staining than wild type mice (Chauvet et al., 2004). These results implicate a dynamic interaction between TRPP subunits in the regulation of the AP-1 and JNK pathways, although the physiological role of this signaling remains to be clarified. However, because these channels have also been implicated in cell cycle regulation and

differentiation (Bhunia et al., 2002; Grimm et al., 2006), it is possible that those effects are a result of proteolysis-mediated signaling via TRPP1.

Lastly, Cav1 channels have been shown to undergo intracellular C-terminal cleavage to generate fragments with multiple effects. In hippocampal neurons, Hell and colleagues showed that postsynaptic Ca^{2+} channels are converted to a shorter form by calpain following the stimulation of NMDA receptors (Hell et al., 1996). This result confirmed previous reports that truncation of these channels increases conductance (Wei et al., 1994), and supports a role for proteolytic cleavage in the enhancement of postsynaptic Ca^{2+} current during neuronal activity. Subsequent studies of Cav1.1, which is expressed in skeletal muscle, used mass spectroscopy and deletion analysis to identify the site of proteolytic cleavage in the C-terminus and showed that the fragment remains bound to the channel complex as a scaffolding protein (Hulme et al., 2005). The cleaved C-terminal peptide helps to form the leucine zipper motif that targets PKA to the channel via AKAP15, contributing to the enhancement of current by PKA phosphorylation (Hulme et al., 2002).

In addition to regulating channel function, the proteolysis of L-type Ca^{2+} channels has recently been shown to yield a transcription factor (Gomez-Ospina et al., 2006). The Dolmetsch group found that a fluorescently labeled C-terminal fragment of Cav1.2 is enriched in the nucleus of cortical neurons. The nuclear expression of this Ca^{2+} channel-associated transcription regulator (CCAT) is regulated by changes in Ca^{2+}; chelation of extracellular Ca^{2+} increases nuclear CCAT labeling, while the stimulation of Cav1.2 channel activity using KCl or glutamate has the opposite effect (Gomez-Ospina et al., 2006). In coimmunoprecipitation experiments, CCAT interacts with the nuclear protein

p54(nrb)/NonO, which regulates transcription and RNA splicing. Interaction between the proteins induces the expression of a luciferase reporter gene. Moreover, microarray analysis show that CCAT-mediated transcription affects the expression of many endogenous genes, including gap junction proteins, axon guidance factors, K^+ and TRP channels, glutamate receptors, several kinases, and a host of other proteins involved in neuronal function (Gomez-Ospina et al., 2006). Clearly, CCAT provides an important mechanism for coupling Ca^{2+} channel activity to protein expression and may contribute to neuronal homeostasis or plasticity. Although Cav1.2 conductance is technically required for CCAT activation, CCAT itself, rather than Ca^{2+} influx, regulates transcription.

F. THE EAG POTASSIUM CHANNEL

To this point, I have reviewed many examples of ion channels that function beyond their classic role as arbitrators of membrane excitability, including channels that affect cell cycle regulation, channels with specific ion-independent functions, and channel-associated proteins that contribute to nontraditional channel activity. I now focus on EAG, a multifunctional K^+ channel that encompasses all of these properties. As described above, EAG contributes to oncogenesis and cell cycle progression (Pardo et al., 1999), and also binds and locally activates CaMKII (Sun et al., 2004). The central focus of this thesis is that EAG activates intracellular signaling pathways via voltage-dependent regulation of CaMKII activity, and that this function is independent of ion flux. Here, I provide a general background of the EAG channel, including discussions of its electro-

physiological properties, topology and amino acid sequence, associated proteins, and putative role *in vivo*.

F.1. Characterization and physiological significance

The *Drosophila* Ether à-go-go (EAG) K^+ channel is the founding member of a superfamily of K^+ channels related to both voltage-gated and cyclic nucleotide-gated K^+ channels (Ganetzky et al., 1999). The *eag* gene was originally discovered in *Drosophila* mutants that exhibit leg-shaking behavior under ether anesthesia (Kaplan and Trout, 1969), but its identity as an ion channel gene was not appreciated until later studies that found an enhancement of neurotransmission defects in *eag/Shaker* double mutants when compared to either individual mutation (Ganetzky and Wu, 1983). Motivated by these phenotypes, the EAG polypeptide was cloned using chromosomal analysis (Drysdale et al., 1991; Warmke et al., 1991) and soon thereafter, an *eag* homology screen identified a family of highly conserved genes in several invertebrate and mammalian species, which could be separated into three subfamilies: *eag*, *eag*-related gene (*erg*), and *eag*-like K^+ channel (*elk*). The amino acid sequences encoded by these genes contain the characteristic transmembrane, pore-forming and voltage sensing domains found in Shaker-like voltage-gated channels, as well as a cyclic nucleotide-binding domain similar to that of CNG channels (Warmke and Ganetzky, 1994). Interestingly, sequence comparison suggests that the EAG family of channels is more closely related to CNG channels than voltage-gated K^+ channels (Guy et al., 1991), and consequently they are now considered part of the same phylogenetic branch of channel evolution (Yu and Catterall, 2004).

In addition to leg shaking behavior, *Drosophila eag* mutants display hyperexcitability in recordings from the larval neuromuscular junction (NMJ). This is characterized by both a high degree of spontaneous action potential firing from the motor neuron and broadened spontaneous and evoked excitatory junctional potentials (EJPs) in the body wall muscle fibers (Ganetzky and Wu, 1985). Both of these defects have been attributed to increases in excitability, and consequently neurotransmitter release, in the motor neurons in the absence of the hyperpolarizing influence of EAG. In contrast, *Shaker* mutants also exhibit repetitive neuron firing, but only do so in response to motor neuron stimulation (Ganetzky and Wu, 1985). Finally, in the absence of EAG, several K^+ currents in muscle are also down-regulated (Wu et al., 1983). However, this effect appears to be an indirect, activity-dependent regulation of the expression of multiple K^+ channels in muscle, given that EAG protein is undectable in wild type muscle fibers (Sun et al., 2004; Wang et al., 2002c). The physiological role of this down-regulation remains unclear.

Consistent with its role in neuronal excitability in *Drosophila*, EAG is expressed throughout the fly neuropil and optic lobes, and is present in the axon and terminals of motor neurons innervating body wall muscle (Sun et al., 2004; Wang et al., 2002c). Importantly, in the larval ventral ganglion, the distribution of EAG overlaps with that of synaptobrevin, a marker for pre-synaptic terminals. In mammals, EAG is widely expressed in the nervous system, including the CA1 and CA3 regions of the hippocampus, neocortex, olfactory bulb, retinal ganglion, photoreceptors, cochlear spiral ligament, and skeletal muscle (Frings et al., 1998; Lecain et al., 1999; Ludwig et al., 1994; Occhiodoro et al., 1998). As discussed above, EAG is also expressed in several

cancer cell lines, including human neuroblastoma and melanoma cells (Meyer and Heinemann, 1998; Meyer et al., 1999).

The presence of EAG throughout the sensory and motor systems suggests that it may be important for behavior. In fact, adult *eag* mutant flies display a number of behavioral phenotypes, which include defects in olfactory discrimination (Dubin et al., 1998), locomotion (Wang et al., 2002b) and habituation of the giant fiber escape pathway (Engel and Wu, 1998). Moreover, *eag* mutants have impaired associative learning in courtship conditioning assays (Griffith et al., 1994). In these experiments, male flies are paired with previously mated females, which are unresponsive to male courtship behavior. Wild type males quickly respond to these cues by decreasing courtship, whereas *eag* flies exhibit an overall increase in courtship over the same period, indicating that learning is disrupted (Griffith et al., 1994). This deficiency is very similar to that seen in flies overexpressing *ala*, a peptide corresponding to the CaMKII autoinhibitory domain. Because larvae expressing *ala* exhibit an increase in EJP frequency that is similar to *eag* mutants, and double mutants do not have an additive effect, EAG and CaMKII are likely to be part of a common pathway mediating synaptic plasticity and homeostasis (Griffith et al., 1994).

F.2. Electrophysiological properties

The heterologous expression of *Drosophila* EAG (dEAG) in *Xenopus* oocytes results in a voltage-dependent outward K^+ current that activates between -40 and -50 mV and increases with depolarizing voltage steps (Robertson et al., 1996; Wilson et al., 1998). Both dEAG and mammalian EAG (mEAG) isoforms exhibit relatively slow activation

and partial inactivation, although this inactivation is much less pronounced than in Shaker channels. Despite the presence of the cyclic nucleotide-binding domain, application of cAMP or cGMP has no effect on EAG gating, and unlike CNG channels, EAG shows a much higher selectivity for K^+ over Na^+ ions (Robertson et al., 1996). Given the absence of specifically pharmacological blockers of the EAG channel, the most distinctive electrophysiological indicator of the presence of EAG channels in native tissues (Bauer and Schwarz, 2001) is a phenomenon reminiscent of the Cole-Moore shift first described for K^+ currents of the squid giant axon (Cole and Moore, 1960; Ludwig et al., 1994). Specifically, the Cole-Moore effect is characterized by increasingly delayed activation kinetics in response to increasingly hyperpolarized prepulse potentials, and is enhanced by increasing extracellular concentrations of Mg^{2+} or H^+ (Terlau et al., 1996). Recent studies have identified the Mg^{2+} binding site in the S3-S4 linker region, and suggest that modulation is due to the stabilization of a closed channel state that results in slower transitions to open states in the presence of Mg^{2+} (Schonherr et al., 2002; Tang et al., 2000). Pharmacologically, EAG is sensitive to Ba^{2+} and quinidine (Ludwig et al., 1994), and although specific EAG blockers have remained elusive, the tricyclic antidepressants imipramine and astemizole have been shown to selectively inhibit human EAG channels by binding the intracellular side of the channel pore (Garcia-Ferreiro et al., 2004). In addition, human EAG (hEAG) current in both heterologous and native tissue can be blocked by increases in intracellular Ca^{2+} concentrations (Meyer et al., 1999; Stansfeld et al., 1996), due to a C-terminal interaction between hEAG and Ca^{2+}-bound CaM, discussed below (Schonherr et al., 2000).

In heterologous expression systems, EAG also has been shown to interact with the K^+ channel β-subunit, Hyperkinetic (Hk) (Wilson et al., 1998). Hk coimmunoprecipitates with EAG, and produces an increase in amplitude and activation kinetics of EAG current when coexpressed in oocytes. Hk also enhances mEAG and hERG currents, as well as those of Shaker (Chouinard et al., 1995) suggesting a promiscuous role for Hk in the modulation of different K^+ channels. It should be noted, however, that the interaction of Hk with EAG family members has yet to be established for channels *in vivo*. As discussed above, Hk has sequence similarity to aldo-keto reductases (Chouinard et al., 1995).

In contrast to EAG, ERG only exhibits small outward current upon depolarization, yet produces large tail currents when repolarized to negative potentials (Trudeau et al., 1995). This is the result of an inactivation mechanism that is more rapid than activation, which confers inward rectification properties on ERG (Schonherr and Heinemann, 1996; Smith and Yellen, 2002). The resulting inverse current (compared to outward rectifiers) has important implications for ERG in cardiac tissue, where it functions alongside HCN pacemaker channels to regulate rhythmic contractions (Trudeau et al., 1995). Indeed, mutations in human ERG have been well-characterized as contributing to long Q-T syndrome in humans (Curran et al., 1995). The current properties of ELK channels are less well-characterized but seem to depend on the isoform expressed: ELK1 channels, which are expressed throughout the human nervous system, are EAG-like but do not exhibit the Cole-Moore shift (Engeland et al., 1998; Zou et al., 2003). ELK2 appears to be intermediate of EAG and ERG, producing large outward currents that then rapidly inactivate (Trudeau et al., 1999). This fast inactivation mechanism is similar to that of

ERG, but shifted to more positive potentials, accounting for the delayed inactivation upon depolarization (Engeland et al., 1998).

F.3. Topology and amino acid sequence

The complete amino acid sequence of *Drosophila* EAG is presented in Figure 1.1, and highlights structural domains, putative sites of protein-protein interaction, and specific residues mutated for experiments throughout this thesis. Each EAG subunit contains 1174 amino acids that form six transmembrane helices (S1-S6) with intracellular N- and C- termini. A series of positively charged residues in S4 constitute the voltage sensor, and an additional hydrophobic domain between S5 and S6 contains the signature GFG motif that forms the K^+ selectivity filter. Using the crystallized KcsA structure as a model, four EAG subunits are thought to coassemble into a tetrameric protein that is able to selectively pass K^+ ions through a central, water-filled pore (Doyle et al., 1998).

In its N-terminus, EAG contains a stretch of amino acids that form a PER-ARNT-SIM (PAS) dimerization domain. This domain is particularly unusual for an ion channel, because nearly all eukaryote proteins that contain a PAS domain are transcription factors that reside within the nucleus or shuttle between the nucleus and cytoplasm (Crews and Fan, 1999). PAS domains are usually found in proteins that act as internal sensors of light, hypoxia, and redox potential, such as the *Drosophila* circadian protein Period (Taylor and Zhulin, 1999). In the case of Period, this domain facilitates dimerization with Timeless, another PAS-containing circadian protein. This association reveals a nuclear localization signal (NLS) in the Per/Tim complex that allows it to directly downregulate transcription of both proteins (Scully and Kay, 2000). It is yet to be

FIGURE 1.1

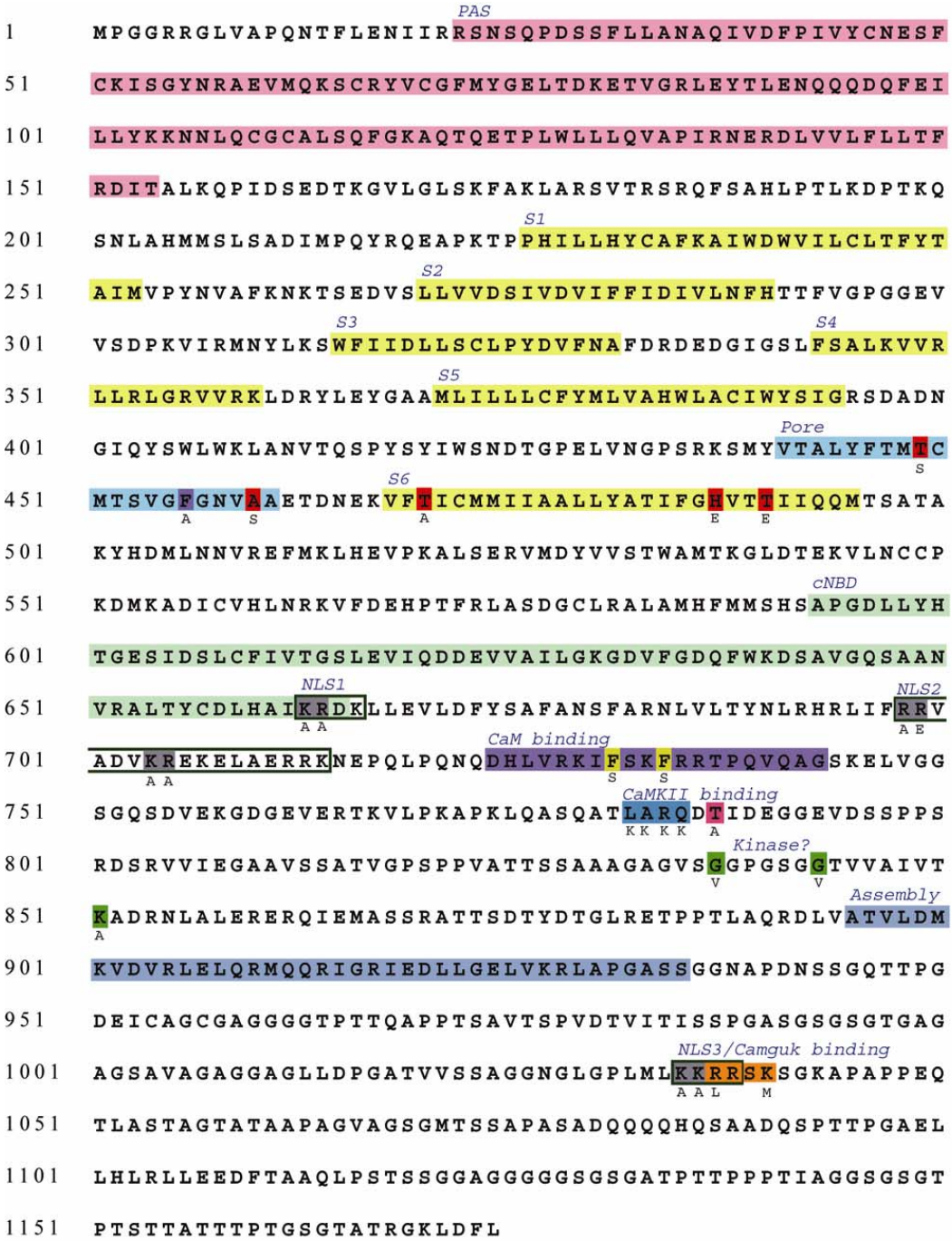

Figure 1.1: *Drosophila* EAG amino acid sequence. Regions of interest are highlighted in color; transmembrane domains are indicated in yellow. Putative nuclear localization signals are boxed. Point mutations used throughout this thesis are specified below the respective amino acids.

determined whether the EAG PAS domain is functional, although it is conserved throughout the EAG family of K^+ channels (Bauer and Schwarz, 2001) and has been suggested to operate as an oxygen sensor in both EAG and hERG (Crociani et al., 2003; Morais Cabral et al., 1998).

The EAG intracellular C-terminus is nearly twice as long as those of K^+ channels of the *Shaker* superfamily, and contains many putative protein interaction domains. In addition to the cyclic nucleotide-binding domain, the C-terminus includes a region with high similarity to the autoinhibitory domain of CaMKII, a CaM binding domain, three putative nuclear localization (NLS) signals, a Src-Homology 3 (SH3) motif, and at least two potential PKA phosphorylation sites. Additionally, there is a stretch of glycine residues with similarity to the conserved ATP-binding and catalytic domains of known kinases (Hanks et al., 1988). Our lab and others have performed site-directed mutagenesis on key residues within these sites as a preliminary test of their functionality. As discussed below, EAG associates with CaM and CaMKII, as well as with the membrane-associated guanylate kinase (MAGUK) adapter protein Camguk (CMG), which binds to a novel SH3 motif. I have also created and tested several point mutations in most of these domains for possible involvement in EAG-mediated signaling. These experiments are described in detail in chapter III of this thesis.

F.4. The EAG protein complex

EAG current is regulated via independent associations with CaM and CaMKII, which have opposing effects on channel function: Ca^{2+}/CaM binding acutely decreases EAG current, most likely by shifting the voltage-dependence of activation to more positive

potentials (Schonherr et al., 2000) while phosphorylation by CaMKII enhances current by increasing the surface expression of EAG channels (Schonherr et al., 2000; Wang et al., 2002c). The rivaling modulatory effects of these proteins suggests that the relationship between intracellular Ca^{2+} and EAG function is finely tuned. Here I discuss the interactions between EAG, CaM, CaMKII, and CMG, which together form a protein complex that may be capable of two-way communication between membrane excitability and Ca^{2+} signaling pathways.

As mentioned above, hEAG current is inhibited by increases in intracellular Ca^{2+}, reaching half-maximal inhibition at approximately 100 nM (Stansfeld et al., 1996). In *Xenopus* oocytes expressing hEAG, current is inhibited when inside-out patches are excised into a bath solution containing ~200 nM free Ca^{2+}, but can restored by exposure to an EGTA-buffered Ca^{2+}-free solution. However, if the same patch is reintroduced to high [Ca^{2+}], inhibition is not observed, suggesting that the loss of a cytosolic factor regulates the effect. Indeed, if the patch is again exposed to the oocyte cytoplasm, Ca^{2+} inhibition is restored (Schonherr et al., 2000). These experiments were the first indication that a cytoplasmic protein such as CaM might be mediating the Ca^{2+} inhibition of hEAG. When excised patches washed in Ca^{2+}-free solution are exposed to recombinant CaM protein, the Ca^{2+} sensitivity of hEAG current is reestablished, confirming that the inhibition is mediated by CaM (Schonherr et al., 2000).

In vitro binding assays identify a 20 residue CaM-binding domain in the hEAG C-terminus (Schonherr et al., 2000). This domain, which putatively forms an amphipathic helix, is conserved in all EAG channels, suggesting that Ca^{2+}/CaM also inhibits *Drosophila* EAG current. Experiments in our lab confirm this hypothesis (Marble et al.,

in preperation). It is interesting to point out that CaM inhibits EAG while at the same time activating Ca^{2+}-regulated K^+ channels, which can be expressed in the same cells (Meyer et al., 1999). The explanation may lie in the stoichiometry of CaM binding; in EAG, the association of one CaM molecule per channel appears sufficient for inhibition (Schonherr et al., 2000), while SK channels may require four Ca^{2+}-bound CaMs for activation (Keen et al., 1999). This difference might establish a $[Ca^{2+}]_i$ threshold below which EAG channels are active, but above which EAG is inactivated and SK channel activity is stimulated.

CaM also regulates EAG indirectly via CaMKII, which binds to EAG via a C-terminal region with homology to its own autoinhibitory domain (Sun et al., 2004) and enhances current by phosphorylating the channel at a key threonine residue (Wang et al., 2002c). As described above, the inhibition of CaMKII in *Drosophila* larvae produces supernumerary EJPs at the NMJ similar to those of *eag* mutants, and both mutants exhibit deficiencies in associative learning assays (Griffith et al., 1994). These findings provided early evidence that CaMKII and EAG share a common pathway regulating synaptic function and plasticity. Subsequent studies using radiolabeled ATP show that EAG is a CaMKII substrate, and that CaMKII phosphorylates the EAG C-terminus at threonine 787 (Wang et al., 2002c). In oocyte recordings, mutation of this residue prevents the inhibition of EAG current by the ala peptide, indicating that T787 is necessary for endogenous CaMKII-mediated increases in EAG current. Subsequent biotinylation assays indicate that phosphorylation increases currents primarily by increasing the number of channels in the plasma membrane (Wang et al., 2002c) and suggest that, in contrast to the effect of CaM binding, which is readily reversible, the effects of CaMKII

on EAG current may be more long-term. Moreover, the independent binding of CaM to EAG does not appear to prevent or enhance phosphorylation at T787 (Marble et al., in preperation). *In vivo*, CaMKII phosphorylation of EAG is observed at the NMJ using phospho-specific antibodies, and can be enhanced by driving the neuronal expression of a constitutively active form of the kinase (Wang et al., 2002c). Together these results show that CaMKII phosphorylation of EAG at T787 enhances current, and suggests that CaMKII regulates EAG function at synaptic terminals.

Coimmunoprecipitation assays from *Drosophila* heads confirm that CaMKII associates with EAG in native tissue, and *in vitro* binding assays show that this occurs via the region of the EAG C-terminus (K_{773}-V_{794}) with homology to the regulatory domain of CaMKII (Sun et al., 2004). Initial CaMKII binding depends on the presence of Ca^{2+}/CaM and therefore the kinase must be activated to associate with EAG. However, sustained binding is Ca^{2+}/CaM-independent, because CaMKII remains associated after EGTA washes, which strip CaM from the complex (Sun et al., 2004). Recent studies in our lab have shown that EAG also associates with the MAGUK adapter protein Camguk (CMG), which is the *Drosophila* ortholog of mammalian CASK and nematode LIN-2 (Marble et al., 2005). When coexpressed in oocytes, CMG can increase EAG current and whole-cell conductance by as much as three-fold, and this effect requires the integrity of the T787 phosphorylation site (see Appendix, Fig A.1). Biotinylation experiments show that, as with the effect of phosphorylation, the enhancement of EAG current is accounted for by an increase in channel surface expression (Fig A.2). Indeed, CMG coexpression increases T787 phosphorylation and surface expression of EAG above the levels observed in the absence of the adaptor protein. This suggests that CMG enhances or

stabilizes the interaction between EAG and CaMKII (Marble et al., 2005). *In vitro* binding assays show that CMG binds to a novel SH3 domain on the EAG C-terminus (Fig A.5). Mutation of this domain prevents the enhancement of current and, in addition, prevents the ability of EAG to recruit CMG to the membrane when heterologously expressed in COS-7 cells (Fig A.6).

F.5. CaMKII activity is regulated by EAG

The association of EAG with CaMKII and CMG can not only regulate EAG current, but also the activity of CaMKII. EAG-bound CaMKII retains catalytic activity, because it can still phosphorylate EAG and other substrates after Ca^{2+}/CaM is removed (Sun et al., 2004). This activity, which is approximately 5-10% of maximum Ca^{2+}-stimulated activity, is independent of CaMKII autophosphorylation, suggesting that the physical association with EAG puts CaMKII into a catalytically active conformation (Sun et al., 2004). Thus, EAG-bound CaMKII remains locally active even after $[Ca^{2+}]_i$ declines, providing a novel mechanism by which the kinase can function in a Ca^{2+}-independent manner.

The interaction between CMG and CaMKII also regulates CaMKII activity, even in the absence of EAG. CMG can activate CaMKII in the presence of Ca^{2+}/CaM (Lu et al., 2003). However, in contrast to the effect of EAG on kinase activity, when Ca^{2+}/CaM is removed, CMG promotes autophosphorylation-mediated CaMKII inactivation, resulting in a cytoplasmic pool of inactive kinase. Although this inactivation may seems contradictory to the increases in EAG current mediated by CaMKII and CMG, it is possible that the role of CMG is to associate active CaMKII with EAG, creating a local

membrane compartment in which the EAG-kinase can remain active even when a decline in cytoplasmic Ca^{2+}/CaM inactivates the remaining pool of CaMKII. Alternatively, the association with EAG may prevent inactivation of kinase by preventing its release from the complex. Either way, the protein complex has the potential of operating as a positive feedback loop: increased phosphorylation and surface expression of EAG would be predicted to recruit more CaMKII and CMG to the plasma membrane, which should further increase channel phosphorylation and surface expression. These effects may extend to other, as yet uncharacterized, members of the protein complex as well as other targets of CaMKII.

G. EAG REGULATES INTRACELLULAR SIGNALING PATHWAYS

In summary, substantial evidence exists to show that ion channels can have cellular functions that are independent of the regulation of ion flux. Several lines of evidence suggest that the EAG K^+ channel is able to affect the activity of intracellular signaling pathways. First, as discussed above, the association between EAG and CaMKII can result in constituitively active kinase. In addition, hEAG has been implicated in cell cycle regulation and cancer: hEAG can induce oncogenic transformation of NIH 3T3 and CHO cells, is present in certain human cancer cell lines (but absent in the corresponding healthy tissues) and favors tumor progression when EAG-expressing cells are implanted into immune-suppressed mice (Pardo et al., 1999). My results also suggest that EAG channels have a direct role in intracellular signal transduction. Specifically, when examining NIH 3T3 fibroblasts using 5-bromo-2'-deoxyuridine (BrdU), a fluorescent indicator of cell proliferation, transfection of wild type *eag* results in a dramatic increase

in the percentage of BrdU-labeled cells compared to that observed for vector-transfected controls. Similar results are obtained using manual cell counts, suggesting that the increased incorporation of BrdU indeed reflects an increase in proliferation. This effect is specific to EAG, because overexpression of Shaker does not significantly increase BrdU labeling compared to control cells. The stimulation of proliferation by EAG is consistent with studies implicating a role for hEAG in cell cycle regulation (Pardo, 2004).

Previous studies have reported that K^+ channels are able to indirectly influence intracellular signaling by changing the membrane potential, thereby controlling Ca^{2+} influx through voltage-dependent Ca^{2+} channels (Lewis and Cahalan, 1995). In turn, Ca^{2+} influx through Ca^{2+} channels can stimulate several intracellular pathways. For example, L-type Ca^{2+} channel activity has been linked to Ras activation and leads to sustained MAPK activation (Rosen et al., 1994), the subequent phosphorylation of CREB, and eventual expression of immediate early genes, including *c-fos* (Sheng et al., 1990), which respond to environmental stimuli to direct cell growth and differentiation. Similarly, both K^+ and Ca^{2+} channels are required for lymphocyte activation (Lewis and Cahalan, 1995). However, the extracellular application of EGTA, a Ca^{2+} chelator, does not significantly affect EAG-stimulated proliferation. My experiments provide evidence that EAG signaling is wholly independent of ion flux, and activated directly by the channel itself.

Transfection of NIH 3T3 cells with EAG-F456A, a non-conducting EAG channel containing a point mutation in its selectivity filter, produces an increase in proliferation that is statistically indistinguishable from that observed in wild type-transfected cells. In addition, a myc-epitope tagged EAG, which fails to conduct K^+ for reasons as yet

unclear, produces an increase in proliferation that is similar in magnitude to that observed for wild type and EAG-F456A channels. Therefore, the ability of EAG to stimulate NIH 3T3 proliferation is independent of channel conductance.

Given that the signaling activity of EAG does not depend on the conduction of K^+ ions, one would predict that changes in extracellular K^+ concentrations ($[K^+]_o$) would have no effect on EAG-induced proliferation. In preliminary experiments, the proliferation of *eag*-transfected cells, and thus activation of intracellular signaling, was highest in low $[K^+]_o$, when V_m is most hyperpolarized. The response to $[K^+]_o$ was bimodal: moderate $[K^+]_o$ inhibited EAG-induced proliferation, while further increases in $[K^+]_o$ increased proliferation in both vector and *eag*-transfected cells. Consideration of these results led to the hypothesis that the conformational shift of EAG produced by the change in V_m regulates EAG signaling activity. One goal of this thesis was to determine if the voltage sensor of EAG constitutes a switch for signal activation. Experiments characterizing the voltage-dependence of EAG signaling are detailed in chapter II.

Although my results indicate that EAG stimulates the downstream activation of signaling pathways, it is unclear what domain of EAG is responsible for mediating the effect. As noted above, EAG has unusually long intracellular regions containing several domains important for protein-protein interactions, transcription regulation, and kinase activation. The CaMKII-like autoinhibitory domain of EAG is the most promising region for EAG-mediated signal activation, because it has been shown to directly bind CaMKII, causing the kinase to remain active even at basal Ca^{2+} levels (Lu et al., 2003). In the absence of EAG, disruption of constituitive kinase activity could account for, or at least contribute to, the similarity in the electrophysiological and learning defects observed in

eag mutants and *ala* transgenics (Griffith et al., 1994). CaMKII has been shown to be an essential component of synaptic plasticity and learning in every organism examined (Griffith et al., 1993; Mayford et al., 1996; Nakanishi et al., 1997; Silva et al., 1992a,b; Vianna et al., 2000). A second aim of this thesis was to characterize the mechanism by which EAG mediates signaling. Experiments to investigate the EAG signaling domain are presented in chapter III.

A final goal of this thesis was to determine the function of EAG-mediated signaling *in vivo*. Synaptic function and learning are obvious functions likely to be regulated by EAG, because *eag* mutants are impaired in these areas, and also because proliferation, neuronal plasticity and learning share common signaling mechanisms, such as the MAPK pathway (Morozov et al., 2003). Chapter III describes experiments using *Drosophila* transgenics that investigate the contributions of EAG signaling to known *eag* phenotypes.

CHAPTER II

A VOLTAGE-DRIVEN SWITCH FOR ION-INDEPENDENT SIGNALING BY ETHER À GO-GO K^+ CHANNELS

A. ABSTRACT

Voltage-gated channels maintain cellular resting potentials and generate neuronal action potentials by regulating ion flux. Here, we show that Ether à go-go (EAG) K^+ channels also regulate intracellular signaling pathways by a mechanism that is independent of ion flux and depends on the position of the voltage sensor. Regulation of intracellular signaling was initially inferred from changes in proliferation. Specifically, transfection of NIH 3T3 fibroblasts or C2C12 myoblasts with either wild type or non-conducting (F456A) *eag* resulted in dramatic increases in cell density and BrdU incorporation over vector- and *Shaker*-transfected controls. The effect of EAG was independent of serum and unaffected by changes in extracellular calcium. Inhibitors of p38 mitogen-activated protein (MAP) kinases, but not p44/42 MAP kinases (extracellular signal-regulated kinases), blocked the proliferation induced by non-conducting EAG in serum-free media, and EAG increased p38 MAP kinase activity. Importantly, mutations that increased the proportion of channels in the open state inhibited EAG-induced proliferation, and this effect could not be explained by changes in the surface expression

of EAG. These results indicate that channel conformation is a switch for the signaling activity of EAG and suggest a novel mechanism for linking channel activity to the activity of intracellular messengers, a role that previously has been ascribed only to channels that regulate calcium influx.

B. INTRODUCTION

Voltage-gated ion channels generate neuronal action potentials, the primary units of information transfer in the brain, by regulating ion flux (Hille, 2001). Effects of ion channels on synaptic connectivity, transmitter release, plasticity, and other cellular processes are generally assumed to be a secondary consequence of ion flux. Specifically, changes in membrane potential and action potentials alter Ca^{2+} influx and Ca^{2+} regulates multiple intracellular signaling pathways (Catterall, 2000; Deisseroth et al., 1998; Dineley et al., 2001; Dolmetsch et al., 2001; Hardingham and Bading, 2003; Sutton et al., 1999). Several recent studies, however, have indicated that some voltage-gated ion channels are bifunctional proteins (Dolmetsch et al., 2001; MacLean et al., 2003; Malhotra et al., 2000; Runnels et al., 2001; Wang et al., 1999). These studies show that voltage-gated channels can contribute to transcriptional regulation, protein scaffolding, cell adhesion, and intracellular signaling, and the effects appear largely independent of ion conduction.

Recent studies of Ether à go-go (EAG, KCNH1) voltage-dependent K^+ channels suggest that EAG may also be bifunctional. First, a region of *Drosophila* EAG with similarity to the autoinhibitory domain of Ca^{2+}/calmodulin-dependent protein kinase II (CaMKII) can associate with activated, Ca^{2+}/CaM-bound, CaMKII. *In vitro* assays

indicate that once Ca^{2+} levels decline, EAG-bound kinase retains five to ten percent of its maximum Ca^{2+}-stimulated activity (Sun et al., 2004). Second, human EAG has been implicated in cell cycle regulation and cancer: transfection can induce oncogenic transformation, EAG is present in some cancer cell lines but absent in the corresponding healthy tissues, and implanting EAG-expressing cells into immune-suppressed mice results in tumor progression (Farias et al., 2004; Pardo et al., 1999). These studies implicate EAG as a component of one or more intracellular signaling pathways.

Our investigation of the involvement of EAG in intracellular signaling was prompted by experiments in which we observed an increase in NIH 3T3 fibroblast density following transient transfection with *Drosophila eag*. Our findings indicate that conformational changes of EAG associated with the position of the voltage-sensor may be an alternative mechanism, independent of ion flux, by which ion channels can affect intracellular signaling.

C. RESULTS

C.1. Transfection with EAG stimulates proliferation

Figure 2.1A shows a representative experiment demonstrating an increase in NIH 3T3 cell density following transfection with *eag*. Cell density was significantly higher for coverslips transfected with *eag* than for controls transfected with empty vector ($p < 0.01$; similar results obtained for two other experiments). To determine the mechanism underlying this increase, cells were labeled with BrdU, a marker for proliferation. Coverslips transfected with *eag* displayed substantial increases in BrdU incorporation when compared to vector-transfected controls (Fig 2.1B; $p < 0.0001$, $n = 3$). In

FIGURE 2.1

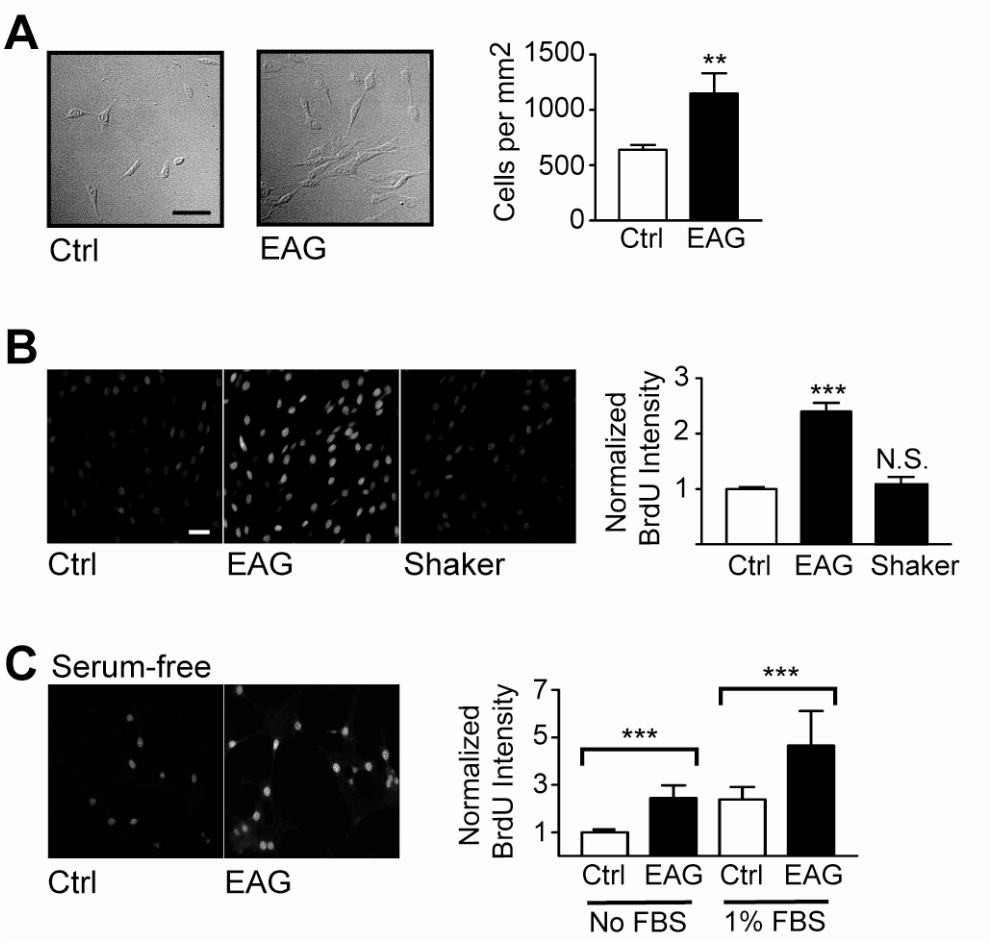

Figure 2.1: EAG stimulates proliferation of NIH 3T3 fibroblasts.
(A) Differential interference contrast microscopy images and cell densities for coverslips transfected with pCS2-*eag* or vector alone. For each condition, cell numbers were averaged across at least 6 visual fields (0.05 mm^2 / field). Similar results were documented for two additional experiments. **(B)** *Left*, representative scans showing BrdU labeling of cells transfected as indicated. BrdU labeling was detected by using secondary antibody conjugated to a fluorescent indicator. *Right*, Average fluorescence intensities normalized to vector-transfected controls (n = 3). Compared with fluorescence intensity measurements, the percent of BrdU-positive versus total cells was 14.0 ± 4.9, 47.1 ± 4.1 and 18.3 ± 2.0, for vector-, *eag*-, and *Shaker*- transfected coverslips, respectively.
(C) *Left*, BrdU incorporation in cells deprived of FBS. *Right*, Normalized fluorescence intensities for three experiments. (Scalebar = 10 μm.) Data are presented as the mean ± SEM. * $p < 0.05$; ** $p < 0.01$, *** $p < 0.0001$; N.S., not significant (ANOVA); Ctrl, control.

contrast, transfection with the gene encoding Shaker, another voltage-dependent K^+ channel, resulted in BrdU incorporation that was indistinguishable from control levels, indicating that the effect was specific to EAG. Increased proliferation also was observed by using phospho-histone labeling, another marker for proliferation (data not shown). These results indicate that proliferation accounts, at least in part, for the observed increase in cell density. EAG-induced proliferation was not limited to NIH 3T3 cells because EAG also increased proliferation in C2C12 myoblasts (data not shown). Finally, increased proliferation was also observed in response to EAG when cells were "synchronized" in serum-free media before reintroduction of fetal bovine serum (FBS). However, proliferation was increased even in the complete absence of FBS (Fig 2.1C; $p < 0.0001$, $n = 3$); thus, the growth factors present in serum were not required for the effect of EAG on signaling.

C.2. EAG-induced proliferation is independent of ion flux

K^+ currents are essential for the proliferation of numerous cell types, including T-lymphocytes and Schwann cells (DeCoursey et al., 1984; Wilson and Chiu, 1993). The role of K^+ channels in proliferation, as well as other cellular processes, is generally assumed to be indirect. K^+ channels alter the membrane potential to modulate Ca^{2+} influx through voltage-dependent Ca^{2+} channels, which, in turn, affects numerous intracellular messenger pathways (Lewis and Cahalan, 1995; Rosen et al., 1994). However, in the present experiments, ion conduction was not required for the effect of EAG on proliferation. Figure 2.2A shows recordings from *Xenopus* oocytes expressing wild type EAG, myc-tagged EAG or EAG-F456A, which contains a point mutation in the

Figure 2.2: EAG-mediated signaling is independent of K^+ conductance.
(A) Representative currents and average current-voltage relations for oocytes injected with *eag* (n = 10), myc-*eag* (n = 4), *eag*-F456A (n = 8), or water (n = 7) as indicated. Currents were elicited by using steps from -110 to +60 mV (holding potential of -120 mV), and peak currents were plotted as a function of voltage. **(B)** *Left,* Non-conducting channels increased BrdU incorporation similar to wild type EAG. *Right*, Normalized fluorescence intensities (n = 3). **(C)** SB-203580 (20 μM), an inhibitor of p38 MAP kinase, inhibits proliferation induced by non-conducting EAG in the absence of serum. *Right*, average data (n = 3). (Scalebar, 10 μm.) **(D)** Average data for the "p38 MAP kinase inhibitor" (25 μM, n = 3), the control compound SB-202474 (25 μM, n = 2), and PD-98059 (40 μM, n = 3) effects on EAG-F456A-induced proliferation in serum-free media. **(E)** EAG increases p38 MAP kinase activity. *Left*, Representative blots of NIH 3T3 cell extracts run out in parallel were probed with antibodies for total p38 (1:500), phosphorylated (active) p38 (1:100), and actin, followed by anti-rabbit HRP-conjugated secondary antibody. *Right*, average data (n = 4). Asterisks and error bars as in Figure 1.

FIGURE 2.2

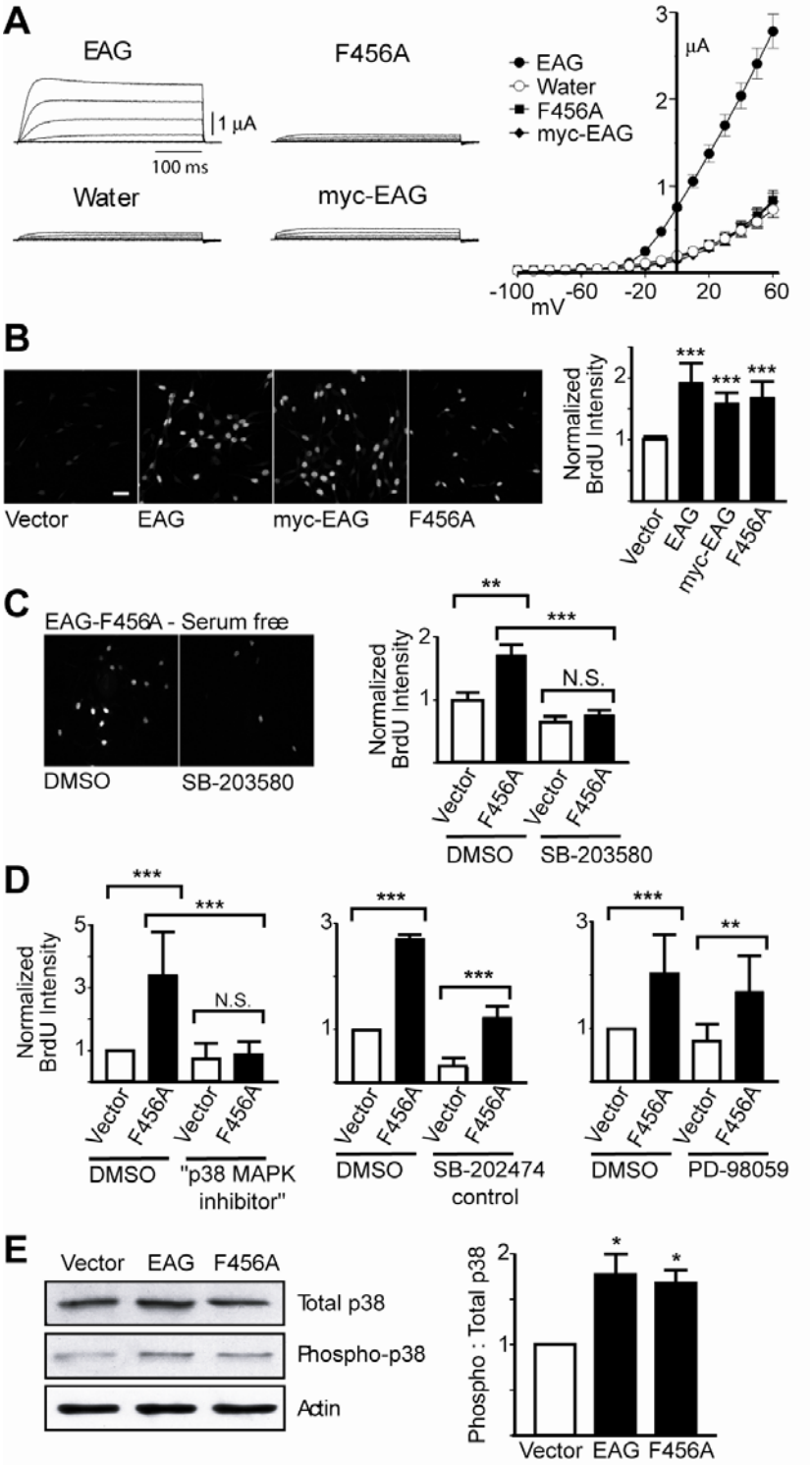
A
EAG
F456A
1 µA
100 ms
Water
myc-EAG
EAG
Water
F456A
myc-EAG
µA
mV
B
Vector
EAG
myc-EAG
F456A
Normalized BrdU Intensity
C
EAG-F456A - Serum free
DMSO
SB-203580
Normalized BrdU Intensity
N.S.
DMSO
SB-203580
D
Normalized BrdU Intensity
N.S.
DMSO
"p38 MAPK inhibitor"
SB-202474 control
PD-98059
E
Vector
EAG
F456A
Total p38
Phospho-p38
Actin
Phospho : Total p38

selectivity filter of the channel pore. The selectivity filter sequence is conserved in all K^+ channels (Doyle et al., 1998) and point mutations in this sequence eliminate conduction in Shaker, as well as numerous other K^+ channels (Heginbotham et al., 1994; MacLean et al., 2003; Preisig-Muller et al., 2002). Both myc-EAG and EAG-F456A failed to produce the outward currents characteristic of the wild type channel. Comparison of current-voltage relations (Fig 2.2A, *right*) revealed little difference between myc-EAG and EAG-F456A currents and currents recorded from water-injected controls, which are carried by channels endogenous to oocytes. Although the mechanism underlying the absence of current in myc-EAG is unclear, both myc-EAG and EAG-F456A produced detectable gating currents (data not shown), indicating that defects in the folding or trafficking of EAG cannot wholly account for the absence of K^+ current.

Myc-EAG and EAG-F456A increased proliferation to a degree similar to wild type channels (Fig 2.2B). The increases in BrdU incorporation were significant in comparisons to vector-transfected controls ($p < 0.0001$; $n = 3$). Moreover, the effects of myc-EAG and EAG-F456A were not significantly different from the effect of the wild type channel. In short, changes in K^+ flux, and the changes in membrane potential and Ca^{2+} influx that are presumed to result, cannot account for the proliferation induced by EAG. Additional evidence that the signaling mechanism of EAG does not include an indirect effect on Ca^{2+} influx was obtained by incubating cells in EGTA-buffered media prior to and during incubation of cells with BrdU. EAG-induced proliferation in the presence of EGTA (1 mM, 5 hrs) was 90.1 ±11.2% and 95.1 ± 3.7% of the proliferation in standard Ca^{2+}-containing media for wild type EAG and EAG-F456A channels respectively ($n = 3$, not significant). Higher concentrations of EGTA caused cells to

detach and, therefore, were not assessed.

C.3. EAG-induced proliferation requires the p38 MAP kinase pathway

MAP kinase signaling is central to proliferation in numerous cell types and in response to a variety of signals (Pearson et al., 2001). To determine whether the proliferation induced by non-conducting EAG channels requires this pathway, cells were treated with inhibitors of MAP kinase signaling in serum-free media. The p38 MAP kinase inhibitor SB-203580 [4-(4-fluorophenyl)-2-(4-methylsufinylphenyl)-5-(4-pyridyl)-1*H*-imidazole] (20 μM) blocked the proliferation observed in response to EAG-F456A (Fig 2.2C; $p < 0.0001$, $n = 3$), reducing proliferation to levels that were no different from the proliferation observed for controls ($p > 0.05$, $n = 3$). Similar results were obtained by using the "p38 MAP kinase inhibitor" [2-(4-chlorophenyl)-4-(4-fluorophenyl)-5-pyridin-4-yl-1,2-dihydropyrazol-3-one] (Fig 2D, *left*). In contrast, although the control compound, SB-202474, [4-ethyl-2(*p*-methoxyphenyl)-5-(4'-pyridyl)-1*H*-imidazole] reduced the overall level of proliferation in both vector- and *eag*-F456A-transfected conditions, it failed to inhibit the EAG-specific increase (Fig 2.2D, *center*; $p < 0.0001$, $n = 2$). Finally, although PD-98059 [2'-amino-3'-methoxyflavone], an inhibitor of the p44/42 extracellular signal-regulated kinases, reduced proliferation in the presence of FBS (data not shown), PD-98059 (40 μM) had little effect on the increase in proliferation specifically induced by non-conducting EAG in serum-free media (Fig 2.2D, *right*; $p < 0.01$, $n = 3$). These results suggest that p38, but not p44/42, MAP kinase signaling is required for the proliferation stimulated by non-conducting EAG-F456A channels.

To determine whether EAG affects p38 MAP kinase activity, we immunoblotted NIH 3T3 cell lysates with antibodies that detect either total p38 MAP kinase or, specifically, the phosphorylated, active kinase. As shown in Figure 2E, p38 phosphorylation nearly doubled in the presence of either wild type or non-conducting EAG (Fig 2.2E; $p < 0.05$, $n = 4$) and the magnitude of the effect appeared to approximate the average increase in BrdU incorporation (Fig 2.2 B,C).

C.4. EAG-induced proliferation is regulated by the position of the voltage-sensor

The observation that the signaling activity of EAG does not depend on ion conduction predicts that changes in extracellular K^+ concentration ($[K^+]_o$) should not affect EAG-induced proliferation. However, although increased $[K^+]_o$ increased proliferation in vector-transfected controls, increasing $[K^+]_o$ by 10 mM inhibited EAG-induced proliferation, returning proliferation to control levels. Specifically, at 15 mM $(K^+]_o$, EAG-induced proliferation was 93.9 ± 1.5 % of controls compared to 151.4 ± 7.3 percent in normal 5.3 mM $[K^+]_o$. (Measurements were normalized to vector-transfected controls in 5.3 mM; $p < 0.001$). Similar results were observed in two additional experiments. Because increases in $[K^+]_o$ will depolarize the membrane and shift the position of the voltage sensor even in non-conducting EAG channels, we hypothesized that the signaling activity of EAG might depend on voltage-sensitive conformations of the channel. Specifically, the $[K^+]_o$ experiments predict that increases in the proportion of channels in the open state should decrease EAG signaling activity.

To explore the possibility that the signaling activity of EAG might be regulated by the position of the voltage sensor, we examined the effects of EAG channels containing

mutations in the sixth transmembrane segment that shifted their voltage-dependence of activation. Figure 2.3A shows representative currents obtained for the wild type channel and two mutants, EAG-TATSSA (T449S/K460S/T470A) and EAG-HTEE (H487E/T490E), when expressed in *Xenopus* oocytes. Comparison of the conductance-voltage (GV) relations (Fig 2.3B) reveals that the predominant effect of both mutations was to produce hyperpolarizing shifts in the midpoints of activation from 8.0 ± 1.1 mV (wild type, n = 6) to -10.8 ± 1.2 mV (n = 9) and -31.6 ± 2.0 mV (n = 7) for EAG-TATSSA and EAG-HTEE channels, respectively. In addition, the TATSSA and HTEE mutations also produced changes in kinetics; however, these changes were in opposite directions (Fig 2.3A). Comparison of the average resting potentials of oocytes expressing EAG channels (Fig 2.3C) revealed that the resting potentials closely followed the changes in the V_{10} for activation (the voltage at which 10% of channels are activated; Fig 2.3D). This would be expected if EAG is the major channel contributing to the membrane potential. Wild type EAG produced only a small shift in the resting potential from -44.5 ± 2.8 to -52.8 ± 1.9 mV. In contrast, EAG-TATSSA and EAG-HTEE shifted the resting potential to -82.8 ± 1.1 and -90.7 ± 0.9 mV, respectively. It is important to note that, given that K^+ channel conformation and membrane potential act as a negative feedback loop, the proportion of channels in the closed state should be similar in each case, provided that each of the constructs contributes to the membrane potential to a similar extent.

The above EAG constructs were used to address whether the signaling activity of EAG is regulated by channel conformation. As shown in Figure 2.4A, there was an approximately 2-fold increase in the proliferation of NIH 3T3 cells regardless of whether

FIGURE 2.3

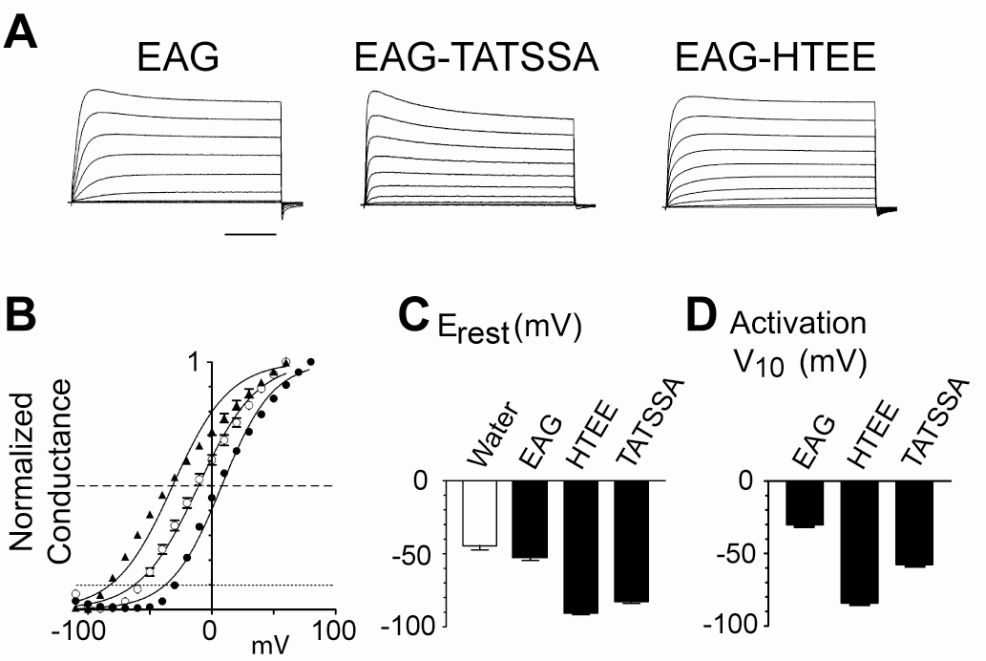

Figure 2.3: Comparison of the properties of wild type and mutant EAG channels. **(A)** Recordings from oocytes expressing EAG constructs as indicated. Voltages were stepped from -110 to +80 mV (holding potential of -120 mV). (Bar, 100 msec.) **(B)** Normalized G-V relations obtained for EAG (●), EAG-TATSSA(○) and EAG-HTEE (▲). GV curves were generated using the relation $G = I_{peak}/ (V_{test} - E_K)$, where E_K was assumed to be -120 mV. Conductances were normalized to the maximum conductance observed. Boltzmann fits to the data had slopes of 20.7 ± 0.9 and 23.5 ± 1.0 for EAG and EAG-TATSSA, respectively. For EAG-HTEE, the slope was constrained to 23. Horizontal dotted and dashed lines represent 10% and 50% maximal activation, respectively. **(C)** Averaged resting potentials for the same oocytes. **(D)** Average V_{10} for activation obtained from GV curves.

wild type *eag*, *eag*-TATSSA or *eag*-HTEE were used. Given the negative feedback of conducting EAG channels on channel conformation, these results suggest that proliferation depends on the position of the voltage sensor of EAG channels rather than on a specific resting membrane potential. Indeed, measurement of the resting potentials of NIH 3T3 cells transfected with these constructs indicated that, although EAG channels contributed to the membrane potential to a lesser degree than in oocytes, each construct shifted the resting potential closer to the respective activation threshold (Fig 2.4B).

Additional evidence in support of the hypothesis that channel conformation is a "switch" for the signaling activity of EAG was obtained using *eag*-TATSSA and *eag*-HTEE constructs that had been rendered non-conducting by including the F456A mutation, in effect short-circuiting the negative feedback function of EAG. As expected, the resting potentials of cells expressing these double mutants were similar to the resting potentials of vector-transfected controls (Fig 2.4B). The shifted voltage-dependence of these channels, combined with their inability to shift the resting potential, should result in a larger proportion of TATSSA-F456A and HTEE-F456A channels in the open conformation. On the basis of the prediction above, increasing the proportion of channels in the open state should decrease EAG-induced proliferation. As predicted, both EAG-TATSSA/F456A and EAG-HTEE/F456A failed to increase proliferation above control levels (Fig 2.4A). In contrast, as observed in our earlier experiments, proliferation was robust for EAG-F456A. Finally, neither changes in expression level or changes in the surface expression of EAG (Fig 2.4C) could account for the changes in proliferation observed with the double-mutant constructs. Together, these results suggest that the signaling activity of EAG depends on voltage-sensitive conformations of the channel.

FIGURE 2.4

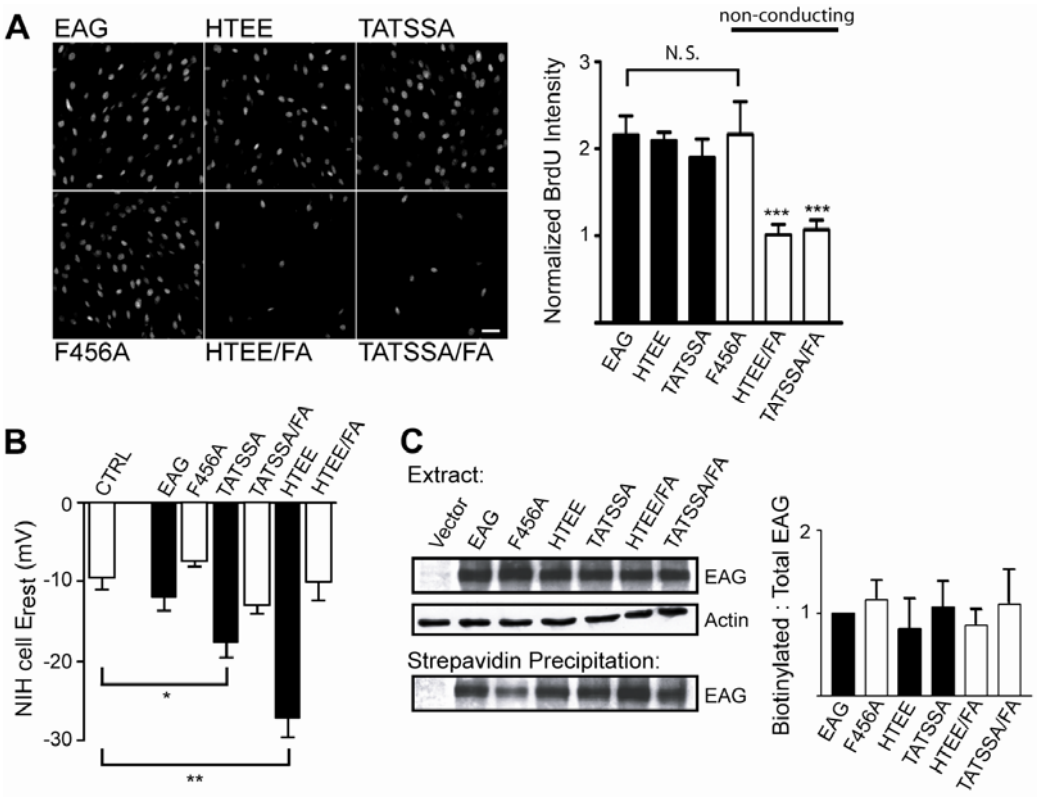

Figure 2.4: EAG-mediated signaling is regulated by channel conformation. **(A)** *Left*, BrdU labeling for EAG, EAG-HTEE or EAG-TATSSA (upper panels) and corresponding non-conducting mutants (lower panels). *Right*, Proliferation is inhibited when EAG is predominantly open but non-conducting (n = 3). (Scalebar = 10 μm.) Asterisks and error bars as in Figure 1. **(B)** Whole recordings of NIH 3T3 cell resting potentials. Individual isolated cells were selected for recordings on the basis of EGFP fluorescence. Resting potentials were more depolarized than observed in oocytes, presumably because of the presence of channels, in particular Ca^{2+} channels, endogenous to NIH 3T3 cells (Chen et al., 1988; Pemberton et al., 2000). The number of oocytes examined for each condition were, from left to right, 16, 13, 8, 12, 11, 13, and 8. **(C)** Total expression and surface expression of wild type and mutant EAG channels. *Left*, Representative blots. *Right*, average data for three experiments. Before preparation of extracts and precipitation with streptavidin agarose, cells were labeled with biotin and then quenched with glycine as described in Methods. Equal amounts of either the extract (upper panels) or the precipitates (lower panels) were separated by SDS-PAGE and probed with EAG (CT) or actin antisera. Bands were quantified by densitometry and normalized to the band observed for wild type EAG in each experiment.

D. DISCUSSION

Our results indicate that EAG is a bifunctional protein that not only regulates K^+ flux, but also regulates intracellular signaling pathways. The effect of EAG on intracellular signaling was evident as an increase in proliferation of NIH 3T3 cells and did not appear to be due to an indirect effect of K^+ ions because it was observed even with non-conducting channels. To date, other examples of bifunctional channels include α1C Ca^{2+} channels whose carboxyl-terminal regions regulate transcription (Dolmetsch et al., 2001), a member of the TRP family of cation channels (TRP-PLIK) that contains a functional kinase domain (Runnels et al., 2001), and voltage-gated sodium channels whose β-subunits not only modulate channel function but also act as cell adhesion molecules (Malhotra et al., 2000). EAG appears to differ from the above channels in that signaling activity is linked to channel conformations determined by the position of the voltage sensor. The signaling function of EAG is a novel mechanism that may link channel gating to intracellular messenger pathways. This role has typically been ascribed only to channels that regulate Ca^{2+} influx. Recently, however, *Ci*-VSP, a novel protein containing a transmembrane voltage sensor linked to a functional cytoplasmic phosphatase and tensin (PTEN) domain, has been reported to regulate phosphoinositide turnover in a voltage-dependent manner (Murata et al., 2005).

The signaling activity of EAG characterized in the present study appears negatively correlated with the proportion of channels in the open state or, at the single channel level, the magnitude of the single channel open probability (p_o). It is tempting to speculate that EAG-induced signaling is limited to channels in a specific conformation, presumably one of two previously characterized EAG closed states (Schonherr et al., 2002; Tang et al.,

2000). Comparison of NIH 3T3 cell resting potentials (Fig 2.4B) to the GV curves obtained in oocytes (Fig 2.3B) predicts that > 50% of the channels must be closed or that the single channel p_o must be < 50% of the maximum for a significant increase in proliferation to occur. However, given the reduced effect of EAG on the NIH 3T3 cell versus oocyte resting potentials, this correlation appears to break down for more quantitative comparisons. For example, at the mean resting potentials of -12, -18, and -28 mV for cells expressing wild type, TATSSA, and HTEE channels (Fig 2.4B), the GV curves indicate that approximately 68, 56, and 49% of channels will be closed, respectively. This observation predicts that proliferation response should be highest for wild type channels and lowest for EAG-HTEE, a trend that is not observed in our data. There are several possible explanations of this discrepancy. First, the resting potentials measured in NIH 3T3 cells may not accurately reflect the resting potentials of cells in our proliferation assays given that the cells are treated differently. Secondly, the GV curves obtained in oocytes may not be representative of channel behavior in NIH 3T3 cells. Unfortunately, EAG current could not be effectively isolated from the other outward currents endogenous to NIH 3T3 cells to address this concern. Third, it is possible that proliferation is not as sensitive an indicator of voltage-dependence as the GV curve. GV curves, which are continuous functions, represent the average behavior of a million or more channels, whereas proliferation, which is a step function, represents the average behavior of hundreds of cells at best. Fourth, EAG-induced proliferation may be limited by the availability or activity of downstream components of the affected signaling pathway. Finally, voltage-dependent enzymatic activity or protein-protein interactions may require that channels occupy a given conformation for a specific duration. Although

channel conformation may serve as a switch for the signaling activity of EAG, the domain underlying signaling remains under investigation. Possibilities include an amino-terminal PER-ARNT-SIM (PAS) domain, several putative nuclear localization signals in the carboxy-terminal domain, and a region with homology to the autoinhibitory domain of CaMKII that has been shown recently to regulate kinase activity in *in vitro* assays (Wang et al., 2002c).

The proliferation induced by EAG was unaffected by changes in extracellular Ca^{2+}, suggesting that increased Ca^{2+} influx is not an essential downstream component of EAG-induced signaling. Nonetheless, our experiments do not address intracellular Ca^{2+} concentrations or the possible role of Ca^{2+} released from intracellular stores. Moreover, although Ca^{2+} influx may not be a downstream component of the EAG-induced pathway, our results suggest that any mechanism that regulates EAG surface expression or voltage-dependence may be an upstream regulator of EAG signaling. Indeed, Ca^{2+}/calmodulin binding to EAG decreases EAG current by shifting channel activation to more positive potentials (Clyne et al., submitted) and, Ca^{2+}, by increasing CaMKII activity and phosphorylation of EAG, increases EAG surface expression (Marble et al., 2005). Thus, both of these Ca^{2+}-dependent mechanisms could act upstream of EAG to increase EAG signaling in an activity-dependent manner, and the role of Ca^{2+} should be further explored.

In the present study, the voltage-dependent signaling activity of EAG increased proliferation of NIH 3T3 cells and C2C12 myoblasts; however, it is unclear whether EAG-induced signaling normally regulates proliferation *in vivo*. No gross morphological defects have been observed in *Drosophila eag* mutants at any developmental stage. It

should be noted, however, that a role for *Drosophila ras* in proliferation was only uncovered by using overexpression of mutant *ras* constructs (Karim and Rubin, 1998), despite the well-established role of *ras* in proliferation in other systems. Although the developmental profile of EAG expression is unknown, EAG transcripts and protein appear most highly expressed in mature neurons in both *Drosophila* and mammals (Jeng et al., 2005; Ludwig et al., 1994; Saganich et al., 2001; Sun et al., 2004). Thus, there is little evidence to suggest that EAG regulates proliferation in normal tissues at present. However, abnormally expressed EAG may have a role in proliferation and transformation, given that human EAG has been suggested to have an oncogenic potential and EAG appears abnormally expressed in several tumor cell lines (Pardo et al., 1999; Patt et al., 2004).

Intracellular signaling pathways typically have a variety of possible roles; the output of a pathway in any given cell at any given developmental stage will depend on context and crosstalk between other pathways. In the present study, proliferation may simply be the "read-out" of a change in the activity of one or more intracellular signaling pathways. Given that EAG appears largely neuron specific and localized at synapses (Jeng et al., 2005; Sun et al., 2004; Wang et al., 2002c), and given that synaptic plasticity and memory acquisition are disrupted in *eag* mutants (Engel and Wu, 1998; Griffith et al., 1994), EAG signaling may normally regulate activity-dependent changes in neuronal function. Indeed, EAG-mediated proliferation was blocked by inhibitors of the p38 MAP kinase pathway, and transfection of EAG increased p38 MAP kinase activity. An important future question concerns whether the link between EAG and p38 activity is

conserved in neurons. MAP kinase signaling is central to not only proliferation but also synaptic plasticity and learning (Sweatt, 2004; Thomas and Huganir, 2004).

E. MATERIALS & METHODS

E.1. Plasmids and construction

pCS2-myc-*eag* contains a myc tag added to the amino-terminus (Wang et al., 2002c). For the wild type construct, EcoRI and XbaI sites flanking the coding sequence were used to subclone *eag* (without the myc tag) into the pCS2 vector. A Kozak sequence (GCCACC) was added to improve channel expression. *Shaker* was subcloned into pCS2 by using *EcoRI* sites flanking the coding sequence of pGH19-*Shaker* (Chouinard et al., 1995). *Eag*-F456A, *eag*-H487E/T490E (HTEE), *eag*-T449S/A460S/T470A (TATSSA) and double mutants were generated by site-directed mutagenesis using QuikChange (Stratagene). For oocyte expression, mutant constructs were subcloned into pGH19-*eag* (Wilson et al., 1998). All constructs were verified by sequencing.

E.2. Immunocytochemistry and proliferation assays

NIH 3T3 fibroblasts were maintained at 37°C and 5% CO_2 in Dulbecco's modified Eagle's medium (DMEM, Invitrogen) supplemented with 10% fetal bovine serum (FBS) as previously described (Chouinard et al., 1995). For transfection, coverslips were washed with Opti-MEM and incubated for 8-10 hrs in 350 µl of Opti-MEM containing 0.4 µl of the indicated cDNAs and 1.5 µl of LipofectAMINE (Invitrogen). Coverslips were then washed and incubated in standard media for 12 hrs. For serum-free experiments, this was followed by incubation in FBS-free DMEM for 12 hrs, with 1%

FBS added to a subset of wells as a positive control. MAP kinase inhibitors or control compounds were added following washout of LipofectAMINE.

For BrdU labeling, 10 μM BrdU was added to each well for ~ 60 min. Coverslips were washed with phosphate-buffered saline (PBS) and fixed with a 3:7 mixture of 50 mM glycine (pH 2.0)/100% ethanol for 1 hr at room temperature (RT), then denatured with 4 M HCl for 15 min. Cells were labeled with anti-BrdU fluorescein-conjugated antibody (Molecular Probes) for 45 min at 37 ^{o}C. Labeling was visualized using an Olympus BX51W1 microscope equipped with a Qimaging Retiga Exi camera and IPlab 3.6 software. Coverslips from the same experiment were viewed using identical settings, and multiple representative scans were taken for each coverslip. To quantify fluorescence, scans were background subtracted, and the intensity of all pixels above background was summed across the total area of each scan. Total intensities were averaged across all scans for each condition before normalizing to the average intensity for controls. Normalized data were then averaged across experiments (N). Data were analyzed using a two-way analysis of variance (ANOVA) with Tukey's post-hoc analysis with the condition and experiment number as variables (* $p < 0.05$, ** $p < 0.01$, *** $p < 0.0001$; N.S., not significant). Data are presented as the mean ± SEM. MAP kinase inhibitors were purchased from Calbiochem.

E.3. Biochemistry

Cells grown on culture plates were dissociated with trypsin-EDTA 48 hrs after transfection, washed and resuspended in PBS. Biotinylation and precipitation of EAG was performed as described (Marble et al., 2005). Briefly, cell suspensions were

incubated in 2 mM sulfo-NHS-LC-biotin (Pierce) and the reaction was quenched by washing with 100 mM glycine in PBS. Cells were lysed in PBS supplemented with 1% IGEPAL CA-630, 0.5% sodium deoxycholate, 0.1% SDS, 1 mM DTT and protease inhibitors, and the homogenate was centrifuged twice for 10 min at 20,000 x *g*. Protein concentrations of supernatants were determined by Bradford assay and diluted to ~ 0.5 mg/ml. Surface proteins were precipitated with strepavidin agarose and the precipitate washed extensively before addition of sample loading buffer. Blots were probed with antisera directed against the carboxyl-terminal domain of EAG (EAG (CT); 1:2000) in blocking buffer, followed by horseradish peroxidase (HRP)-conjugated secondary antibody (1:2000), and visualized with ECL (Amersham Biosciences). Protein bands were quantified by using Quantity One software (BioRad). Assays of p38 MAP kinase activity were performed by using extracts prepared in buffer containing the following: 20 mM Tris (pH 7.4), 100 mM NaCl, 50 mM NaF, 1 mM Na_3V0_4, 1 mM EDTA, 1 mM DTT, 1 mM benzamidine, and 0.001 mM microcystin-LR with 1% IGEPAL CA-630, 0.5% sodium deoxycholate, 0.1% SDS, and protease inhibitors.

E.4. Electrophysiology

Experiments using *Xenopus* oocytes were performed as described (Marble et al., 2005). Oocytes were typically injected with 0.1-0.2 ng of RNA; non-conducting constructs were injected at 1-2 ng. The recording solution contained the following: 140 mM NaCl, 2 mM KCl, 1 mM $MgCl_2$ and 10 mM Hepes (pH 7.1 with NaOH). Pipettes had resistances of 0.3 - 0.6 MΩ. Experiments were performed at RT. Leak and capacitative currents were subtracted using P/4 methods.

For NIH 3T3 cell recordings with an Axopatch200B amplifier, cells maintained on plates were co-transfected with pCDNA3-EGFP and the indicated constructs and were then replated onto coverslips. Pipette resistances ranged from 3 to 6 MΩ. The extracellular solution contained the following: 40 mM sodium aspartate, 100 mM NaCl, 4 mM KCl, 1.5 mM $MgCl_2$, 1 mM $CaCl_2$, 2 mM glucose and 10 mM Hepes (pH 7.4 with NaOH). The pipette solution contained the following: 35 mM potassium aspartate, 110 mM KCl, 2 mM MgATP, 1 mM NaATP, 3 mM sodium phosphocreatine, 0.1 mM NaGTP, 8 mM EGTA and 10 mM Hepes (pH 7.4 with KOH).

CHAPTER III

CONDUCTANCE-INDEPENDENT GATING OF CAMKII ASSOCIATED WITH ETHER À GO-GO K^+ CHANNELS

A. ABSTRACT & INTRODUCTION

Recent studies suggest that voltage-gated channels can regulate biochemical events independently of ion flux (Dolmetsch et al., 2001; Gomez-Ospina et al., 2006; Kaczmarek, 2006; MacLean et al., 2003; Malhotra et al., 2000; Runnels et al., 2001). *Drosophila* Ether à go-go (EAG) potassium (K^+) channels regulate intracellular signaling by a mechanism that is independent of conductance and is gated by the position of the voltage sensor (Hegle et al., 2006). Here we present evidence that EAG signaling is mediated via voltage-dependent regulation of Ca^{2+}/calmodulin-dependent protein kinase II (CaMKII), and that this signaling mechanism is conserved in mammalian EAG. Mutation of key residues in the EAG carboxyl-terminal CaMKII-binding domain abolishes EAG-mediated signaling, and biotinylation assays using mutations that shift the voltage-dependence of EAG suggest that membrane-associated CaMKII activity is modulated by voltage-driven conformational changes in EAG. Although the above experiments assess signaling in NIH 3T3 cells heterologously expressing EAG, we also assessed the role of the EAG-CaMKII complex in transgenic *Drosophila*. In recordings

at the larval neuromuscular junction (NMJ), EAG channels with mutations in the CaMKII binding domain largely failed to rescue the high levels of spontaneous activity characteristic of *eag* mutants, whereas non-conducting EAG-F456A channels rescued spontaneous activity with an efficiency nearly overlapping that observed for wild type channels. These results suggest that voltage-dependent, conductance-independent EAG signaling plays a role in synaptic homeostasis *in vivo* and implicate EAG signaling as a novel mechanism for linking neuronal activity to the state of intracellular messenger pathways.

B. RESULTS

The EAG K^+ channel was originally implicated as a possible bifunctional channel in studies showing a role for human EAG in cell cycle progression and oncogenesis (Farias et al., 2004; Meyer and Heinemann, 1998; Pardo et al., 1999; Patt et al., 2004), although the mechanism underlying the effects of abnormally expressed EAG remained unclear. In studies of the *Drosophila* ortholog, we have shown that EAG acts independently of conductance as an upstream regulator of the activity of p38 mitogen-activated protein kinase (MAPK) and proliferation (Hegle et al., 2006). Specifically, when studies are performed in serum-free media to eliminate the possible confounding effects of growth factor stimulated pathways, both wild type EAG and the non-conducting selectivity filter mutant, EAG-F456A, increase p38 MAPK activity, and the proliferation induced by either channel is blocked by p38 MAPK inhibitors (Hegle et al., 2006). However, p38 MAPK is likely to be several steps downstream of the EAG events that mediate signaling. To determine the EAG domain and mechanism directly mediating voltage-

dependent, conductance-independent signaling, we first examined the effects of deletions and mutations in the cytoplasmic tails in BrdU assays of NIH 3T3 cell proliferation. Figure 3.1A shows a representative experiment comparing the effects of wild type and non-conducting channels with the effects of truncated channels that lack the cytoplasmic N- or C-terminal domains. As observed previously, incorporation of 5-bromo-2'-deoxyuridine (BrdU), a fluorescent indicator of cell proliferation, was significantly increased over control levels ($p < 0.01$, $n = 6$) for coverslips transfected with wild type EAG and EAG-F456A (Fig 3.1C). In addition, although the N-terminal deletion (EAG-ΔNT, containing amino acids 213-1174), which lacks the PER-ARNT-SIM (PAS) dimerization domain (Crews and Fan, 1999), failed to disrupt EAG-induced proliferation, the C-terminal deletion (EAG-ΔCT, containing amino acids 1-514) decreased proliferation ($p < 0.05$ in comparison to EAG, $n = 3$) to a level comparable to vector-transfected controls (Fig 3.1A,C). These results suggested that a key domain underlying EAG-induced proliferation resides in the cytoplasmic C-terminal tail of EAG.

The EAG C-terminus is nearly twice as long as that of Shaker channels and contains several domains that could mediate the signaling activity of EAG. In addition to a domain with homology to the cyclic nucleotide-binding domains of other channels (Guy et al., 1991), it contains a functional CaMKII binding domain with high similarity to the autoinhibitory domain of the kinase (Hanks et al., 1988; Sun et al., 2004), a functional calmodulin (CaM) binding domain (Schonherr et al., 2000), three putative nuclear localization signals (NLS), and a series of putative Src-Homology 3 (SH3) motifs, one of which is known to interact with the Camguk/CASK adapter protein (Marble et al., 2005). To identify the domain(s) contributing to the signaling activity of EAG, we generated

Figure 3.1: CaMKII binding is essential for EAG signaling.
(A) C-terminal domain is required for EAG signaling. Representative scans showing BrdU labeling of coverslips transfected with the pCS2 vector, pCS2-*eag*, pCS2-*eag*-F456A, and N- and C-terminal deletion mutants. BrdU labeling was detected by using secondary antibody conjugated to a fluorescent indicator. (Scalebar = 10 μm for these and all scans in subsequent figures.) **(B)** Representative scans showing BrdU labeling of coverslips transfected with *eag* CaMKII-binding domain mutants as indicated.
C) Average fluorescence intensities for coverslips examining the role of the N- and C-terminal cytoplasmic domains, normalized to vector-transfected controls ($p = 0.0034$ overall; $p < 0.01$ for individual comparisons of WT-EAG and EAG-F456A to vector controls, $n = 6$; $p < 0.05$ for comparisons of the CT-deletion to WT-EAG, $n = 3$).
(D) Average fluorescence intensities of coverslips transfected with all domain mutations, including those shown in (b), normalized to vector-transfected controls (overall $p = 0.0167$, $n = 5$). **(E)** Representative blots showing total expression and surface expression of wild type and mutant channels, with actin as the loading control. **(F)** Average surface expression as in (e). For each experiment, bands were quantified by densitometry and normalized to the band for wild type EAG in the extract, prior to determining the ratio of EAG in the streptavidin precipitate to total EAG (overall $p = 0.4623$, $n = 3$). **(G)** Representative recordings from oocytes expressing wild type EAG or EAG-LAKK. Oocytes were stepped from -100 to +60 mV in 10 mV increments (holding potential, -80 mV); every other trace is shown. Capacitative and leak currents were subtracted using a P/4 protocol. (Bars, 5 μA and 100 ms). **(H)** Average conductance-voltage (GV) relations obtained for WT-EAG ($n = 9$) and EAG-LAKK ($n = 4$). Conductances were calculated from currents using the relation $G = I_{peak}/ (V_{test} - E_K)$, where E_K was assumed to be -100 mV, and then normalized to the maximum conductance observed. Boltzmann fits had midpoints of 1.2 ± 0.4 and 2.8 ± 3.2 mV and slopes of 16.1 ± 0.3 and 19.9 ± 2.9, for EAG and EAG-LAKK, respectively. Data are presented as the mean ± SEM. N.S., not significant; WT, wild type; Ctrl, control.

FIGURE 3.1

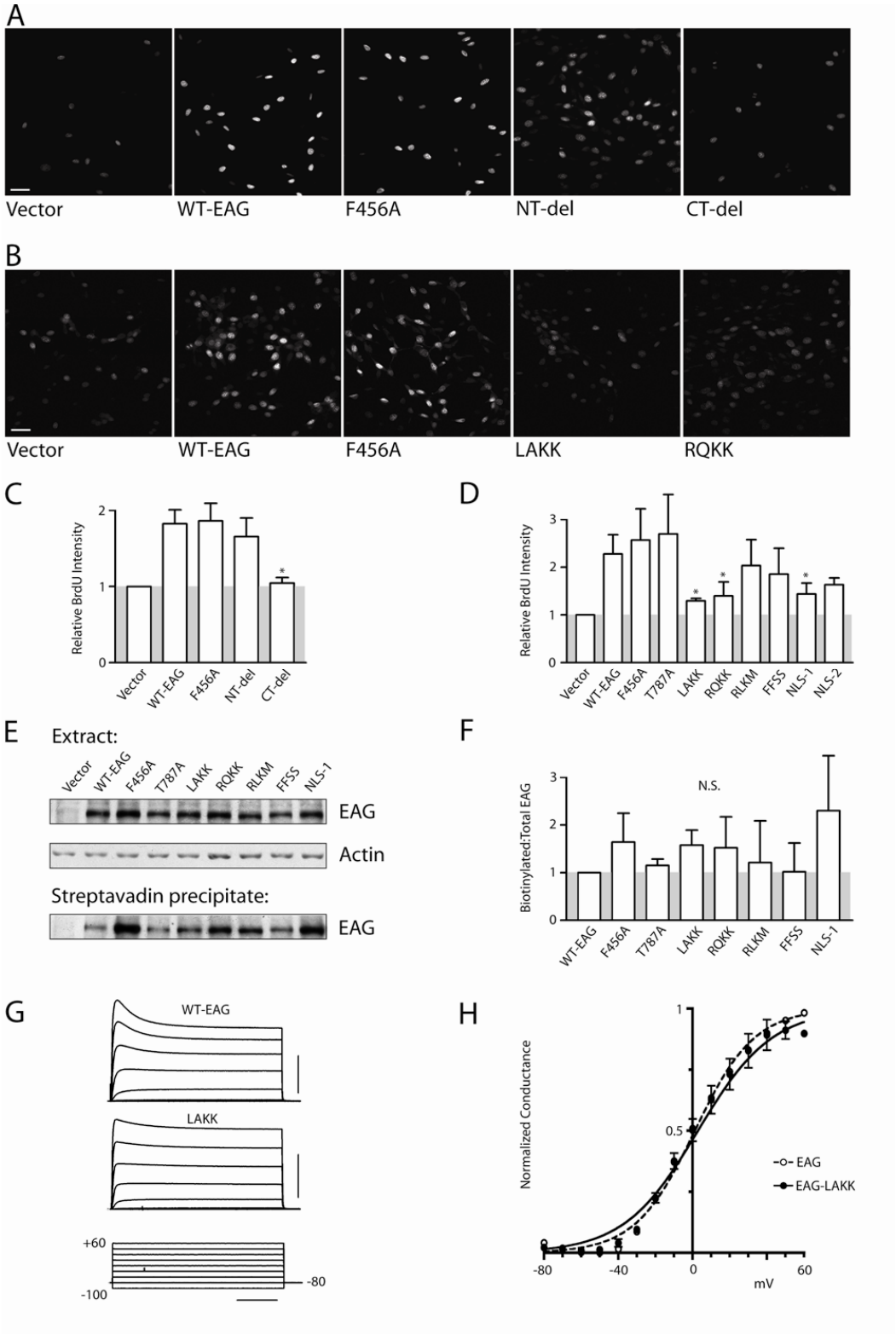
A
Vector
WT-EAG
F456A
NT-del
CT-del
B
Vector
WT-EAG
F456A
LAKK
RQKK
C
Relative BrdU Intensity
Vector
WT-EAG
F456A
NT-del
CT-del
D
Relative BrdU Intensity
Vector
WT-EAG
F456A
T787A
LAKK
RQKK
RLKM
FFSS
NLS-1
NLS-2
E
Extract:
Vector
WT-EAG
F456A
T787A
LAKK
RQKK
RLKM
FFSS
NLS-1
EAG
Actin
Streptavadin precipitate:
EAG
F
Biotinylated:Total EAG
N.S.
WT-EAG
F456A
T787A
LAKK
RQKK
RLKM
FFSS
NLS-1
G
WT-EAG
LAKK
+60
-100
-80
H
Normalized Conductance
EAG
EAG-LAKK
mV

mutations in candidate domains, including the CaMKII (EAG-LAKK), CaM (EAG-FFSS), and Camguk (EAG-RLKM) binding domains, the CaMKII phosphorylation site (EAG-T787A), and two putative NLS domains (EAG-NLS-1 and -2). The third putative NLS overlaps with the Camguk binding domain and should also be disrupted by the RLKM mutation. Subsequent assays of BrdU incorporation revealed that the most predominant inhibition was produced by the CaMKII binding domain mutation, EAG-LAKK (Fig 3.1B,D; $p < 0.05$ for EAG-LAKK, $n = 5$). The proliferation observed using EAG-LAKK was statistically indistinguishable from that observed for vector-transfected controls (Fig 3.1D). Further verification of the importance of the CaMKII binding domain was obtained using EAG-RQKK, in which residues neighboring LA were replaced with lysines. This mutant also significantly inhibited proliferation (Fig 3.1B,D; $p < 0.05$ for EAG-RQKK, $n = 5$).

The reduced proliferation observed with mutations in the CaMKII domain could not be explained by changes in surface expression, because precipitation of biotinylated cell extracts revealed no significant difference in expression levels between the various C-terminal domain mutations (Fig 3.1E,F). Furthermore, when expressed in *Xenopus* oocytes, the EAG-LAKK and EAG- RQKK mutants exhibited outward currents comparable to those observed for wild type EAG, although inactivation was slower and less extensive for EAG-LAKK channels (Fig 3.1G). Comparison of normalized conductance-voltage (GV) relationships revealed no obvious difference in the voltage-dependence of the CaMKII binding mutants and wild type channels (e.g., Fig 3.1H). Together, these data suggest that CaMKII binding is essential for EAG-mediated proliferation; however, they do not rule out possible contributions of other regions of the

channel. In particular, a mutation in NLS-1 also inhibited EAG-induced proliferation, but surface expression of this construct was quite variable (Fig 3.1D,F).

The most notable feature of EAG-mediated proliferation is that EAG signaling is regulated by channel conformations associated with the position of the voltage sensor. Specifically, mutations in the sixth transmembrane domain that shift the voltage-dependence of activation to more negative potentials (EAG-HTEE and EAG-TATSSA) disrupt EAG-mediated proliferation when coupled with the F456A mutation to render channels non-conducting (referred to as EAG-HFA and EAG-TFA, respectively). By short-circuiting the negative feedback effect of ion conduction on membrane potential, EAG-HFA and EAG-TFA channels are forced into a predominantly open conformation and, in this state, EAG-mediated proliferation is inhibited (Hegle et al., 2006). If CaMKII is the most immediate downstream target of EAG signaling, then either CaMKII activity or localization also should be regulated by voltage-dependent conformations of EAG. Recent *in vitro* studies suggest that kinase activity may be regulated, because CaMKII associated with the C-terminal cytoplasmic tail of EAG retains 5-10% of its maximal activity when the complex is washed in Ca^{2+}-free buffer (Sun et al., 2004). This constitutive activity is distinct from that mediated by phosphorylation of T287 of the kinase, although T287 can still be autophosphorylated.

To determine whether EAG regulates CaMKII in a voltage-dependent manner, we probed extracts of cells transfected with EAG-HTEE, EAG-TATSSA or their non-conducting counterparts for phosphorylated kinase, given that autophosphorylation is a reliable indicator of kinase activity. As shown in Figure 3.2A, in extracts, the ratio of phosphorylated to total CaMKII was uniform for the different EAG constructs. In

FIGURE 3.2

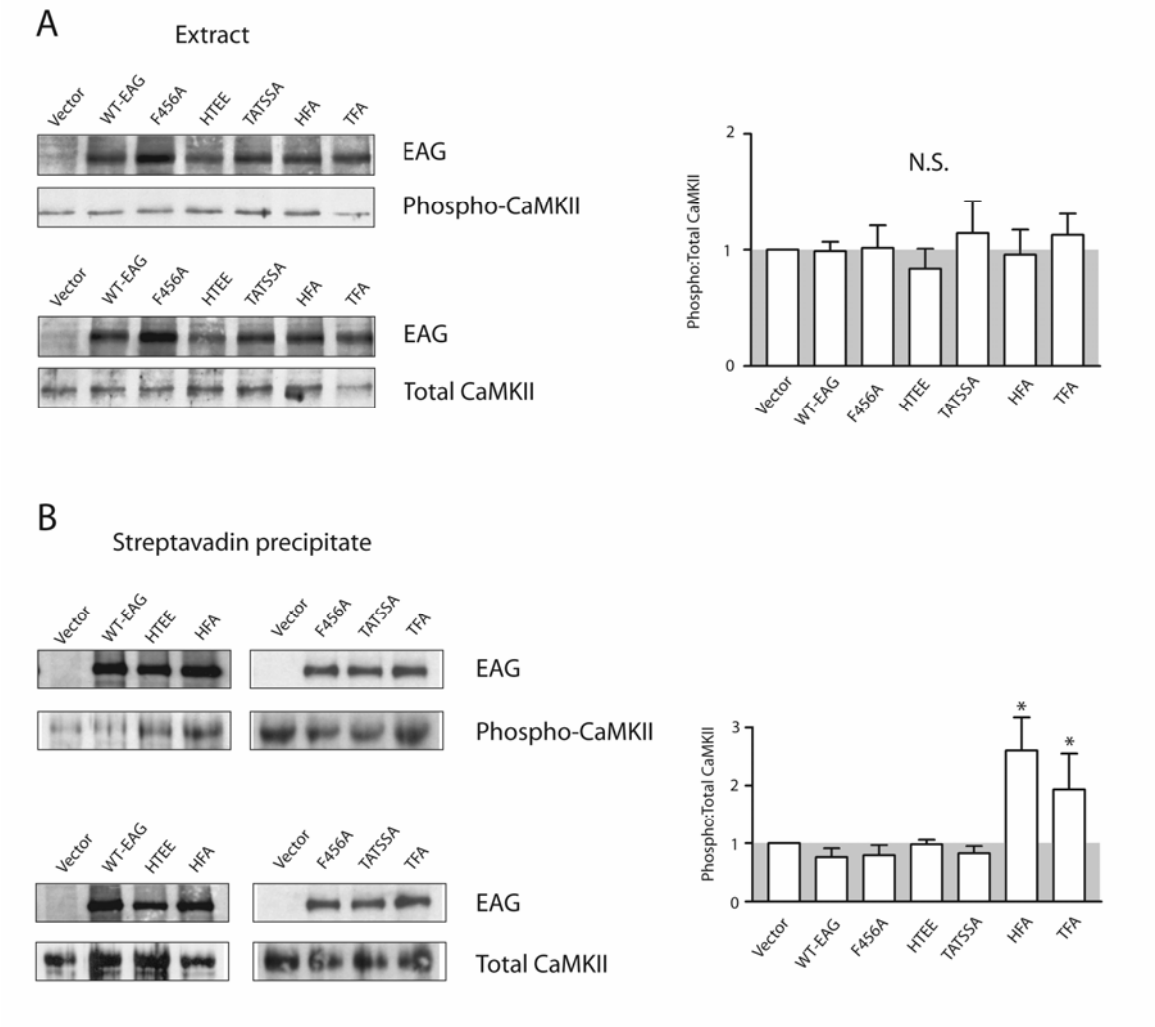

Figure 3.2: EAG gating regulates membrane-associated CaMKII activity.
(A) *Left*, Representative blots showing EAG, phospho-CaMKII and total CaMKII in extracts of NIH 3T3 cells expressing the indicated EAG constructs. *Right*, Averaged densitometric quantification of CaMKII activity, shown as the ratio of phospho:total CaMKII and normalized to the activity observed for vector-transfected controls (overall $p = 0.8314$, $n = 4$). **(B)** Membrane-associated CaMKII activity. *Left*, Representative blots for the indicated EAG constructs. Biotinylation and precipitation were performed as described in Methods. *Right*, Average ratio of phospho:total CaMKII analyzed as described in (a). Overall $p = 0.0028$, $n = 4$. In both (a) and (b), equal amounts of either extracts (a) or precipitates (b) were separated by SDS-PAGE and probed with EAG (CT), phospho-CaMKII or CaMKII antisera as indicated.

contrast, however, when the membrane fraction was isolated using biotinylation and precipitation with streptavadin, there was an approximate two-fold increase in membrane-associated kinase activity for the EAG-HFA and EAG-TFA conditions when compared to controls (Fig 3.2A,B, $p < 0.05$, $n = 4$). In addition, there appeared to be a consistent, though small, decrease in CaMKII activity for EAG constructs that induce proliferation. A local decrease in CaMKII activity, or a shift in localization to different membrane-associated complexes, could explain why mutations in the CaMKII binding domain inhibit the proliferation response. Together, these results suggest that the effect of EAG on CaMKII activity depends on voltage-dependent conformations of the channel and, further, that EAG-mediated increases in kinase activity negatively regulate the proliferation pathway.

If p38 MAPK is downstream and inhibited by CaMKII in the proliferation pathway, then EAG-dependent regulation of p38 MAPK activity also should be voltage-dependent. However, we were unable to detect voltage-dependent regulation of p38 MAPK in either the cytoplasmic or membrane-associated fractions. As observed previously (Hegle et al., 2006), p38 MAPK activity was consistently increased over control levels for all EAG constructs examined (data not shown). Either the effects on p38 MAPK are limited to molecules in close proximity to EAG or voltage-dependent regulation affects the localization of p38 MAPK to a compartment that is not adequately represented by the cytoplasmic or membrane fractions. Lastly, it is possible that CaMKII regulates a step that is downstream of p38 MAPK to inhibit proliferation.

Further support for the role of CaMKII in EAG-induced proliferation was obtained in experiments examining the conservation of EAG signaling in mouse EAG channels

(mEAG). As with *Drosophila eag*, transfection of either wild type or non-conducting (F466A) *meag* resulted in a significant increase in BrdU incorporation (Fig 3.3A; $p < 0.05, 0.001$ for mEAG and mEAG-F466A, respectively, $n = 4$). Recordings from NIH 3T3 cells expressing mEAG revealed a robust outward current, which exhibited voltage-dependent activation kinetics reminiscent of the Cole-Moore shift as expected for EAG channels (Cole and Moore, 1960; Ludwig et al., 1994) (Fig 3.3B). In contrast, the outward currents observed in cells transfected with mEAG-F466A overlapped with the currents observed in vector transfected controls, and, in both cases, changes in prepulse voltage had an effect on kinetics that was opposite that observed for currents recorded from cells transfected with the wild type channel (Fig 3.3B).

The mEAG C-terminal cytoplasmic tail contains a stretch of amino acids with homology to the CaMKII binding domain in the *Drosophila* channel, as well as the CaMKII autoinhibitory domain (Fig 3.3B). To examine whether this domain is also required for mEAG-mediated proliferation, two mEAG mutants, mEAG-RQEE and mEAG-QKEE, were generated based on homology to key residues in the other sequences. Both constructs produce an outward current that is comparable to that observed for the wild type channel in amplitude and voltage-dependence, although activation is slower (Fig 3.3E). Coverslips transfected with either mutant exhibit substantially reduced BrdU incorporation compared to coverslips transfected with wild type *meag* ($p < 0.05$, N=3; Fig 3.3D, *right*), indicating that the CaMKII binding domain plays a critical role in proliferation induced by both the mouse and fly channels.

Voltage-dependent proliferation is also conserved in mEAG channels (Fig 3.3F,G). Because mEAG outward currents are more robust than those generated by the *Drosophila*

Figure 3.3: CaMKII-dependent signaling is conserved in mammalian EAG.
(A) *Left*, Representative scans showing BrdU labeling of coverslips transfected with vector, *meag* or *meag*-F466A. *Right*, Average fluorescence intensities for the conditions shown in (a), normalized to vector-transfected controls (overall $p = 0.0105$; $n = 4$). **(B)** *Left*, Averaged currents elicited by ~160 ms voltage ramps from -100 to +100 mV for NIH 3T3 cells transfected with wild type mEAG ($n = 16$), mEAG-F466A ($n = 6$), or empty vector ($n = 4$). Capacitative and leak currents were subtracted using a P/8 protocol. *Right*, Prepulse voltage regulation of the kinetics of mEAG current. Currents elicited using a voltage step to +40 mV were preceded by a 500 ms prepulse to the following potentials: for mEAG, -120 (dotted trace), -100 (dashed trace), -80 (dashed trace) and -60 mV (solid trace) in 10 mV increments; for mEAG-F466A, -120 (dotted trace) and -70 mV (solid trace). (Bars, 100 ms and 50 ms for mEAG and mEAG-F466A respectively.) **(C)** Amino acid sequence alignment of the catalytic domain of CaMKII with the dEAG and mEAG C-terminus. Grey boxes indicate conserved residues. Outlined box identifies dEAG and mEAG residues mutated in this study. **(D)** *Left*, Representative scans showing BrdU labeling of coverslips transfected with *meag* CaMKII-binding domain mutants, as indicated. *Right*, Average fluorescence intensities, normalized to vector-transfected controls (overall $p = 0.0113$, $n = 3$). **(E)** *Left*, Representative recordings from NIH 3T3 cells expressing wild type mEAG, mEAG-RQEE or mEAG-QKEE. (Bars, 1 nA and 100 ms.) *Right*, Normalized G-V relations obtained for mEAG ($n = 5$), mEAG-RQEE ($n = 3$) and mEAG-QKEE ($n = 3$) obtained from tail currents enhanced using a recording solution containing 20 mM KCl. GV curves were generated using the relation $G = I_{peak}/ (V_{tail} - E_K)$, where E_K was assumed to be -100 mV. Conductances were normalized to the maximum conductance observed. Boltzmann fits had midpoints of -9.2 ± 1.4, -8.2 ± 1.4 and -7.4 ± 1.5 mV and slopes of 22.5 ± 1.3, 21.9 ± 1.2 and 25.1 ± 1.3, for mEAG, EAG-QKEE and EAG-RQEE, respectively. **(F)** *Left*, Representative recording showing the changes in membrane potential observed during perfusion with solutions containing the indicated K^+ concentrations. *Right*, Averaged membrane potentials (N equals at least 8 for each concentration) compared to the values estimated using the Goldman equation assuming a pK:pCl ratio of 1:0.67. **(G)** *Left*, Proliferation-Voltage (PV) curve generated using the voltages estimated for different K^+ concentrations based on the data in (f). The Boltzmann fit to the data has a midpoint of -23.5 mV and a slope of -8.9. The mEAG GV curve shown in (e) has been added for comparison. *Right*, Proliferation induced by mEAG and the CaMKII binding mutant mEAG-RQEE, at K^+ concentrations predicted to result in membrane potentials of -58 and -25 mV as indicated. Only proliferation induced by the wild type channel is regulated by the membrane potential, in spite of the fact that mEAG-RQEE channels are as efficient as the mEAG in driving the membrane potential to more negative values. In paired two-tailed t-tests, $p = 0.0109$ for mEAG and 0.5069 for mEAG-RQEE, $n = 4$.

FIGURE 3.3

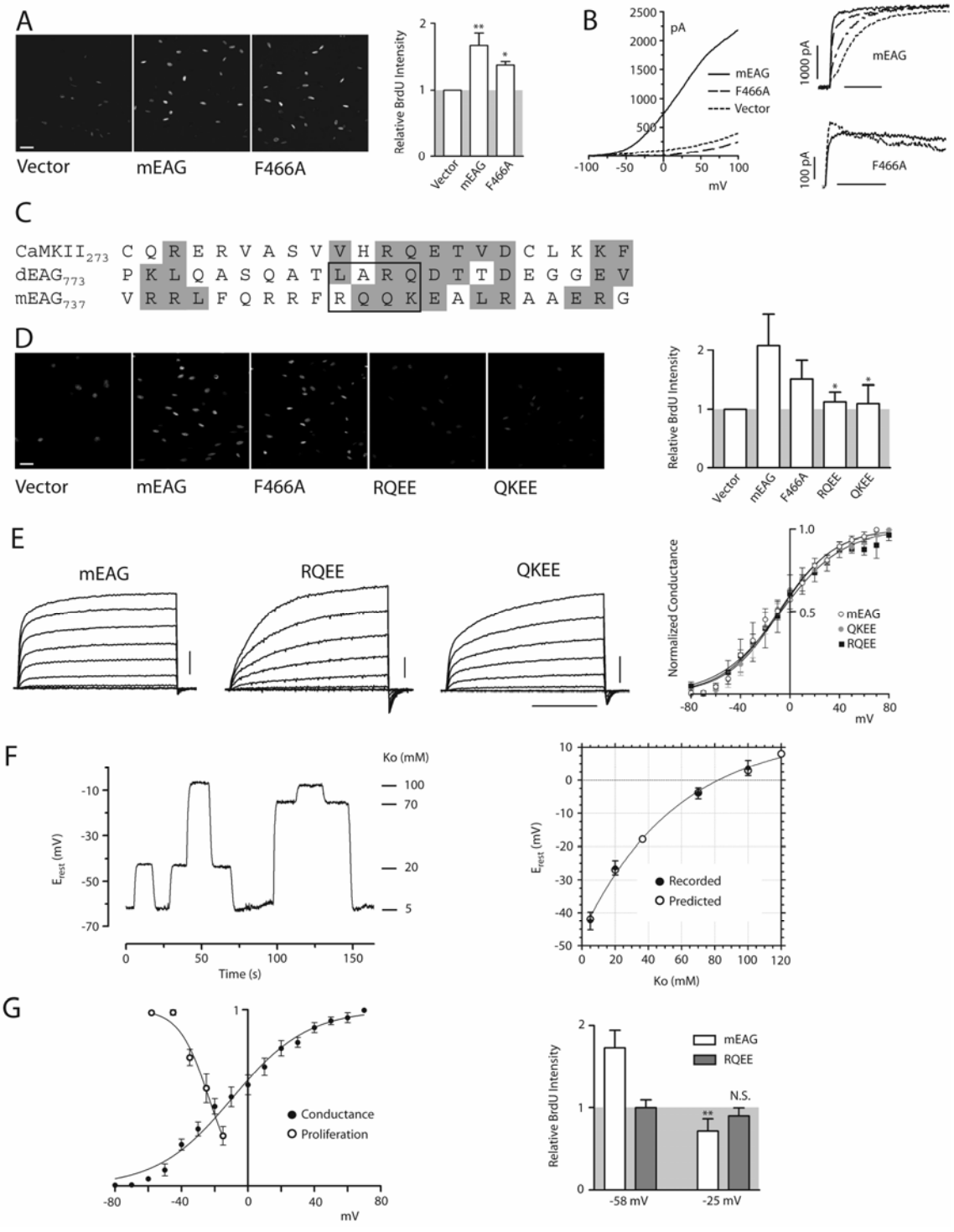
A
Vector
mEAG
F466A
Relative BrdU Intensity
B
pA
mEAG
F466A
Vector
mV
1000 pA
100 pA
C
CaMKII273 C Q R E R V A S V V H R Q E T V D C L K K F
dEAG773 P K L Q A S Q A T L A R Q D T T D E G G E V
mEAG737 V R R L F Q R R F R Q Q K E A L R A A E R G
D
Vector
mEAG
F466A
RQEE
QKEE
Relative BrdU Intensity
E
mEAG
RQEE
QKEE
Normalized Conductance
mV
F
Ko (mM)
Erest (mV)
Time (s)
Recorded
Predicted
Ko (mM)
G
Conductance
Proliferation
mV
mEAG
RQEE
N.S.
Relative BrdU Intensity
-58 mV
-25 mV

channel (Hegle et al., 2006), mEAG expression results in membrane potentials that are substantially more hyperpolarized (~ -45 mV) than those observed using dEAG (~ -12 mV). The increased working range allowed us to pursue the voltage-dependence of mEAG signaling using iso-osmotic substitution of K^+ for Na^+ in the media. The effect of $[K^+]$ on the membrane potential was determined in current clamp recordings during perfusion of extracellular solutions containing a range of K^+ concentrations; a representative experiment is shown in Figure 3.3F (*left*). Averaged membrane potentials each concentration are plotted in Figure 3.3F (*right*) and were well-approximated using the Goldman equation, assuming a permeability ratio of 1.0:0.67 for K^+ to Cl^-, respectively.

The above measurements allowed us to estimate the resting potentials of cells in proliferation assays at various extracellular $[K^+]$ concentrations. Figure 3.3G (*left*) depicts a 'proliferation-voltage' (PV) curve, in which normalized BrdU intensity is plotted as a function of voltage. The PV curve was well-fit by a Boltzmann function with half maximal activation (V_{50}) at -23.5 mV and a slope of -8.9. Comparison of the PV and GV curves suggests that that proliferation is maximal when the channels are predominantly in a closed conformation, as previously suggested for the *Drosophila* channel (Hegle et al., 2006). In addition, the steeper slope of the PV curve raises the question of subunit stoichiometry, suggesting that all four subunits may need to be closed for proliferation, and, conversely, that only one subunit of the channel may need to switch conformation for activation of CaMKII to occur. It should be noted, however, that the GV curve reflects the opening of the channel and that more accurate measurement of the movement of the voltage sensor, by assessing gating charge movement, could

eliminate this difference. Although further experiments will be needed to examine the validity of this suggestion, previous measurements of the charge and open probability valences for *Drosophila* channels indicate that the difference is negligible (Tang et al., 2000). Finally, two additional observations further support the hypothesized voltage-dependence of signaling. First, in contrast to *Drosophila* EAG, which has a minimal effect on membrane potential, non-conducting mEAG-F466A is less effective in stimulating proliferation than the wild type channel, an observation that is readily explained by its inability to shift the membrane potential. Second, voltage-dependent proliferation is not observed for the CaMKII-binding mutant, mEAG-RQEE, in spite of its ability to shift the membrane potential, indicating that voltage-dependent proliferation requires the association of CaMKII and mEAG and is not due to a voltage-dependent mechanism endogenous to NIH 3T3 cells (Fig 3.3G).

To investigate the role of EAG signaling *in vivo*, we used the GAL4-UAS system (Phelps and Brand, 1998) to express various channel constructs in the null, eag^{sc29}, background. As observed in mammals (Jeng et al., 2005; Ludwig et al., 1994; Saganich et al., 2001), *Drosophila* EAG is largely neuron-specific: EAG is expressed throughout the brain and optic lobes, and, in larvae, is enriched in the axons and terminals of motor neurons that synapse on the body wall muscle fibers (Sun et al., 2004; Wang et al., 2002c). We therefore used the neuron-specific *elav* promoter to drive EAG expression. The two primary defects observed at the larval neuromuscular junctions (NMJs) of eag^{sc29} mutants are a high frequency of spontaneous excitatory junctional potentials (EJPs) and increased amplitudes of both spontaneous and evoked excitatory junctional currents (EJCs) (Fig 3.4). In extracellular recordings of motor nerve activity, these

Figure 3.4: EAG signaling contributes to synaptic function *in vivo*.
(A) *Left*, Representative EJCs elicited by electrical stimulation of the motor nerve for w^- males (WT) and homozygous eag^{sc29} larvae, compared to EJCs observed for heterozygous wild type (WT-rescue), eag^{LAKK}, and eag^{F456A} constructs transgenically expressed using the neuron-specific *elav* promoter. Recording solution contained 0.15 mM Ca^{2+}. This low concentration of Ca^{2+} enhances amplitude differences presumably by minimizing evoked neurotransmitter release. Bars, 0.5 μA and 100 ms. *Right*, Averaged EJC amplitude data for w^- male (WT) and eag^{sc29} larvae compared to transgenically expressed eag constructs as indicated. Statistical comparisons are to the rescue condition indicated by the gray background shading, overall $p < 0.0001$. N equals a minimum of 20 muscle fibers for each condition. **(B)** *Left*, Representative recordings of spontaneous EJP activity in wild type and eag^{sc29} larvae compared to recordings from transgenic larvae expressing either wild type or LAKK channels. HL3 saline contained 0.4 mM external Ca^{2+}. Each of the 3 traces shown is a recording from a different fiber. (Bars: 20 mV and 500 ms). *Right*, Average data for the genotypes as indicated. Overall $p < 0.0001$. N equals a minimum of 20 muscle fibers for each condition. Note: There are no spontaneous EJPs in recordings from wild type larvae. In both (a) and (b) only data from muscle fibers 6 and 7 were included. For individual comparisons to the rescue condition: * $p < 0.05$; *** $p < 0.001$; N.S., not significant.

FIGURE 3.4

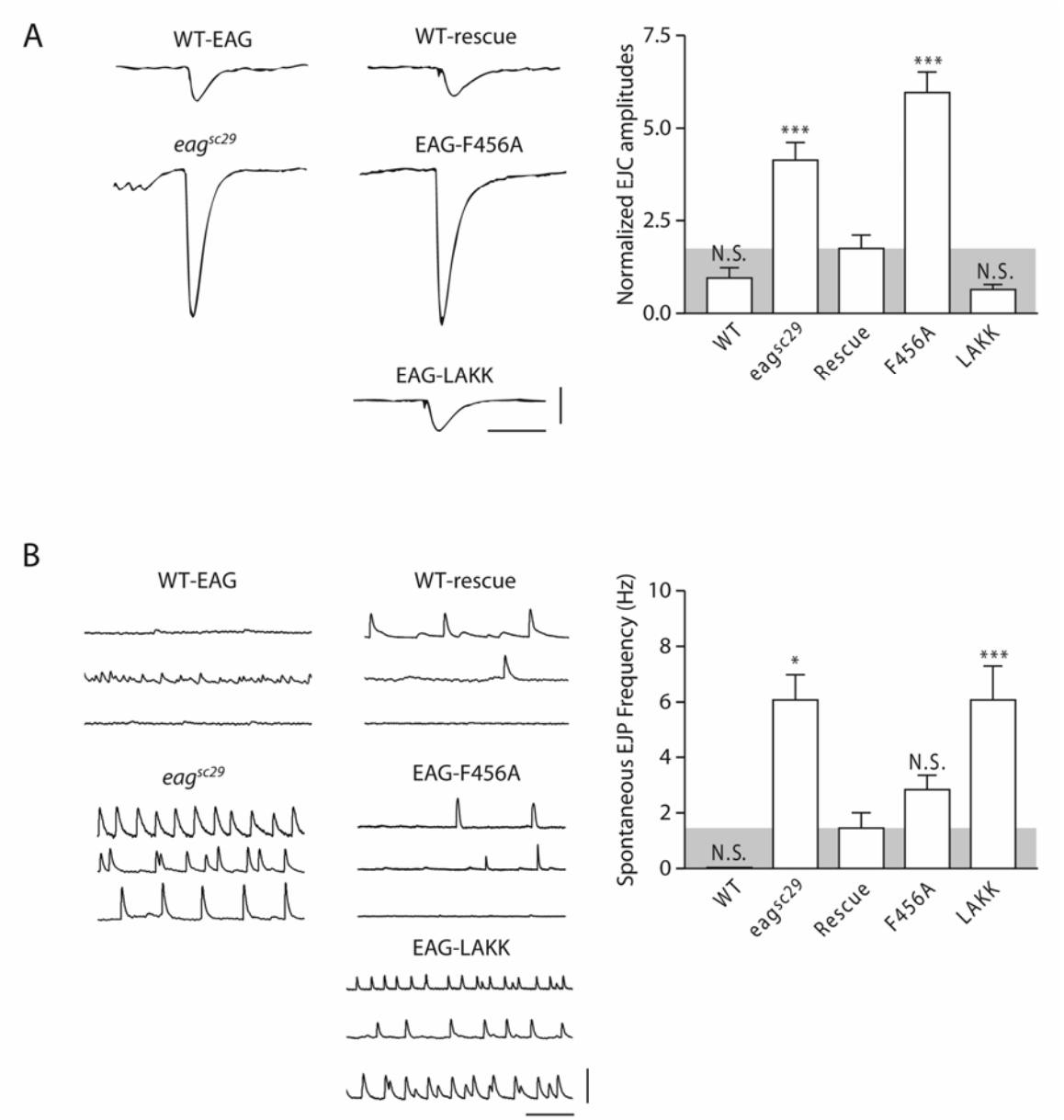
A
WT-EAG
WT-rescue
eag^sc29
EAG-F456A
EAG-LAKK
Normalized EJC amplitudes
7.5
5.0
2.5
0.0
***
***
N.S.
N.S.
WT
eag^sc29
Rescue
F456A
LAKK
B
WT-EAG
WT-rescue
eag^sc29
EAG-F456A
EAG-LAKK
Spontaneous EJP Frequency (Hz)
10
8
6
4
2
0
*
***
N.S.
N.S.
WT
eag^sc29
Rescue
F456A
LAKK

defects are readily seen to reflect hyperexcitability of the motor nerve and/or terminals (Ganetzky and Wu, 1985) and have led to the suggestion that EAG current normally contributes to the maintenance of the resting potential, in addition to the repolarization of evoked action potentials.

In comparisons of wild type, signaling- (EAG-LAKK), and conductance- (EAG-F456A) deficient constructs, both wild type and signaling-deficient (EAG-LAKK) channels restore evoked EJC amplitudes to a level that is statistically indistinguishable from wild type larvae (Fig 3.4A), whereas non-conducting EAG-F456A channels fail to rescue. These results suggest that EAG-LAKK is reasonably well-expressed and that EAG current plays the predominant role in repolarizing the motor neuron action potential. In contrast, whereas EAG-F456A expressing lines reduce the frequency of spontaneous activity to levels comparable to that observed using wild type EAG, the spontaneous activity observed in EAG-LAKK expressing larvae remains at a level comparable to that observed in eag^{sc29} (Fig 3.4B). Thus, EAG signaling, not current, plays the predominant role in maintaining a stable level of motorneuron activity, suggesting that EAG signaling may be a key player in homeostatic regulation of this synapse.

C. DISCUSSION

In summary, the EAG signaling mechanism described here suggests a novel function for the voltage sensors of ion channels that is distinct from their role in regulating ion flux. EAG signaling depends on voltage-dependent conformations of the channel: proliferation is highest when channels are predominantly in a closed conformation and

the activity of membrane-associated CaMKII is inhibited. Given that an intact CaMKII binding domain is essential for both EAG- and mEAG- mediated proliferation, and given our previous observations for p38 MAPK, our data support a model in which the suppression of CaMKII activity by closed EAG conformations relieves downstream inhibition of p38 MAPK pathway either by changing the localization or activity of a component in this pathway. This pathway also may underlie the oncogenic potential of abnormally expressed human EAG (Farias et al., 2004; Meyer and Heinemann, 1998; Pardo et al., 1999; Patt et al., 2004).

Our experiments do not address the identity of the target(s) of EAG-CaMKII signaling in either NIH 3T3 fibroblasts or *in vivo*. However, CaMKII has been well-established as a key component of synaptic plasticity and learning in a number of systems, including *Drosophila* and mammals (Griffith et al., 1993; Silva et al., 1992a,b). Through the regulation of small GTPases such as Ras, CaMKII activity regulates MAPK pathways that activate nuclear transcription factors, such as the cAMP response element binding protein (CREB), that control the transcription of activity-dependent genes (Thomas and Huganir, 2004). Specifically, Ras-mediated activation of p42/44 MAPK contributes to facilitation and long-term potentiation (LTP) (Bolshakov et al., 2000; Zhu et al., 2002), whereas p38 MAPK regulates long-term depression (LTD) (Guan et al., 2003; Thomas and Huganir, 2004; Zhu et al., 2002). CaMKII activity also contributes to p38 MAPK inactivation through the regulation of ASK1 and SynGAP (Krapivinsky et al., 2004; Takeda et al., 2004). It is therefore not unreasonable to hypothesize that EAG/CaMKII signaling may influence plasticity pathways via the downstream activation of MAPKs that mediate potentiation, depression, and learning, especially given that *eag* mutants also

have impaired associative learning, a deficiency similar to that seen in flies with inhibited CaMKII activity (Griffith et al., 1994).

D. MATERIALS & METHODS

D.1. Plasmids and construction

Wild type *eag* was subcloned into pCS2 and pPUAST vectors using EcoRI and XbaI sites flanking the coding sequence. A modified Cavener/Kozak initiation sequence on *eag* was added via PCR as a 5' extension on an oligonucleotide primer. All *eag* mutant constructs, including *eag*-F456A, *eag*-T787A, *eag*-L782K/A783K (LAKK), *eag*-R784K/Q785K (RQKK), *eag*-R1037L/K1040M (RLKM), *eag*-F731S/F734S (FFSS), *eag*-K663A/R664A (NLS1), *eag*-R698A/R699E (NLS-2), *eag*-H487E/T490E (HTEE), *eag*-T449S/A460S/T470A (TATSSA), *eag*-HTEE-F456A (HFA), *eag*-TATSSA-F456A (TFA), *meag*-F466A, *meag*-R746E/Q747E (RQEE) and *meag*-Q748E/K749E (QKEE) were generated by site-directed mutagenesis using QuikChange (Stratagene). *Eag*-ΔCT was generated by introducing a stop codon at E511. *Eag*-ΔNT was constructed using PCR by replacing the first 212 N-terminal residues with a short sequence (MRLHVWRV) to allow proper S1 membrane insertion. pCDNA3 and the pCDNA3-*meag* construct were gifts from Yi Zhou, University of Alabama at Birmingham. For oocyte expression, mutant constructs were subcloned into pGH19-*eag* (Wilson et al., 1998). All constructs were verified by sequencing. pPUAST-*eag* was co-injected along with the Δ2,3 recombinant helper plasmid into w^- *Drosophila* larvae and positive transgenics were scored for the w^+ phenotype in F1. To assess the ability of transgenic

EAG to rescue neuronal activity, UAS-*eag* was expressed using the pan-neuronal (elav5147-Gal4) driver and crossed into the eag^{sc29} null background.

D.2. Immunocytochemistry and proliferation assays

NIH 3T3 fibroblasts were maintained at 37°C and 5% CO_2 in Dulbecco's modified Eagle's medium (DMEM, Invitrogen) supplemented with 10% fetal bovine serum (FBS) as previously described (Chouinard et al., 1995). For transfection, coverslips were incubated for at least 5 hrs in DMEM containing containing 1.6 µg of the indicated cDNAs and 4 µl LipofectAMINE-2000 (Invitrogen). Coverslips were then washed and incubated in standard media for 12 hrs. Cell density at the time of transfection was critical to allow effective transfection while minimizing cell loss due to dissociation of cells from coverslips during subsequent growth. Experiments using increased concentrations of KCl were performed by equimolar substitution of KCl for NaCl in DMEM prepared according to standard formula. For BrdU labeling, 10 µM BrdU was added to each well for 3 hrs. Coverslips were washed with phosphate-buffered saline (PBS) and fixed with a 3:7 mixture of 50 mM glycine (pH 2.0)/100% ethanol for 1 hr at room temperature (RT), then denatured with 4 M HCl for 15 min. Cells were labeled with anti-BrdU fluorescein-conjugated antibody (Molecular Probes) for 45 min at 37 ^{o}C. Labeling was visualized using an Olympus BX51W1 microscope equipped with a Qimaging Retiga Exi camera and IPlab 3.6 software. BrdU fluorescence was quantified using NIH ImageJ software as described (Hegle et al., 2006). For quantification of BrdU incorporation, we scanned the regions of each coverslip with the highest cell density; this likely underestimates EAG-induced proliferation given that the blank areas on each

coverslip were excluded. Scans were background subtracted, and the intensity of all pixels above background was summed across the total area of each scan. Total intensities were averaged across all scans for each condition before normalizing to the average intensity for controls. Normalized data were then averaged across experiments (N).

D.3. Biochemistry

Cells grown on culture plates were transfected with 8μg of the indicated cDNAs and 20 μl of LipofectAMINE-2000 (Invitrogen). Cells were dissociated with trypsin-EDTA 48 hrs after transfection, washed and resuspended in PBS. Biotinylation and precipitation of EAG was performed as described (Marble et al., 2005). Briefly, cell suspensions were incubated in 2 mM sulfo-NHS-LC-biotin (Pierce) and the reaction was quenched by washing with 100 mM glycine in PBS. Cells were lysed in PBS supplemented with 1% IGEPAL CA-630, 0.5% sodium deoxycholate, 0.1% SDS, 1 mM DTT and protease inhibitors, and the homogenate was centrifuged twice for 10 min at 20,000 x *g*. Protein concentrations of supernatants were determined by Bradford assay and diluted to ~ 0.5 mg/ml. Surface proteins were precipitated with strepavidin agarose and the precipitate washed extensively before addition of sample loading buffer. Blots were probed with antisera directed against the carboxyl-terminal domain of EAG (EAG (CT); 1:2000) in blocking buffer, followed by horseradish peroxidase (HRP)-conjugated secondary antibody (1:2000), and visualized with ECL (Amersham Biosciences). Assays of CaMKII and p38 MAP kinase activity were performed using extracts prepared in buffer containing the following (in mM): 20 Tris (pH 7.4), 100 NaCl, 50 NaF, 1 Na_3V0_4, 1 EDTA, 1 DTT, 1 benzamidine, and 0.005 microcystin-LR with 1% IGEPAL CA-630,

0.5% sodium deoxycholate, 0.1% SDS, and protease inhibitors. For CaMKII activity blots, antisera were directed against phospho-Thr-286 (1:200) or total CaMKII (1:1000) (Santa Cruz). For p38 MAPK activity blots, antisera were directed against phospho-Thr180/Tyr182 (1:250) or total p38 MAPK (1:500) (Cell Signaling Technologies). Protein bands were quantified using ImageJ.

D.4. Electrophysiology

Experiments using *Xenopus* oocytes were performed as described (Marble et al., 2005). Oocytes were typically injected with 0.1-0.2 ng of RNA; non-conducting constructs were injected at 1-2 ng. The recording solution contained the following (in mM): 140 NaCl, 2 KCl, 1 $MgCl_2$ and 10 Hepes (pH 7.1 with NaOH). Pipettes had resistances of 0.3 - 0.6 MΩ. For NIH 3T3 cell recordings with an Axopatch200B amplifier, cells maintained on plates were co-transfected with pCDNA3-EGFP and the indicated constructs, and were replated onto coverslips prior to recording. Pipette resistances ranged from 3 to 6 MΩ. Unless otherwise noted, the extracellular solution contained the following (in mM): 40 sodium aspartate, 100 NaCl, 4 KCl, 1.5 $MgCl_2$, 1 $CaCl_2$, 2 glucose and 10 Hepes (pH 7.4 with NaOH). The pipette solution contained the following (in mM): 35 potassium aspartate, 110 KCl, 2 MgATP, 1 NaATP, 3 sodium phosphocreatine, 0.1 NaGTP, 8 EGTA and 10 Hepes (pH 7.4 with KOH). Larval recordings were obtained from body wall muscle fibers 6 and 7 in 3rd-instar WT, eag^{sc29} and *eag*-rescue larvae using HL3 media containing (in mM): 70 NaCl, 5 KCl, 4 $MgCl_2$, 10 $NaHCO_3$, 5 trehalose, 115 sucrose and 5 Hepes (pH7.1) with either 0.4 or 0.15 mM

$CaCl_2$. Data were collected and analyzed using an AxoClamp 20B and pClamp 9 software. All experiments were performed at room temperature.

D.5. Statistics

Unless otherwise noted, data were analyzed using one way analysis of variance (ANOVA) with Bonferroni post-hoc analysis for selected conditions. The repeated measures ANOVA was used for proliferation and biochemical assays. Data are presented as the mean ± SEM.

CHAPTER IV

DISCUSSION

Voltage-dependent signaling by EAG K^+ channels is a novel mechanism by which changes in membrane potential can directly regulate intracellular signaling pathways. Membrane-associated CaMKII activity is modulated by the EAG voltage sensor in a manner independent of channel conductance, creating a dynamic signaling complex that may underlie synaptic homeostasis *in vivo*. The aims of this thesis were to determine the mechanism underlying the ability of *Drosophila* EAG K^+ channels to stimulate proliferation when heterologously expressed in NIH 3T3 cells, to determine whether the mechanism is conserved in other EAG isoforms, and to determine whether disruption of this mechanism contributes to the phenotypes observed in *Drosophila eag* mutants. As presented in Chapter II, my studies show that EAG acts as an upstream regulator of intracellular signaling pathways and that this function is distinct from the ability of EAG to conduct K^+ ions. Most importantly, EAG signaling activity is regulated by the voltage sensor, as revealed by experiments using depolarizing concentrations of KCl or EAG mutations that shift the voltage-dependence of channel gating.

The effects of ion channels on intracellular communication have, in the past, been assumed to be indirect consequences of ion conduction. My studies on EAG contribute

to a growing body of evidence that voltage-gated ion channels are multifunctional proteins. In contrast to most other conductance-independent functions of voltage-gated channels, however, the signaling activity of EAG is regulated by changes in channel conformation associated with the position of the voltage sensor. This finding is particularly relevant to neuronal function, because it provides a novel mechanism for linking neuronal excitability to the activity of intracellular messengers. A screen of mutations in several candidate intracellular domains shows that EAG signaling requires an intact CaMKII binding domain, and biochemical experiments confirm that the activity of membrane-associated CaMKII is regulated by EAG in a voltage-dependent manner. The effect of EAG on CaMKII activity is the inverse of the effect on proliferation: decreased CaMKII activity results in increased proliferation, while mutations of the channel that increase CaMKII activity decrease proliferation. These results support a model in which CaMKII and EAG operate as a signaling complex that translates voltage-sensitive conformational changes in EAG into modulation of CaMKII, in turn regulating downstream effectors to affect the proliferative state of the cell. Voltage-dependent, conductance-independent signaling is also observed using the mammalian isoform of EAG, and similarly requires CaMKII binding, indicating that CaMKII-mediated EAG signaling is conserved.

Finally, *in vivo* experiments suggest that some of the defects observed in *Drosophila eag* mutants are due to disrupted regulation of CaMKII. Transgenic flies expressing the EAG-LAKK construct, which contains mutations in the CaMKII binding domain, yield functional currents at the neuromuscular junction as evidenced by the ability to rescue EJC amplitudes as effectively as a the wild type channel, yet the frequency of

spontaneous activity remains high. Conversely, transgenic expression of the non-conducting EAG-F456A construct fails to rescue EJC amplitudes, but restores spontaneous activity to a level much nearer to that obtained following transgenic expression of the wild type channel. These results strongly suggest that the high level of spontaneous activity characteristic of *eag* mutants is predominantly due to disrupted regulation and/or localization of CaMKII, and that the absence of EAG current only moderately contributes to this phenotype. These results are presented in Chapter III.

In this chapter I suggest further experiments that would clarify specific aspects of the EAG signaling model, including the biophysical mechanism of signaling by the EAG voltage sensor, the regulation of EAG and CaMKII surface expression by the adapter protein Camguk, and the downstream consequences of EAG-regulated CaMKII activation. In addition, I consider how these findings impact the physiological significance of EAG at the synapse, and discuss the implications for EAG signaling in cell cycle progression and oncogenesis.

A. BIOPHYSICAL MECHANISMS OF EAG SIGNALING

In formulating a model of the biophysical mechanism of EAG signaling, one must consider several questions: Do individual channel conformations permit signal activation, or do transitions between states drive signaling? How many EAG subunits are required? Moreover, how is voltage sensor movement linked to CaMKII activity? Does the voltage sensor physically interact with C-terminal-bound CaMKII, or is the link indirect? Resolving these questions will be central to a complete understanding of the voltage-

dependence of EAG signaling. Here I propose various models of voltage-dependent EAG signaling and experiments that would help to distinguish between them.

A.1. Kinetic models of EAG-regulated proliferation

Preliminary investigations showed that increasing extracellular KCl to depolarize cell membranes has an inhibitory effect on the proliferation induced by non-conducting EAG channels. Because there is presumably no difference in K^+ flux for the vector and non-conducting EAG conditions, this result led to the hypothesis that EAG-induced proliferation is maximal when the channel is predominantly in a closed conformation. Subsequent analysis of EAG mutants with shifted voltage-dependence confirmed that closed channel conformations induce proliferation, whereas the open conformation appears inhibitory (Figs 2.3, 2.4). In addition, mEAG-mediated proliferation sharply decreases upon membrane depolarization (Fig 3.3), providing further evidence that proliferation is attenuated at positive potentials. Reinterpretation of this model in its simplest form, based on the findings with CaMKII (Fig 3.2), suggests that EAG inhibits CaMKII activity when at rest, and increases CaMKII activity when the channel is open.

Several observations suggest that this model is an oversimplification of the signaling mechanism. If EAG signaling follows a Boltzmann distribution, as would be expected for a voltage-gated event, then the magnitude of the proliferation response (or kinase activity) should vary precisely in accord with changes in the half-maximal activation ($V_{1/2}$) for the wild type, TATSSA, and HTEE EAG constructs. At the mean resting potentials of -12, -18, and -28 mV for NIH 3T3 cells expressing wild type, TATSSA, and HTEE channels (Fig 2.4B), conductance-voltage (GV) curves indicate that roughly 68,

56, and 49 percent of channels are in a closed conformation, respectively. The above model then predicts that proliferation response should be highest for wild type channels and lowest for EAG-HTEE, a trend that is not observed. There are several possible mundane explanations of this discrepancy. Most notably, the measurements obtained in Chapter II are single data points and therefore do not control for subtle differences in the expression, localization, or regulation of different EAG constructs.

To begin to address the above issue, we coexpressed non-conducting EAG-F456A with Shaker to hyperpolarize the membrane potential to a level nearer the activation threshold for EAG. This was necessary because, even though *Drosophila* EAG channels are at the membrane of NIH 3T3 cells, the currents generated are minimal. Thus the average resting potential of NIH 3T3 cells expressing EAG is very depolarized, limiting the range of potentials in which to examine signaling. Coexpression with Shaker shifts the resting potential from an average of -12 mV to -45 mV, allowing proliferation to be assayed at potentials for which EAG should have a much lower p_o. By recording the membrane potential of cells coexpressing EAG-F456A and Shaker at a range of extracellular K^+ concentrations ($[K^+]_o$) and fitting the resulting data points with the Goldman equation, we were able to calculate appropriate values of $[K^+]_o$ with which to measure the effects of depolarization on BrdU incorporation. The resulting "proliferation-voltage" (PV) curve permits a direct comparison of proliferation and conductance data in NIH 3T3 cells, allowing for a more precise assessment of the basic model. Our initial results showed that driving the membrane potential to more negative values with Shaker increases proliferation compared to that stimulated by non-conducting EAG alone, again suggesting that occupancy of a closed state regulates EAG induced

proliferation. However, further interpretation of this result is difficult, because coexpression with Shaker may affect the voltage-dependence of EAG.

The possible confounding effects of Shaker were circumvented through the use of mammalian EAG, which also exhibits conductance-independent signaling activity (Fig 3.3A). In contrast to the *Drosophila* channel, mEAG exhibits robust outward current when expressed in NIH 3T3 cells and is therefore able to drive the membrane to much more negative potentials. Comparison of the voltage-dependence of mEAG proliferation with whole-cell conductance (Figure 3.3G) shows that proliferation appears to plateau at more negative potentials, for which mEAG conductance is close to zero. However, a more exacting comparison reveals that the voltage for half-maximal activation ($V_{1/2}$) of proliferation is -23.5 mV, which is more negative than the $V_{1/2}$ for activation of current (-9.2 mV). If occupancy of the open state underlies kinase activation and inhibits proliferation, the $V_{1/2}$ for proliferation and current should be similar. Secondly, the slope of the Boltzmann fit to the proliferation data (-8.9) is steeper than the slope of the Boltzmann fit to the mEAG current (22.5). It should be noted that the GV curve reflects the opening of the channel and that more accurate measurement of the movement of the voltage sensor, namely by assessing gating charge movement, could account for these differences. Alternatively, the differences in the PV and GV curves may offer important clues regarding the mechanism of voltage-dependent signaling.

One possible explanation of the different $V_{1/2}$ for proliferation and conductance is that proliferation resulting from inhibition of the constitutive activity of CaMKII occurs from a specific closed state of the channel, as opposed to occurring from all non-open states. Studies of the Cole-Moore shift of EAG activation have revealed that EAG has at least

two closed states, designated C_{slow} and C_{fast}, and at least one open state (Schonherr et al., 2002; Tang et al., 2000). During hyperpolarization, a Mg^{2+} binding pocket forms between S2/S3 and S4, that, when occupied, stabilizes C_{slow} via allosteric hindrance of S4 movement (Schonherr et al., 2002). Extracellular application of Mg^{2+} also stabilizes C_{slow}, resulting in a delay of EAG activation kinetics (Tang et al., 2000). A simplified model of EAG activation can be written

$$\mathbf{(C_{slow} \rightarrow C_{fast})_4 \rightarrow O}$$

where O is the open or activated state (modified from (Schonherr et al., 2002). Note that in this model, all four subunits must move into C_{fast} before the channel can open to conduct ions.

In order to fully characterize the state-dependence of EAG signaling, experiments that isolate specific EAG conformations will be useful for comparison to proliferation or kinase activation at C_{slow}, C_{fast}, and O states. Because the application of extracellular Mg^{2+} stabilizes C_{slow} by slowing the $C_{slow} \rightarrow C_{fast}$ transition (Tang et al., 2000), BrdU assays performed in the presence of various concentrations of Mg^{2+} may clarify the role of C_{slow} in signal activation. If C_{slow} is the main determinant of signaling, proliferation should be higher in EAG-expressing cells exposed to Mg^{2+} than for control cells. Indeed, preliminary experiments testing the effects of Mg^{2+} on EAG signaling show that proliferation of *eag*-transfected NIH 3T3 cells in the presence of 2 mM $MgCl_2$ is increased by ~50% compared to that of cells in standard media (unpublished observations). This result suggests that proliferation can only occur when channels occupy C_{slow}; however, because Mg^{2+} may affect other cellular processes, other

techniques, including altering the proportion of channels in C_{fast} (see below), would help to strengthen this conclusion.

One approach to distinguishing between the contributions of C_{slow} and C_{fast} on the activation of EAG signaling is the use of cysteine substitution and modification. In bovine EAG (bEAG), the extracellular residues L322 and S325, which reside in the S3-S4 linker region, are critical for the $C_{slow} \rightarrow C_{fast}$ transition. Replacement of L322 with cysteine decreases both the proportion of channels in C_{slow} and the time constant of slow activation (τ_{slow}), whereas cysteine substitution at S325 has the opposite effects (Schonherr et al., 2002). Homologous mutations in *Drosophila* EAG, L342C and A345C, have been generated in our lab, but the kinetic properties of these channels have yet to be characterized. If L342C and A345C have similar activation kinetics as the bEAG mutations, these mutants may be useful for determining the relative contribution of C_{slow} and C_{fast} to EAG signaling. If C_{slow} mediates signaling, cells expressing the EAG-A345C mutant should exhibit increased proliferation beyond that stimulated by wild type EAG, and the proliferation of cells expressing EAG-L322C should approach that of vector controls. In contrast, if C_{fast} contributes to signaling, EAG-L322C would be expected to stimulate some increase in proliferation compared to control cells.

Replacement of these key residues with cysteines also allows for chemical modification of the channel by charged methanethiosulfonate compounds such as MTSET and MTSES. For the bEAG mutations, application of MTSET or MTSES "locks" the channel into fast gating modes, effectively eliminating the C_{slow} state (Schonherr et al., 2002). If these compounds have a similar effect on EAG-L322C and EAG-A345C, they may also be used to test whether C_{slow} or C_{fast} regulate signaling.

Sustained application of MTSET or MTSES to cells expressing these mutants would be expected to eliminate C_{slow}-mediated signaling, and the immobilization of channels by these compounds would also inhibit any signaling mediated by state transitions. Similarly, if C_{fast} mediates EAG signaling, MTSET or MTSES application would be expected to increase signaling, or at least have no inhibitory effect on proliferation. Preliminary experiments show that these compounds do not affect proliferation stimulated by wild type EAG or EAG-F456A, indicating that nonspecific effects would be minimal.

Finally, mutations could be made in the voltage-sensing residues of S4 to disrupt channel gating or eliminate S4 movement altogether. Certainly, further support for voltage-dependent signaling could be obtained using mEAG constructs with shifted voltage-dependence, akin to the HTEE and TATSSA mutations made for the *Drosophila* channel. In addition, the creation of a "constitutively active" EAG, for example by using cysteine mutations to force disulfide bond formation, would be useful to examine the effects of EAG signaling independently of voltage-dependent regulation in both NIH 3T3 cells and flies.

A.2. EAG subunit stoichiometry

Another aspect of the voltage-switch mechanism of EAG signaling is the question of subunit stoichiometry. Must all four subunits occupy the same conformation for activation to occur, or is the conformation of one subunit alone sufficient for pathway activation? The fact that the slope of the Boltzmann curve for proliferation (-8.9) is much steeper than that for normalized mEAG conductance (22.5) suggests the hypothesis that

the movement of one subunit may be sufficient to inhibit EAG-induced proliferation, whereas all four subunits must move in order to activate the channel. As noted above, measurement of the gating charge movement during depolarization would provide a more exact comparison of EAG signaling and voltage-gated conformational shifts of the channel.

To more precisely address the subunit stoichiometry of EAG signaling, mutations of the positively charged S4 residues within individual EAG subunits could be introduced into concatameric channels. By shifting the voltage-dependence of only one subunit or, alternatively, by fusing the voltage sensor of one or more subunits into a constitutively open or closed position, the contributions of single subunits to EAG signaling may be more fully resolved.

A.3. The link between CaMKII and voltage sensor

EAG signaling is mediated through the regulation of CaMKII, both because mutation of the C-terminal CaMKII binding domain eliminates the effects of EAG on proliferation (Fig 3.1B,C), and because membrane-associated CaMKII phosphorylation is sensitive to different conformations of EAG (Fig 3.2). EAG mutations that activate proliferation correspond to decreased CaMKII activity, while mutations that inhibit proliferation are associated with increased CaMKII activity. Thus, EAG-induced proliferation appears to be propagated through a voltage-dependent reduction in the constitutive activity of CaMKII bound to the EAG C-terminus. However, the actual mechanism linking specific EAG conformations to changes in CaMKII activity remains unclear.

There are several possible models to explain the link between EAG gating and CaMKII modulation, taking into account both the specific voltage sensing mechanism of EAG, and the proximity of the voltage sensor to the kinase. In the classic "axial translation" model of K^+ channel voltage sensing, the positively charged S4 helix responds to changes in membrane potential by sliding or rotating within an aqueous gating canal formed by the other helices (Gandhi and Isacoff, 2002). If the voltage sensor of EAG operates in this fashion, the movement of S4 through the gating canal may affect CaMKII via a variety of mechanisms. In the direct model, the cytoplasmic end of S4 or the S4-S5 linker is close enough to the C-terminal-bound CaMKII to have an allosteric or electrostatic influence on kinase conformation, inhibiting bound CaMKII activity when the channel is closed. Outward translation of S4 during channel activation would thus remove the inhibition at positive potentials, leading to an increase in CaMKII activity. A second possibility is that S4 movement affects CaMKII conformation indirectly, by exerting conformational changes in the intracellular C terminus that in turn modulate the kinase. A third model supposes that S4 movement affects the availability of the CaMKII binding domain to the kinase, occluding association at rest and allowing CaMKII to bind and activate when EAG is open. These three modes of CaMKII regulation will be referred to as the 'direct', 'indirect' and 'conditional binding' models.

In contrast to the axial translation model of voltage-sensing, recent crystallization of KvAP suggests that the K^+ channel voltage sensor may actually move externally, rather than through an enclosed gating canal. In this model, S4 and a portion of S3 form a charged "paddle" that extends outward from the pore-forming helices into the lipid bilayer (Jiang et al., 2003a). The paddles are thought to respond to voltage changes by

sweeping through the hydrophobic interior of the membrane, coupling their movement to conformational shifts in the pore leading to channel activation (Jiang et al., 2003b). More recent studies have found that the voltage sensor does not extend as far into the membrane as the KvAP crystal structure suggests, but may instead lie at the protein/lipid interface (Cuello et al., 2004; Gandhi et al., 2003). In either case, voltage sensor residues that would be obscured in the classical model may be exposed and available to directly induce conformational changes in C-terminal-bound CaMKII. Alternatively, the movement of the sensor could indirectly influence CaMKII activation via conformational shifts elsewhere in the C-terminus, or affect the ability of CaMKII to bind to the channel altogether. Thus, the three models proposed above would also apply to more current models of voltage sensing. However, the specific residues responsible for modulating CaMKII activity would likely differ between the mechanisms: specifically, if the paddle model is correct, the residues at the tip of the paddle, which move the greatest distance, would be expected to exert the greatest influence on kinase activity, whereas in the axial translation model, residues near the cytoplasmic end of S4 or in the S4-S5 linker would be expected to have the greatest effect.

Regardless of the voltage sensor structure, the three basic models of CaMKII modulation described above can be experimentally distinguished. Fluorescence resonance energy transfer (FRET) is a well-established technique used to examine interactions between nearby molecules (Kenworthy, 2001; Selvin, 1995). FRET makes use of a phenomenon by which the energy of excitation of a "donor" fluorophore such as Cy2 is transferred to a nearby "acceptor" dye, which may or may not also be fluorescent. The quenching of the fluorescent donor thus indicates the presence of a nearby acceptor

molecule. Because the efficiency of energy transfer is inversely proportional to the sixth power of the distance between molecules, this technique also allows for near-angstrom measurements of separation when the dyes are attached to proteins of interest (Selvin, 1995).

Although EAG has not been crystallized, accessibility studies have identified key residues important for gating and further suggest that the EAG voltage sensor may operate via a mechanism very similar to that of Shaker (Schonherr et al., 2002; Silverman et al., 2003). With the knowledge of voltage sensor residues accessible from the cytoplasmic face of the membrane, FRET would be a powerful tool to further characterize either direct or indirect modes of CaMKII regulation. Specifically, if regulation occurs via direct interactions with the voltage sensor, one should be able to assess the distances between various residues of the EAG voltage sensor and CaMKII by attaching a donor fluorophore to accessible voltage sensor residues of EAG and measuring quenching in the presence of dye-labeled CaMKII. Labeled channels would first be characterized in oocyte recordings to determine the effects on current and gating properties, and tested biochemically for the ability to regulate CaMKII activity. If dye attachment does not interfere with voltage-dependent modulation of CaMKII, a library of FRET-ready channels could be generated by labeling residues on various EAG mutants known to affect CaMKII activity, such as EAG-HTEE/F456A (HFA) and EAG-TATSSA/F456A (TFA), and other channels with altered gating properties, such as EAG-L322C and EAG-A345C. In tests of the indirect model of CaMKII regulation, FRET could be used to investigate intramolecular interactions between the EAG voltage sensor

and C-terminal residues, including those that form the CaMKII binding domain, thus determining the extent of the voltage sensor's influence on C-terminal conformations.

One difficulty posed by this approach is the accessibility of FRET fluorophores to the EAG complex. This may be overcome by performing the experiments in cut-open oocytes, excised patches or by whole-cell perfusion of transfected cells, so that the dyes can be directly applied to the cytoplasmic face of the membrane. Moreover, although FRET would provide much information about the proximity of labeled EAG and CaMKII residues, if the key amino acids cannot be predicted via the available accessibility data, this strategy may prove to be fruitless. Another way to identify the specific EAG residues important for interactions between CaMKII and the voltage sensor would be to first characterize voltage sensor movement using compounds such as the Cys-reactive probe aminophenoxazone maleimide (APM). This compound has been used in studies of Shaker to report specific conformational shifts during gating events (Cohen et al., 2005). By comparing voltage sensor movements between EAG mutants that regulate CaMKII differently, it may be possible to narrow down the most probable residues involved, providing a clear starting point for FRET analysis.

In contrast to the direct versus indirect models, the conditional binding model of CaMKII regulation can be easily tested by coimmunoprecipitating CaMKII with EAG mutants known to affect signaling, such as EAG-HFA and EAG-TFA. Preliminarily, this model seems less able to account for data suggesting that EAG inhibits CaMKII when in the closed conformation (Fig 3.2). Nevertheless, if CaMKII coimmunoprecipi-tates with these channels, but does not coimmunoprecipitate with EAG-HTEE and EAG-TATSSA, it would indicate that the shifted voltage sensor prevents CaMKII binding. An important

technical consideration that may limit the interpretation of these results is that it is possible that CaMKII remains associated with EAG via CMG or other scaffolding proteins, even if direct binding to the EAG C-terminus is occluded by the voltage sensor at depolarized potentials.

In summary, although much work is yet to be done to identify the specific biophysical model of voltage-dependent CaMKII regulation by EAG, the results presented in this thesis suggest that EAG -induced proliferation is the result of the attenuation of CaMKII activity by closed states of EAG. Thus, CaMKII appears to be regulated by the voltage sensor, although it is unclear whether signaling is due to the inhibition of bound CaMKII activity or to dissociation of the kinase from the EAG C-terminus. A combination of site-directed mutagenesis and analysis with fluorescent probes may be able to fully resolve this issue.

B. CELLULAR MECHANISMS OF EAG SIGNALING

As presented in Chapter II, the presence of EAG promotes increases in p38 MAPK activity as well as proliferation of NIH 3T3 cells, and EAG-induced proliferation requires p38 MAPK activity (Fig 2.1, 2.2). However, p38 MAPK is likely to be several steps removed from the EAG signaling mechanism. Subsequent work, discussed in Chapter III, suggests that the most direct effect of EAG is to regulate CaMKII activity, and that regulation of CaMKII activity by EAG is voltage-dependent, as expected given the voltage-dependence of the proliferation response. Furthermore, CaMKII-mediated signaling appears to be conserved in mEAG (Fig 3.3C-E). The separate observations for p38 MAPK and CaMKII can be combined into a model in which EAG-induced

proliferation is the result of a local attenuation of CaMKII activity near the channel. Inhibition of CaMKII, or a change in CaMKII localization, is important to EAG-induced proliferation; otherwise mutations in the CaMKII binding domain would not disrupt the proliferation response (Fig 3.1B-D). Biochemical assays of CaMKII phosphorylation also show that membrane-associated CaMKII activity is lower in cells expressing EAG constructs that are predominantly closed and stimulate proliferation, and higher in cells expressing EAG constructs that are predominantly open and decrease proliferation (Fig 3.2).

If p38 MAPK is downstream and inhibited by CaMKII in the proliferation pathway, then EAG-dependent regulation of p38 MAPK activity also should be voltage-dependent. However, voltage-dependent regulation of p38 MAPK has not been detected in either the cytoplasmic or membrane-associated fractions. Thus, either the effects on p38 MAPK are limited to molecules in close proximity to EAG or voltage-dependent regulation predominantly affects the localization of p38 MAPK to a compartment that is not adequately represented by the cytoplasmic or membrane fractions. Lastly, it is possible that CaMKII inhibits proliferation by regulating a step that is downstream of p38 MAPK. In either case, the uniform regulation of p38 activity for all EAG constructs tested (data not shown) implies that EAG has effects on two distinct intracellular signaling pathways.

In the sections that follow, I discuss cellular mechanisms of EAG signaling, including other possible targets of EAG-regulated CaMKII activity, the roles of local versus global pools of CaMKII, the regulation of EAG surface expression and CaMKII association, and the possible cytoplasmic and nuclear localization of EAG or EAG fragments.

B.1. Downstream targets of CaMKII

A major unanswered question concerns the identity of downstream effectors regulated by EAG-associated CaMKII activity. According to the model proposed in Chapter III and above, EAG signaling is mediated via downregulation of membrane-associated CaMKII activity, and results in changes in the activation states or localization of downstream signaling molecules, including p38 MAPK. Potential intermediates between CaMKII and p38 MAPK include the synaptic GTPase-activating protein (SynGAP) (Krapivinsky et al., 2004) and the apoptosis-signal regulating kinase (ASK1), a known substrate of CaMKII that also influences p38 MAPK activity (Takeda et al., 2004). In addition, CaMKII activity is central to Ca^{2+} signaling pathways that control numerous cellular functions, including carbohydrate and fatty acid metabolism, muscle contraction, neurotransmitter release and synaptic plasticity (Braun and Schulman, 1995). Because of the ubiquitous nature of CaMKII, a complete analysis of the intracellular pathways mediated by EAG signaling could be a time-consuming endeavor. For example, in synapses alone, CaMKII has at least 28 different substrates (Yoshimura et al., 2000). Furthermore, the specific mechanisms by which decreased CaMKII activity upregulates or downregulates the activity of target proteins are complex and likely depend on the biochemical makeup of the cell or even that of a microdomain within a given cell. Indeed, it is possible that EAG regulation of bound CaMKII directly affects CaMKII targets that are local to EAG complexes, but has little effect on cytoplasmic substrates. *In vivo*, this type of regulation may be the consequence of the partitioning of CaMKII into membrane and cytoplasmic pools via EAG-Camguk interactions (see below).

In pursuing possible downstream targets of CaMKII, it is also important to consider that proliferation may not be the function normally regulated by EAG *in vivo*. Indeed, the effect of heterologous overexpression of EAG is cell-line specific: while EAG-mediated proliferation was observed in C2C12 myoblasts, as well as NIH 3T3 cells, expression of EAG in CHO cells had no effect on BrdU incorporation, but rather promoted cell death (unpublished observations). However, both the p38 and p42/44 MAPK pathways are implicated in learning, as well as cell cycle regulation (Ambrosino and Nebreda, 2001; Chang and Karin, 2001); thus it not clear at which point the pathway activated in NIH 3T3 cells and *in vivo* will diverge.

To date, EAG overexpression in *Drosophila* has not resulted in the appearance of visibly discernable growth defects (unpublished observations). However, a role in growth cannot completely be ruled out, given that more precise indicators such as experiments examining the effects of EAG on patterning in imaginal discs have yet to be performed. The proposed physiological role of EAG signaling is discussed in more detail below. A growth-related phenotype would simplify enhancer and suppressor screens of transgenics to identify components in the EAG signaling pathway *in vivo*.

B.2. Regulation of EAG surface expression by Camguk

If EAG signaling is mediated via changes in CaMKII activity at the membrane, it follows that the surface expression of EAG is an important component of signal regulation. One mechanism by which EAG membrane localization may be regulated is via phosphorylation of T787, which appears to be enhanced through an association with the MAGUK adapter protein Camguk (CMG) (Marble et al., 2005). In transfected COS-

7 cells, CMG normally localizes to the cytoplasm, but translocates to the nucleus when coexpressed with Tbr-1, a T-box transcription factor that is a binding partner of CMG (Hsueh et al., 2000). However, when EAG is coexpressed with CMG and Tbr-1, the channel competes with Tbr-1 to recruit CMG to the plasma membrane (Marble et al., 2005) (See Appendix, Fig A.3). This piece of evidence, along with reciprocal coimmunoprecipitation results, demonstrates a functional association between EAG and CMG. *In vitro* binding assays showed that Camguk binds to a novel SH3 domain (R_{1037}-K_{1040}) on the EAG C-terminus (Fig A.5). When this domain was mutated, EAG failed to successfully compete with Tbr-1 for CMG, resulting in a loss of CMG labeling at the membrane (Fig A.6).

In oocytes, coexpression of CMG and EAG results in increased current and whole-cell conductance (Marble et al., 2005). This enhancement is accounted for by an increase in EAG surface expression, because CMG increases the amount of biotinylated EAG in oocyte preparations (Fig A.2). CMG coexpression also increases the phosphorylation of EAG at T787, the site that has been shown to be phosphorylated by CaMKII to enhance current (Wang et al., 2002c), and suggests that CMG promotes the interaction between EAG and CaMKII (Fig A.2). These results imply that CMG may be able to regulate EAG signaling in two ways: by increasing EAG membrane expression, and by promoting interactions between CaMKII and EAG at the membrane. Indeed, these roles may be dual aspects of the same function. If CMG is normally associated with CaMKII, interactions between EAG and CMG would likely function to further stabilize the EAG-CaMKII complex.

In vitro, CMG has been shown to associate with and activate CaMKII in the presence of Ca^{2+}/CaM (Lu et al., 2003). Importantly, when Ca^{2+}/CaM is removed, CMG promotes CaMKII inactivation via autophosphorylation of T306, releasing the kinase and preventing it from being reactivated by subsequent increases in Ca^{2+}/CaM. This provides a potential mechanism by which separate pools of CaMKII may be established *in vivo*. If CMG promotes interactions between EAG and activated CaMKII during Ca^{2+} influx, it would create a membrane compartment local to EAG in which CaMKII remains active even when a decline in cytoplasmic Ca^{2+}/CaM renders the cytoplasmic pool of CaMKII inactive.

The existence of a distinct pool of CaMKII at the membrane may be important for interpreting the intracellular mechanism of EAG signaling. EAG mutants with shifted voltage-dependence that disrupt signaling have no effect on total cellular CaMKII activity in NIH 3T3 extracts, yet appear to enhance CaMKII activity that immunoprecipitates with biotinylated membrane proteins (Fig 3.2).

It would be interesting to test the effects of CMG on both EAG-mediated proliferation and the regulation of EAG-associated CaMKII activity in NIH 3T3 cells. Coexpressed CMG would be expected to promote the association between EAG and CaMKII and increase the number of channel complexes present on the plasma membrane. It is likely that the percentage of EAG channels associated with CaMKII would be increased in the presence of CMG, affecting the relative sizes of the membrane-associated and cytoplasmic pools of CaMKII. In this case, CMG coexpression would potentially increase the effect of EAG signaling at the resting potential, resulting in a much greater overall decrease in CaMKII signaling, increased proliferation and p38 MAPK activity.

The regulation of EAG surface expression by CMG may be much more relevant to EAG signaling *in vivo*. By promoting an overall increase in the size of the membrane-associated pool of EAG and CaMKII, CMG would maximize the effects of EAG signaling. Because EAG expression is enriched at synaptic terminals (Sun et al., 2004), signaling may be important for regulating homeostatic mechanisms that maintain synaptic fidelity, as discussed below.

B.3. Subcellular localization of EAG

The EAG C-terminus contains three putative nuclear localization signal (NLS) sequences (K_{663}-K_{666}, R_{698}-K_{714}, and K_{1035}-R_{1040}), as well as a leucine-rich region (L_{893}-L_{908}) that may function as a nuclear export signal (NES). If any of the localization signals are functional, proteolytic cleavage could result in the transport of EAG-associated signals to the nucleus. In addition, these sequences may influence EAG localization by counteracting normal channel trafficking to the membrane. Indeed, Figure 3.1E shows that while mutation of NLS-1 does not affect overall EAG expression in NIH 3T3 extracts, the biotinylated fraction is substantially increased compared to wild type EAG. Similar results were observed following mutation of NLS-2 (data not shown), suggesting that these NLS sequences negatively affect surface expression. These mutations also produced a decrease in BrdU incorporation (Fig 3.1D), a result that seems counterintuitive vis-à-vis the model of EAG signaling at the membrane. However, increased membrane localization of EAG may effectively "dilute" EAG signaling if CaMKII or other downstream targets are a limiting factor in these cells.

Further experiments to investigate the function of the NLS and NES domains on EAG signaling should include a characterization of the effects of NLS1 and NLS2 mutants on NIH 3T3 proliferation, as well as on p38 MAPK and CaMKII regulation. In addition, NLS3 and NES mutants as well as combinatory (NLS1/2, NLS2/NES, etc.) mutations, should be generated and analyzed. Because NLS2 is the most well-characterized NLS in EAG (the only NLS identified by ProSite and other domain search engines), it is the most promising candidate for examining the effects of channel localization on EAG signaling. NLS mutations could also be combined with EAG-HTEE, EAG-TATSSA, EAG-HFA and EAG-TFA to determine to what extent surface expression affects the voltage-dependence of CaMKII activation.

Alternatively, the effects of NLS-mediated localization on EAG signaling may be due to disruption of as yet unidentified signaling components in the cytoplasm or nucleus. EAG antibodies on Western blots reliably indicate a ~75kD fragment in addition to the ~180kD full-length EAG band. This band has normally been considered a degradation product of EAG but may actually be the product of alternatively spliced EAG mRNA, consisting of part of the N-terminus and most of the C-terminus, but lacking the transmembrane domains (Leslie Griffith lab observations, unpublished at the time of this writing). Indeed, immunocytochemical staining of EAG at a C-terminal epitope in COS-7 cells reveals some cytoplasmic, nonnuclear labeling in addition to surface expression (unpublished observations). Although the function of this smaller EAG protein is currently unknown, it contains the CaMKII-, Ca^{2+}/CaM-, and cyclic nucleotide-binding domains and may potentially be regulated by other proteins that interact with the NLS and NES sequences. It will be crucial to understand the role of this pseudo-EAG protein

as a potential regulator of cytoplasmic CaMKII activity. Because it lacks a voltage-sensing domain, it would obviously not have the same modulating function as the full-length channel, but if is able to bind and activate CaMKII in the absence of Ca^{2+}/CaM, it may be important for maintaining CaMKII activity in the cytoplasm during periods of low $[Ca^{2+}]_i$. This protein could be cloned and expressed independently of full-length EAG in NIH 3T3 cells to determine any potential contribution EAG signaling. If a comparison to the full-length channel reveals that this protein has some effect on proliferation or p38 MAPK activation, domain mutations that disrupt signaling, such as EAG-LAKK, could be readily introduced to further characterize its function.

C. PHYSIOLOGICAL SIGNIFICANCE OF EAG SIGNALING

What might be the role of EAG-mediated signaling *in vivo*? In *Drosophila* larvae, EAG is present throughout the nervous system, including the brain and optic lobes, and is enriched in the axons and endplates of motor neurons that innervate the body wall muscle (Sun et al., 2004; Wang et al., 2002c). In the larval ventral ganglion, EAG expression overlaps with that of synaptobrevin, a soluble NSF attachment receptor (SNARE) protein, suggesting that it normally functions presynaptically (Sun et al., 2004). *Drosophila eag* mutants display hyperexcitability at the NMJ, characterized by both a high degree of spontaneous action potential firing from the motor neuron and broadened EJPs in the body wall muscle fibers, implying a role for EAG in maintaining the resting membrane potential and repolarization of the action potentials of motor neurons (Ganetzky and Wu, 1985).

The results presented in Figure 3.4 suggest that the spontaneous EJP phenotype of *eag* mutants may be due to a disruption of EAG signaling. EAG-LAKK mutants cannot bind CaMKII, resulting in significantly decreased BrdU incorporation when expressed in NIH 3T3 cells (Fig 3.1B,D). When EAG-LAKK is neuronally expressed in the *Drosophila* eag^{sc29} null mutant background, it rescues the EJC amplitude phenotype as well as wild type EAG (Fig 3.4A), implying that EAG-LAKK is expressed at levels sufficient to allow repolarization of the motor neuron action potential. However, in contrast to wild type EAG, EAG-LAKK fails to rescue the increased frequency of spontaneous EJPs (Fig 3.4B). This result implies that the spontaneous activity observed in *eag* mutants is the result of disrupted EAG signaling, rather than a lack of EAG current. In this section I discuss the possible functions of EAG signaling *in vivo*, and suggest future directions for EAG signaling research.

C.1. Synaptic plasticity & homeostasis

Drosophila eag mutants exhibit impaired associative learning in courtship conditioning assays, a deficiency that is also observed in flies overexpressing *ala*, a peptide corresponding to the CaMKII autoinhibitory domain. Because larvae expressing *ala* exhibit increases in EJP frequency similar to *eag* mutants, and *ala/eag* double mutants do not produce an additive effect, EAG and CaMKII are likely to be part of a common pathway mediating synaptic plasticity and homeostasis (Griffith et al., 1994). This idea is substantiated by experiments showing that the EAG-CaMKII interaction regulates electrical stability at the larval NMJ (Fig 3.4). Together with the finding that EAG modulates CaMKII activity in a voltage-dependent manner, these results suggest an

important role for EAG/CaMKII signaling in mediating cellular responses to changes in excitability. CaMKII has been well-established as a key component of synaptic plasticity and learning in *Drosophila* and mammals (Griffith et al., 1993; Silva et al., 1992a,b). Through the regulation of small GTPases such as Ras, CaMKII activity regulates MAPK pathways that activate nuclear transcription factors, such as the cAMP response element binding protein (CREB), that control the transcription of activity-dependent genes (Thomas and Huganir, 2004). Specifically, Ras-mediated activation of p42/44 MAPK leads to AMPA receptor insertion during facilitation and long-term potentiation (LTP) (Bolshakov et al., 2000; Zhu et al., 2002), whereas p38 MAPK activation regulates synaptic depression and long-term depression (LTD) via removal of AMPA receptors (Guan et al., 2003; Thomas and Huganir, 2004; Zhu et al., 2002). CaMKII activity also contributes to p38 MAPK inactivation through the regulation of ASK1 and SynGAP, as noted above (Krapivinsky et al., 2004; Takeda et al., 2004). In NIH 3T3 cells, inhibitors of both p38 and p42/44 MAPKs inhibited proliferation in the presence of serum (unpublished observations), but only p38 MAPK was essential for serum-independent EAG (Fig 2.2C-E). It is therefore not unreasonable to hypothesize that EAG/CaMKII signaling may influence plasticity pathways via the downstream activation of MAPKs that mediate potentiation, depression, and learning.

When considering the need for homeostatic regulation of excitability, while still allowing for some degree of plasticity, the EAG signaling mechanism gains further appeal. EAG signaling would inherently include both a negative feedback loop to limit electrical excitability and a positive feedback loop on CaMKII that could "tag" the synapse with a marker for the degree of prior activity. Specifically, because one known

target of CaMKII is EAG itself, and because phosphorylation increases the surface expression of the channel, excitability would be limited by an increase in the hyperpolarizing influence of EAG. Concomitantly, the increase in EAG surface expression would lead to an increase in membrane associated CaMKII that could be "activated" by voltage even in response to depolarizations that remain subthreshold. CaMKII activity and downstream targets would be modulated by EAG conformation: at rest, predominantly closed channels would inhibit CaMKII, leading to increased p38 MAPK activity and sustaining synaptic depression. During subthreshold depolarization events, EAG channels would begin to activate, increasing CaMKII activity, thus stimulating a decrease in p38 MAPK and relieving synaptic depression, while potentially activating p42/44 potentiation pathways. This would allow plasticity mechanisms mediated by CaMKII and MAPKs to directly respond to membrane potential fluctuations in the absence of action potential-triggered Ca^{2+} influxes. In addition, this mechanism may help to maintain other intracellular Ca^{2+} pathways between action potentials. Maintaining an active pool of kinase near the membrane may be important for the resting functions at presynaptic terminals, such as neurotransmitter vesicle docking and priming, that occur between excitatory events. A proposed model of EAG/CaMKII signaling based on the results of this thesis is presented in Figure 4.1.

Future research on the physiological role of EAG signaling should include *in vivo* experiments to address synaptic potentiation and depression at the larval NMJ. Such experiments would make use of transgenic larvae expressing the various EAG signaling mutants in the eag^{sc29} null background, and comparing the degree of rescue to wild type EAG transgenics. Post-tetanic potentiation would be assessed by measuring EJC

FIGURE 4.1

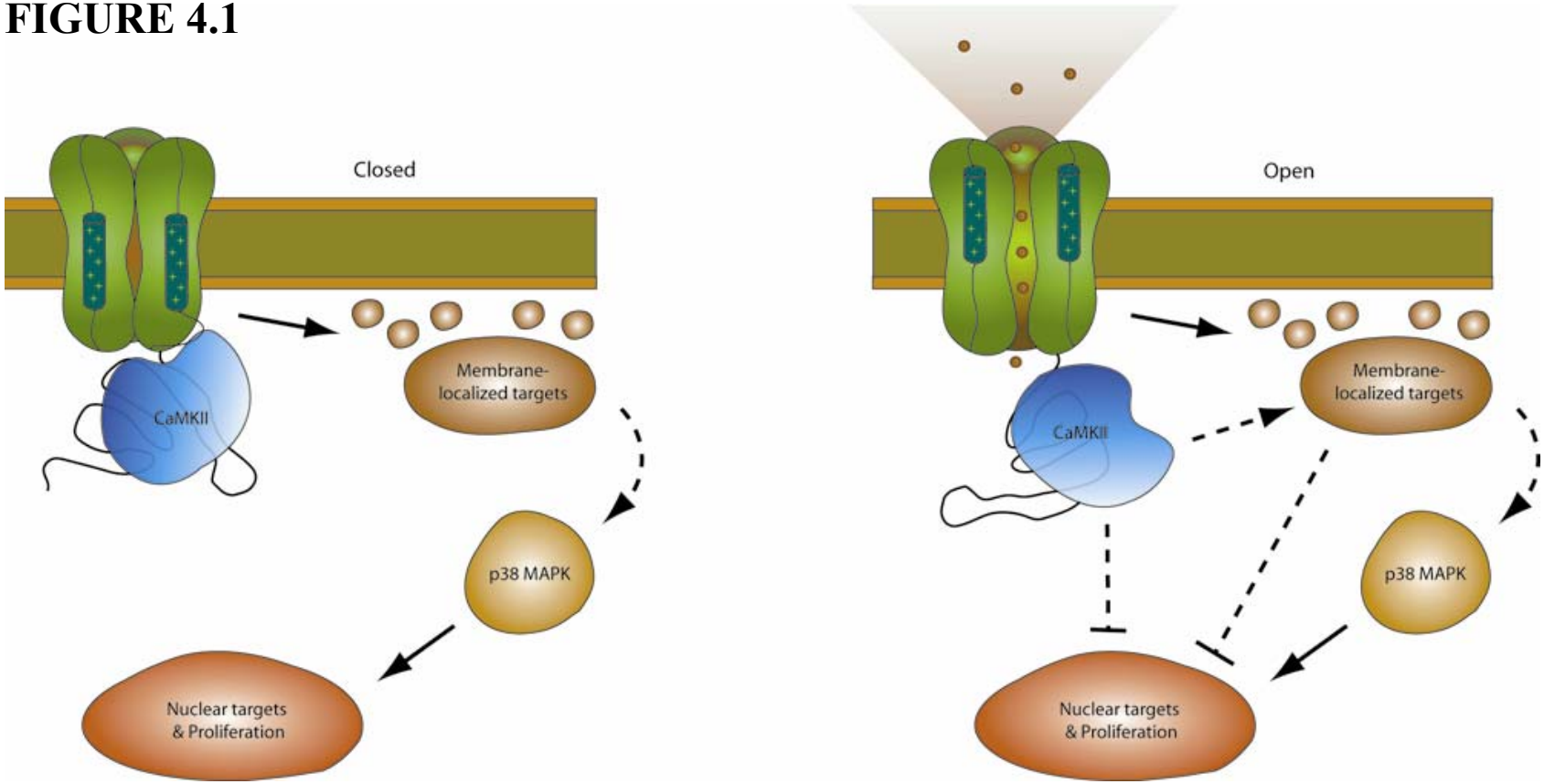

Figure 4.1: Model of EAG/CaMKII signaling. *Left*, EAG stimulates p38 MAPK activity from the closed conformation. In NIH 3T3 cells proliferation is induced, whereas *in vivo* the effect may be to depress excitability. *Right*, When EAG is in the open conformation, membrane-associated CaMKII activity is increased and inhibits proliferation. Because p38 MAPK activity is unchanged, CaMKII must act on either distinct local targets or targets downstream of p38 MAPK to cause inhibition. Solid arrows indicate known pathways; dashed arrows indicate possible pathways that would account for our observations.

amplitude and duration following stimulation by a tetanizing stimulus. Depression would be measured by recording EJCs during sustained low frequency stimulation. EAG mutations that disrupt signaling, such as EAG-HFA and EAG-TFA, which increase CAMKII activity, would likely result in normal potentiation but remove depression, whereas channels that are "locked" into a closed conformation might be expected to cause permanent depression. Biochemically, the effects of various signaling mutants on the *in vivo* phosphorylation of CaMKII, p38 MAPK and p42/44 MAPK could be assessed in immunoblot assays using extracts prepared from larvae or adult heads. The role of EAG signaling on associative learning in flies could be examined using courtship conditioning assays of signaling transgenics, and again comparing the degree of rescue of learning defects to that of wild type EAG.

C.2. Cell cycle & oncogenesis

Several lines of evidence implicate EAG in promoting tumor progression. EAG mRNA has been found in many human somatic cancers, include breast carcinomas, cervical carcinomas, neuroblastomas (Pardo et al., 1999), melanomas (Meyer and Heinemann, 1998) and gliomas (Patt et al., 2004), despite being absent from the corresponding healthy tissues. In addition, hEAG confers oncogenic properties such as increased proliferation, loss of contact inhibition and substrate independence when heterologously overexpressed in mammalian cell lines (Pardo et al., 1999). HEAG-expressing cells can also stimulate tumorogenesis when transplanted into immune-suppressed mice. As with other oncogenic K^+ channels, these effects are typically

rationalized as an effect of K^+ efflux leading to changes in membrane potential and cell volume loss (Pardo et al., 2005).

Could voltage-dependent CaMKII signaling explain the tumor-promoting effects of EAG? p42/44 MAPKs not only have a well-established role in transcriptional activation in response to growth factors and other mitogenic signals (Chang and Karin, 2001; Treisman, 1996), but also directly stimulate DNA synthesis (Graves et al., 2000) and regulate some cell cycle checkpoint proteins (Palmer et al., 1998). p38 MAPK has also been implicated in cell cycle progression (Ambrosino and Nebreda, 2001), and is important for the mitogen-stimulated proliferation of T-lymphocytes (Crawley et al., 1997). Indeed, dEAG signaling stimulates proliferation of transfected NIH 3T3 cells (Fig 2.1). However, overexpression of EAG in *Drosophila* does not appear to result in gross morphological defects (unpublished observations). To more rigorously test whether EAG signaling has an *in vivo* role in proliferation, EAG could be specifically overexpressed in eye imaginal discs, a technique is widely used in *Drosophila* to study mechanisms of proliferation and differentiation, to identify a possible growth phenotype. By comparing potential morphological phenotypes between wild type EAG, EAG-LAKK and the signaling mutants EAG-HFA and EAG-TFA, it would be possible to establish a link between EAG signaling and growth. Furthermore, the tumor-promoting effects of EAG signaling mutants could be compared by implanting transfected cells into immune-suppressed mice and comparing tumor growth with wild type EAG. If signaling regulates EAG oncogenesis, mutations that disrupt signaling would be expected to result in fewer or smaller tumors than those caused by wild type EAG.

Finally, hERG is a channel closely related to EAG that shares many structural features, including the PAS and cyclic-nucleotide binding domains. HERG is also found in variety of tumors (Cherubini et al., 2000; Lastraioli et al., 2004; Pillozzi et al., 2002), and manages to promote both tumor growth and apoptosis (Wang et al., 2002a). The results presented in Figure 3.3 show that EAG signaling is conserved in mammalian EAG channels. If signaling is conserved throughout the EAG superfamily, it may also explain the ability of hERG to regulate the cell cycle. Future investigations could examine whether EAG signaling is conserved in hERG by using BrdU incorporation and biochemical assays of CaMKII and p38 MAPK activation. Furthermore, any potential voltage dependence of hERG signaling could similarly be examined by extracellular application of KCl. Any oncogenic potential of cells overexpressing signaling-deficient mutants could also be studied by implantation into immune-suppressed mice, as proposed above for EAG.

C.3. Final conclusions

In summary, voltage-dependent EAG signaling is a novel mechanism by which changes in membrane potential are directly translated to the activity of intracellular messenger pathways. EAG signaling is mediated via conformation-dependent regulation of bound CaMKII, leading to the downstream activation of p38 MAPK and stimulation of proliferation in NIH 3T3 fibroblasts. Constitutive CaMKII activity appears to be attenuated when EAG occupies closed states, an effect that is relieved as channel conformation shifts during depolarization. Remarkably, this voltage-driven 'switch' is independent of K^+ flux, because mutations of the EAG selectivity filter to block

conductance do not prevent modulation of CaMKII, or the downstream effects of signaling.

EAG signaling is conserved in mammalian channels and may be the primary contribution of EAG at the synapse, because EAG channels that do not bind CaMKII cannot rescue spontaneous activity at the neuromuscular junction of *Drosophila eag* mutants. *In vivo*, the partitioning of CaMKII into membrane and cytoplasmic compartments by the scaffolding protein Camguk may allow the EAG-bound pool of kinase to remain active during periods of low $[Ca^{2+}]_i$, when cytoplasmic CaMKII activity is at a minimum. Membrane associated CaMKII activity would thus be modulated directly in response to local subthreshold fluctuations of the membrane potential, a possibility that has important implications for synaptic plasticity, stability and neurotransmitter release.

In conclusion, the voltage-dependent signaling mechanism presented in this thesis is highly unusual for an ion channel, and suggests that the physical coupling of membrane potential to biochemical events may be an important, previously overlooked component of cellular physiology. It is hoped that these studies will stimulate new ways of thinking about the functions of voltage-gated ion channels, help to refine current models of intracellular signaling, and lead to a better understanding of the roles of EAG and other voltage-gated channels in cancer and disease.

APPENDIX

CAMGUK/CASK ENHANCES ETHER À GO-GO K^+ CURRENT BY A PHOSPHORYLATION-DEPENDENT MECHANISM

A. ABSTRACT

Signaling complexes are essential for the modulation of excitability within restricted neuronal compartments. Adaptor proteins are the scaffold around which signaling complexes are organized. Here, we demonstrate that the Camguk (CMG)/CASK adaptor protein functionally modulates *Drosophila* Ether à go-go (EAG) potassium channels. Coexpression of CMG with EAG in *Xenopus* oocytes results in a more than twofold average increase in EAG whole cell conductance. This effect depends on EAG-T787, the residue phosphorylated by calcium/calmodulin-dependent protein kinase II (Wang et al., 2002c). CMG coimmunoprecipitates with wild type and EAG-T787A channels, indicating that T787, although necessary for the effect of CMG on EAG current, is not required for the formation of the EAG-CMG complex. Both CMG and phosphorylation of T787 increase the surface expression of EAG channels, and in COS-7 cells, EAG recruits CMG to the plasma membrane. The interaction of EAG with CMG requires a noncanonical Src homology 3-binding site beginning at position R1037 of the EAG sequence. Mutation of basic residues, but not neighboring prolines, prevents binding and

prevents the increase in EAG conductance. Our findings demonstrate that membrane-associated guanylate kinase adaptor proteins can modulate ion channel function; in the case of CMG, this occurs via an increase in the surface expression and phosphorylation of the EAG channel.

B. INTRODUCTION

Ether à go-go (EAG), the *Drosophila* ortholog of KCNH1, is the founding member of a family of potassium (K^+) channels identified by the presence of domains with homology to the PAS (Per, Arnt, Sim) and cyclic nucleotide binding domains of other proteins (Drysdale et al., 1991; Guy et al., 1991; Morais Cabral et al., 1998; Warmke et al., 1991). *eag* larvae exhibit spontaneous action potentials in the motor nerve and excitatory junctional potentials in muscle that are broadened compared to those of wild type larvae (Ganetzky and Wu, 1985). EAG is present in the axons and terminals innervating the larval body-wall musculature (Wang et al., 2002c) and is localized with synaptobrevin in the central nervous system (Sun et al., 2004).

In addition to hyperexcitability at the neuromuscular junction, *eag* mutants also exhibit defects in associative learning (Griffith et al., 1994). Intriguingly, there is substantial similarity in the electrophysiological and learning phenotypes of *eag* mutants and transgenic *Drosophila* expressing an inhibitory peptide of calcium and calmodulin (Ca^{2+}/CaM)-dependent protein kinase II (CaMKII) (Griffith et al., 1994), and phosphorylation of EAG by CaMKII results in a dramatic increase in current (Wang et al., 2002c). Recent work has demonstrated that *Drosophila* CaMKII interacts with the Camguk (CMG) adaptor protein (Lu et al., 2003). CMG is a member of the membrane-

associated guanylate kinase (MAGUK) family of adaptor proteins and the *Drosophila* ortholog of CASK and Lin-2 (Butz et al., 1998; Dimitratos et al., 1997; Hata et al., 1996; Hoskins et al., 1996). CMG/CASK/Lin-2 is unique in that the N-terminus (NT) displays considerable homology to CaMKII. The kinase domain of CMG, although appearing nonfunctional as a kinase, associates with CaMKII in an ATP- and Ca^{2+}/CaM-dependent fashion (Lu et al., 2003). Once Ca^{2+} levels decline, CMG downregulates cellular CaMKII activity by releasing the kinase in a form that must be dephosphorylated before it can be activated by subsequent increases in Ca^{2+}.

Given the regulation of EAG function by CaMKII, we sought to determine whether CMG also associates with EAG. Intriguingly, the interaction of CMG with EAG promoted an increase in whole cell conductance and alterations in inactivation kinetics that were reminiscent of the changes in current observed as a consequence of phosphorylation by CaMKII. Indeed, mutation of EAG-T787, the site phosphorylated by CaMKII, prevented the effects of CMG without affecting immunoprecipitation of the complex. Moreover, CMG increased EAG surface expression, whereas mutation of T787 decreased EAG surface expression, indicating that CMG and phosphorylation affect channel function by the same mechanism. One possible model that could account for these findings is that CMG may locally increase kinase efficiency by ensuring that only active kinase is in the vicinity of the channel.

C. RESULTS

C.1. CMG modulates EAG current

To determine whether the CMG adaptor protein might regulate EAG function, we examined EAG channels expressed in *Xenopus* oocytes either alone or together with an excess of CMG. Figure A.1, A and B, shows examples of EAG current traces and average current-voltage relations obtained from a representative batch of oocytes. In response to test pulses to +60 mV (holding potential, -80 mV), co-expression with CMG resulted in peak currents that were increased 2.7-fold over control values (Fig A.1B). CMG produced increases in current in 19 of 21 batches of oocytes examined. The increase averaged 2.3-fold above EAG controls and was significant ($p < 0.0001$) when tested using a two-way ANOVA with oocyte batch and CMG as variables. When CMG was coexpressed with *Shaker*, another *Drosophila* potassium channel, no increase in Shaker current was observed (data not shown). The average peak Shaker currents in response to test pulses to +60 mV (holding potential, -100 mV) were 12.5 ± 0.6 μA (n = 8) and 10.7 ± 0.8 μA (n = 10) in the absence and presence of CMG, respectively.

The primary effect of CMG was on EAG current amplitudes. Analysis of the voltage-dependence of EAG currents in an extracellular solution containing 25 mM KCl to enhance tail currents revealed little change in either the slope or midpoint of activation when EAG was coexpressed with CMG (Fig A.1C). Scaled representative traces for the two conditions are shown in Figure A.1D, *top*. Examination of activation and inactivation kinetics revealed only a modest increase in the inactivation time constant and a decrease in the percentage of inactivation (Fig A.1D, *bottom*). The CMG-mediated

Figure A.1: CMG increases EAG current and conductance.
(A) Coexpression with CMG increases EAG current amplitudes in *Xenopus* oocytes. Macroscopic currents recorded in two electrode voltage clamp from representative oocytes in response to depolarizing voltage steps from -100 to 80 mV in 20 mV increments (holding potential, -80 mV). Linear leakage and capacitative components have been subtracted. Calibration bars apply to both sets of traces. **(B-G)** Dark symbols and bars represent measurements obtained in the presence of CMG. **(B)** Comparison of the average current-voltage relationships obtained for one batch of oocytes (batch refers to oocytes obtained from the same frog) injected with RNA encoding *eag* (n = 7) or *eag* together with an excess of *cmg* (n = 10) as indicated. Currents were elicited by a series of voltage steps from -100 to 80 mV (holding potential, -80 mV). Leak subtraction was performed using a P/4 protocol with pulses of opposite polarity preceding each test pulse (holding potential, -80 mV). **(C)** Normalized conductance-voltage (GV) relations for wild type EAG channels, alone (n = 9) or in the presence of CMG (n = 16). For each oocyte, conductance was determined using the relation $G = I_{tail} / (V_{tail} - E_K)$ and normalized to the maximum conductance. Measurements were made in an extracellular solution containing 25 mM KCl to enhance tail currents. E_K was experimentally determined for each oocyte. Boltzmann functions fit to the averaged data had a midpoint and slope of -12.2 mV and 10.3 for EAG, and a midpoint and slope of -13.6 mV and 9.2 for EAG in the presence of CMG. **(D)** *Top*, Scaled representative traces obtained for EAG alone (I_{peak} = 3.0 μA) or together with CMG (I_{peak} = 4.8 μA). Currents were elicited by a 400 ms pulse to 40 mV from a holding potential of -80 mV. *Bottom*, Kinetics of EAG currents in the absence and presence of CMG. Three batches of oocytes with a mean fold increase in current amplitude that approximated the mean for all oocytes were selected for kinetic analysis. For each oocyte, activation (*left*) and inactivation (*middle*) taus were obtained by fitting two exponentials plus a constant to the first 200 ms of the response to a 400 ms test pulse to 40 mV (holding potential, -80 mV). The percentage of inactivation (inact) was determined by dividing the mean current obtained during the final 10 ms of the pulse by the peak current observed during the pulse. N = 26 and 28 for EAG and EAG with CMG, respectively. The effect of CMG was analyzed using a two way ANOVA with oocyte batch and CMG as variables (* $p < 0.05$; *** $p < 0.001$; N.S., not significant). **(E)** CMG fails to affect EAG-T787A. Experiments performed as in (b). n = 9 and 9 in the absence or presence of CMG, respectively. **(F)** GV relations for EAG channels expressed alone or together with CMG. Currents shown in (b) were converted to conductance using the relation $G = I_{test} / (V_{test} - E_K)$. E_K was assumed to be -80 mV. **(G)** CMG increases the average whole cell conductance in oocytes expressing the wild type, but not mutant, channel. Fold increase in the whole cell conductance for the oocytes described in (d) and three batches of oocytes expressing EAG-T787A alone or with CMG. Conductances were determined as described in (f) in response to a test pulse to 60 mV (holding potential, -80 mV). To normalize for variation in channel expression across different batches of oocytes, the mean conductance in the presence of CMG was normalized to the mean conductance obtained for that batch of oocytes expressing EAG or EAG-T787A alone. The number of oocytes examined for each condition is indicated above each bar. The effect of CMG was statistically analyzed as described in (d). Error bars represent SEM.

FIGURE A.1

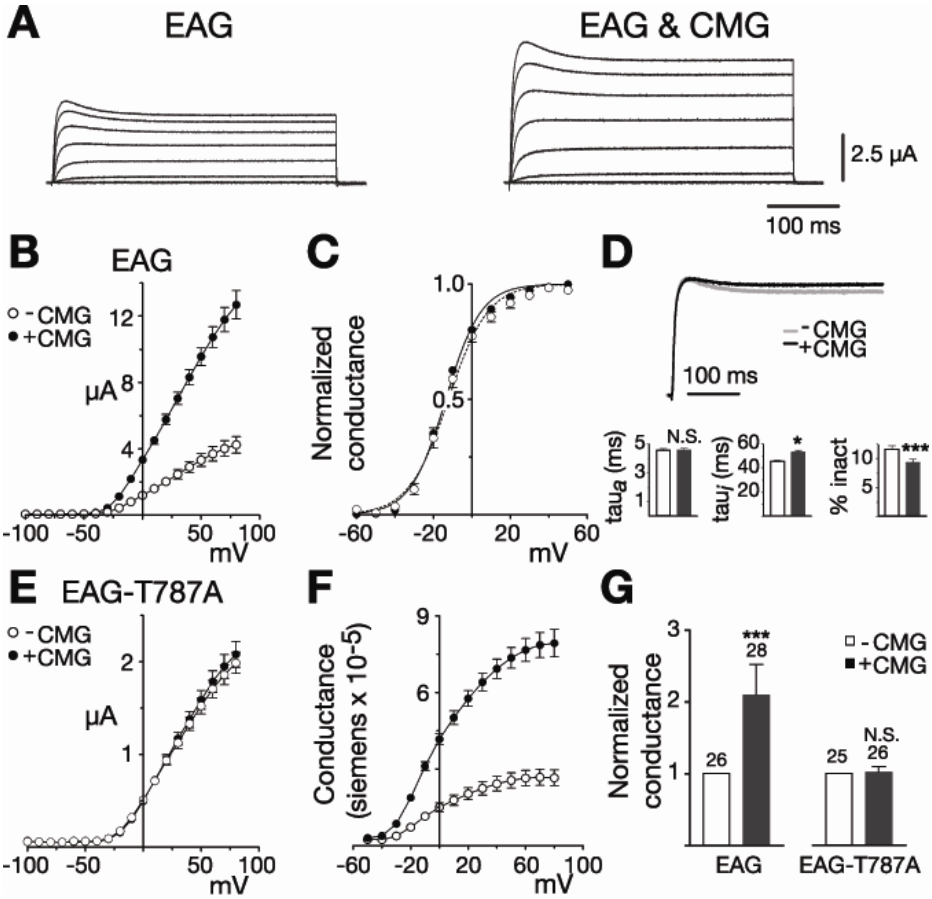
A
EAG
EAG & CMG
2.5 µA
100 ms
B
EAG
- CMG
+CMG
µA
mV
C
Normalized conductance
mV
D
- CMG
+CMG
100 ms
tau_a (ms)
N.S.
tau_i (ms)
*
% inact
***
E
EAG-T787A
- CMG
+CMG
µA
mV
F
Conductance (siemens x 10-5)
mV
G
Normalized conductance
- CMG
+CMG
***
28
26
N.S.
26
25
EAG
EAG-T787A

decrease in inactivation was observed even when comparing oocytes with similar current amplitudes, suggesting that the effect on kinetics was not caused by a decreased efficiency of the voltage clamp for larger currents.

Many adaptor proteins affect the function of associated proteins by colocalizing the proteins with other modulators. Previous work has shown that EAG is phosphorylated by CaMKII activity endogenous to the oocytes even at basal Ca^{2+} levels (Wang et al., 2002c). Both the increase in current amplitude and the changes in inactivation in the presence of CMG are reminiscent of the changes in current observed as a consequence of phosphorylation. Because CaMKII has been shown to associate with CMG in the presence of ATP and Ca^{2+}/CaM (Lu et al., 2003), we sought to determine whether the effect of CMG on EAG currents could be mediated by phosphorylation. As shown in Figure A.1E, the effect of CMG was dependent on EAG-T787, the residue previously shown to be phosphorylated by CaMKII *in vitro* and *in vivo*. When threonine at position 787 was replaced by alanine (EAG-T787A), CMG failed to increase current or affect inactivation.

The increase in current observed for wild type channels in the presence of CMG is most likely a result of an increase in the number of active channels given the lack of an appreciable change in either voltage-dependence or kinetics. Figure A.1F displays the change in EAG activity in terms of the whole cell conductance for the batch of oocytes examined in Figure A.1B. Figure A.1G summarizes and compares the effect of CMG on the whole cell conductance of oocytes expressing EAG and EAG-T787A for three representative oocyte batches. If changes in open probability or single channel conductance do not contribute to the effect of CMG on EAG current, the average increase

in conductance suggests a more than twofold increase in the number of functional channels at the plasma membrane.

C.2. EAG and CMG co-immunoprecipitate from oocyte extracts

When oocyte extracts were probed with EAG (CT) antisera (Fig A.2A, top blot, left three lanes), two protein bands were clearly identified. The primary EAG band ranged between 180 and 200 kDa depending on the protein markers used (Fig A.2A, *top*, lanes 2 & 3). The second, lower molecular weight, band was also reliably observed and is most likely an alternate modification of the protein or a degradation product. Both bands were absent in Western blots of extracts prepared from uninjected oocytes (Fig A.2A, *top*, lane 1). Immunoprecipitation reactions indicated that, in oocytes, EAG and CMG are part of the same protein complex. Immunoprecipitations using anti-CMG, but not preimmune, sera coprecipitated the EAG protein (Fig A.2A, *top*, lanes 3-4). The reverse immunoprecipitation reaction is shown in the bottom blot (right three lanes). Immunoprecipitations using anti-EAG (NT), but not preimmune, sera coprecipitated CMG, which was observed as a single band near the predicted molecular weight of 103 kDa.

C.3. CMG and phosphorylation regulate EAG surface expression

One possible explanation of the failure of CMG to enhance EAG-T787A currents in our electrophysiological experiments is that phosphorylation of T787 may be required for the association of CMG with EAG. As shown in Figure A.2A (*top and bottom*, lanes 6 and 9), there was no appreciable difference in the ability to immunoprecipitate the

Figure A.2: CMG associates with EAG and increases EAG surface expression and phosphorylation. (A) Coimmunoprecipitation of EAG and CMG from *Xenopus* oocyte extracts. Lanes 1-3 show oocyte extracts for comparison; lane 4, immunoprecipitation with pre-immune sera; lanes 5-6, immunoprecipitation with indicated antibody. CMG associates with both wild type and EAG-T787A channels. *Top* (lanes 5-6), immuno-precipitation with CMG antisera. *Bottom* (lanes 5-6), reverse immunoprecipitation with EAG (NT) antisera. Similar results were observed in five experiments. Respective loads were 5, 10 and 20 μl for extracts, immunoprecipitated and coimmunoprecipitated proteins, respectively (see Materials and Methods). **(B)** CMG and phosphorylation of EAG-T787 both increase EAG surface expression. *Top*, Oocytes were labeled with biotin for 30 min and then quenched with glycine as described in Materials and Methods before preparation of oocyte extracts. For each condition, 600 μl of extract obtained from 50 oocytes was used for immunoprecipitation with EAG (NT) antisera. Proteins were separated by SDS-PAGE, transferred to PVDF membranes, blotted with the indicated antisera, and processed with ECL. Gels were run in parallel with equal amounts of the precipitates. *Bottom*, streptavidin-labeled bands were quantified by densitometry and normalized to the intensity of the EAG band in each experiment; data are presented as the mean ± SEM; n = 3 (* $p \leq 0.05$; ** $p \leq 0.01$; *** $p \leq 0.005$). **(C)** CMG increases phosphorylation of EAG-T787. *Top*, EAG was immunoprecipitated from oocyte extracts with EAG (NT) antisera. Gels were run in parallel, proteins transferred to PVDF membranes, which were then probed with either EAG (CT) antisera (*top*) or antibody recognizing EAG phosphorylated at T787 (*bottom*) (Wang et al., 2002c). *Bottom*, EAG labeled by phospho-specific antibody. Bands were quantified by densitometry and normalized to the EAG(CT)-labeled band and the corresponding region of the uninjected oocyte lane for each experiment; data are presented as the mean ± SEM; n = 3; p values as in (c). IP, Immunoprecipitation.

FIGURE A.2

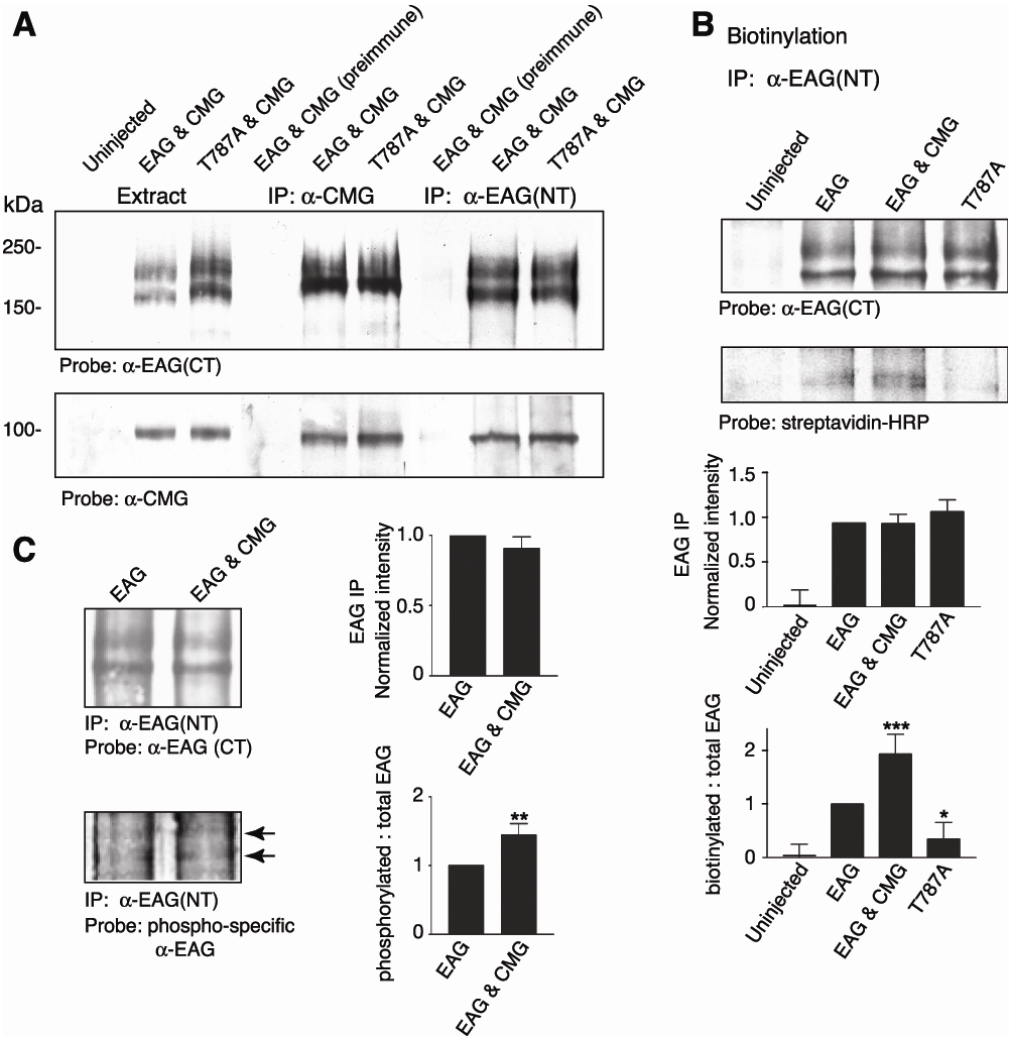
A
Uninjected
EAG & CMG
T787A & CMG
EAG & CMG (preimmune)
EAG & CMG
T787A & CMG
EAG & CMG (preimmune)
EAG & CMG
T787A & CMG
kDa
Extract
IP: α-CMG
IP: α-EAG(NT)
250-
150-
Probe: α-EAG(CT)
100-
Probe: α-CMG
B
Biotinylation
IP: α-EAG(NT)
Uninjected
EAG
EAG & CMG
T787A
Probe: α-EAG(CT)
Probe: streptavidin-HRP
EAG IP
Normalized intensity
1.5
1.0
0.5
0
Uninjected
EAG
EAG & CMG
T787A
biotinylated : total EAG
***
*
2
1
0
C
EAG
EAG & CMG
IP: α-EAG(NT)
Probe: α-EAG (CT)
IP: α-EAG(NT)
Probe: phospho-specific α-EAG
EAG IP
Normalized intensity
1.0
0.5
0
EAG
EAG & CMG
phosphorylated : total EAG
**
2
1
0
EAG
EAG & CMG

complex when EAG-T787A was expressed instead of the wild type channel, indicating that phosphorylation is not a prerequisite for formation of the complex. Either phosphorylation is required for CMG to exert an effect on EAG currents or, alternatively, the increase in current observed in the presence of CMG is the result of an increase in the efficiency of phosphorylation.

To begin to distinguish between these alternatives, we further investigated the mechanism underlying the effect of CMG on EAG current. Oocytes were surface labeled with biotin and, after biotin treatment, EAG was isolated by immunoprecipitation with EAG (NT) antisera (Fig A.2B, top blot). As shown in Figure A.2B (bottom blot) for a parallel blot of the immunoprecipitate probed with streptavidin, only the lower EAG band was detectably biotinylated. More importantly, compared with EAG channels expressed alone, there was a clear increase in the biotinylation of EAG when CMG was coexpressed (bottom blot, lanes 2 and 3). Finally, biotinylated EAG was lowest when expressing EAG-T787A (compare lanes 2 and 4). Semiquantitative comparisons of band intensities normalized to the intensity observed for wild type EAG indicated that the increases in biotinylation of EAG observed as a consequence of CMG and phosphorylation of EAG-T787 were significant (Fig A.2B, *bottom*). The average increase in biotinylation observed for EAG in the presence of CMG was comparable with the increase in whole-cell conductance observed in oocyte recordings (Fig A.1G). In addition, the decrease in biotinylation observed for EAG-T787A when compared with wild type EAG closely approximated the previously reported decrease in current observed when oocytes are injected with approximately equal concentrations of RNA (Wang et al., 2002c). A similar difference is observed in the experiments of Figure A.1

(compare the current levels in B and E). These results suggest that CMG and phosphorylation of EAG-T787 increase EAG current by the same mechanism, namely by increasing the number of EAG channels in the plasma membrane.

C.4. CMG increases phosphorylation of EAG-T787

To determine whether the increase in current observed in the presence of CMG is the result of an increase in the efficiency of phosphorylation of EAG-T787, we immuno-precipitated EAG from oocyte extracts and probed the precipitate with an EAG antibody that specifically recognizes EAG phosphorylated at T787 (Wang et al., 2002c). As shown in Figure A.2C (*left*), whereas there was no detectable difference in the overall level of EAG as a function of CMG (*top*), phosphorylation of T787 was increased when CMG was coexpressed (*bottom*). Comparisons of the level of phosphorylation averaged across multiple experiments (Fig A.2C, *right*) indicated that the change in phosphorylation was significant. In summary, the enhancement of EAG current observed in the presence of CMG appears, at least in part, to be caused by an increase in the phosphorylation of T787. It remains unclear, however, whether phosphorylation is the sole mechanism underlying the increase in conductance and surface expression of EAG given the difference in the magnitudes of the effects. One possible explanation of this difference is that phosphorylation of EAG is more likely for channels in the membrane. Differences in the solubility of cytoplasmic versus membrane-associated channels may obscure differences in phosphorylation. Alternatively, the association with CMG and phosphorylation could have synergistic effects on the surface expression of EAG channels.

C.5. EAG recruits CMG to the plasma membrane in COS-7 cells

Additional indication of a functionally relevant interaction between EAG and CMG was obtained in COS-7 cells. Our ability to examine colocalization of EAG and CMG, as well as changes in the surface expression of EAG, was hampered by the fact that the primary epitope used by the only antibody, α-EAG(CT), that recognizes EAG in immunocytochemical experiments appears to be occluded when CMG is bound; in separate experiments α-EAG(CT) was the only anti-EAG antibody examined that failed to coprecipitate CMG from oocyte extracts (Marble and Wilson, unpublished observations). Although we were unable to examine changes in the localization of EAG, experiments in COS-7 cells suggested that the EAG-CMG complex may play a role in localizing CMG, in addition to its role in the modulation of EAG current. Changes in the localization of CMG as a function of coexpression with EAG were assessed using another binding partner, Tbr-1, a T-box transcription factor known to associate with the mammalian CMG homolog CASK (Hsueh et al., 2000). As shown in Figure A.3A, little or no background labeling was observed when cells were mock-transfected with empty vector (*left top panel*). CMG expressed alone (*right top panel*) was localized to the cytoplasm and displayed a pattern consistent with a distribution to the endoplasmic reticulum as has been observed in the case of CASK (Hsueh et al., 2000). Also consistent with previous experiments, cotransfection with Tbr-1 shifted CMG into the nucleus (*right middle panel*). Most importantly, when EAG was coexpressed with CMG and Tbr-1, EAG successfully recruited a significant fraction of the CMG protein away from the nucleus to the cytoplasm and the plasma membrane (indicated by the arrows in the inset of the *left bottom panel*). In contrast, coexpression with the Shaker K^+ channel,

Figure A.3: EAG-dependent translocation of CMG to the plasma membrane of COS-7 cells. COS-7 cells were transiently transfected with 0.4 μg of each of the cDNAs indicated below each panel. **(A)** The subcellular distribution of CMG as a function of co-expressed proteins was assessed by indirect immunofluorescence using antisera directed against CMG, followed by rhodamine-conjugated anti-guinea pig IgG. The *left top panel* shows the relative absence of CMG staining when cells were transfected with the empty pCDNA3 vector. The distribution of CMG shifts from the cytoplasm *(right top panel)* to the nucleus (*left middle panel*) when Tbr-1 is coexpressed as has previously been reported for the CMG homolog CASK (Hsueh et al., 2000). As shown in the *bottom left panel*, EAG competes with Tbr-1 to recruit a fraction of CMG to the plasma membrane, whereas Shaker fails to shift CMG from the nucleus. GW-CMV-Tbr-1 was a gift from M. Sheng (Massachusetts Institute of Technology, Cambridge, MA). Images were background subtracted for display using NIH Image software. Dashed boxes indicate the magnified areas displayed in the insets. Arrows within insets point to areas exhibiting particularly robust membrane staining. Scale bar, 10 μm. **(B)** Representative line scans of fluorescence intensity for key panels in (a). In each case, the scanned segment is the area between the two arrowheads. Intensity measurements were normalized to the highest intensity point of each image. **(C)** Averaged, normalized line scan data from three separate experiments examining the distribution of CMG to the cytoplasm, nucleus, and membrane for three expression conditions: CMG (C), CMG and Tbr-1 (CT), and CMG, Tbr-1, and EAG (CTE). Note that the bottom left panel of (a) was excluded from the analysis, given our inability to distinguish between the nucleus and cytoplasm. One-way ANOVA comparisons of fluorescence intensity are between C versus CT, and CT versus CTE conditions (* $p < 0.05$; ** $p < 0.01$; *** $p < 0.001$; N.S., not significant). Error bars represent SEM.

FIGURE A.3

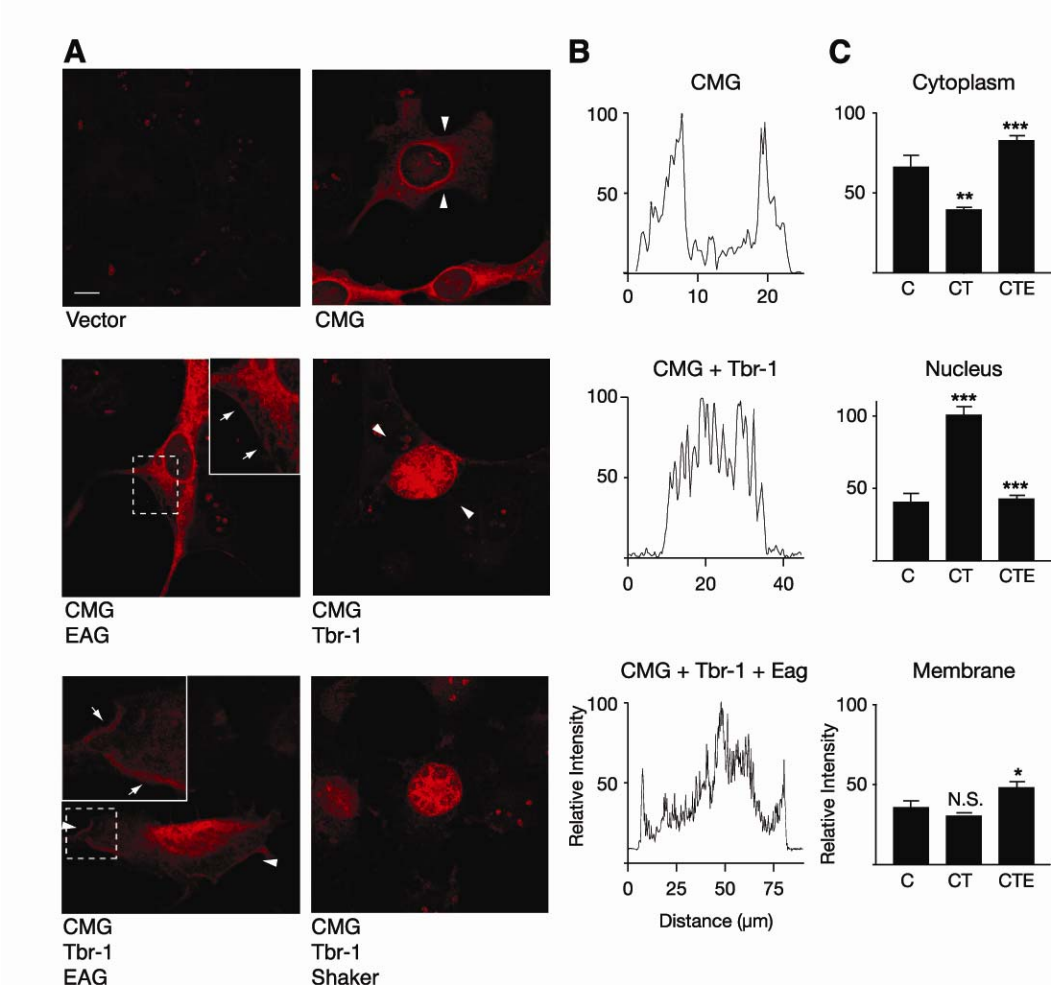
A
Vector
CMG
CMG
EAG
CMG
Tbr-1
CMG
Tbr-1
EAG
CMG
Tbr-1
Shaker
B
CMG
100
50
0
10
20
CMG + Tbr-1
100
50
0
20
40
CMG + Tbr-1 + Eag
Relative Intensity
100
50
0
25
50
75
Distance (μm)
C
Cytoplasm
100
50
***
**
C
CT
CTE
Nucleus
100
50
***
***
C
CT
CTE
Membrane
Relative Intensity
100
50
N.S.
*
C
CT
CTE

another MAGUK-interacting protein (Kim et al., 1995), failed to compete with Tbr-1 to alter CMG localization (*bottom right panel*). Finally, plasma membrane localization of CMG was also observed in the presence of EAG alone (indicated by the arrows in the inset in the *left middle panel*). Differences in CMG localization as a function of co-expression with Tbr-1 and EAG were quantified using line scans of fluorescence intensity normalized to the maximum fluorescence observed in each image examined. Figure A.3B shows representative line scans, taken across the segments indicated by the arrowheads, for the panels shown in Figure A.3A. Figure A.3C displays line scan data for the cytoplasm, nucleus, and membrane averaged across three separate experiments. In each case, EAG produced a significant change in the localization of CMG when compared with the localization of CMG in the presence of Tbr-1 (see also Fig A.6E).

C.6. EAG and CMG co-immunoprecipitate from *Drosophila* extracts

Immunoprecipitation reactions using protein extracts from wandering third-instar larvae indicated that EAG and CMG associate *in vivo*. In the experiment of Figure A.4, CMG was immunoprecipitated and the precipitates separated by SDS-PAGE. Blotting with CMG antisera identified a single band near the molecular weight predicted for CMG, 103 kDa (Fig A.4A), for immunoprecipitates from extracts of both wild type and *eag* null mutants (eag^{sc29}). More importantly, as shown in Figure A.4B, EAG was observed in both extracts (*left panel*) and CMG immunoprecipitates (*right panel*) from wild type larvae, but was absent in eag^{sc29} larvae. As observed for oocytes, the primary EAG band was higher than the molecular weight predicted for EAG, but this band was identified by three antisera raised against different regions of the EAG protein (data not

FIGURE A.4

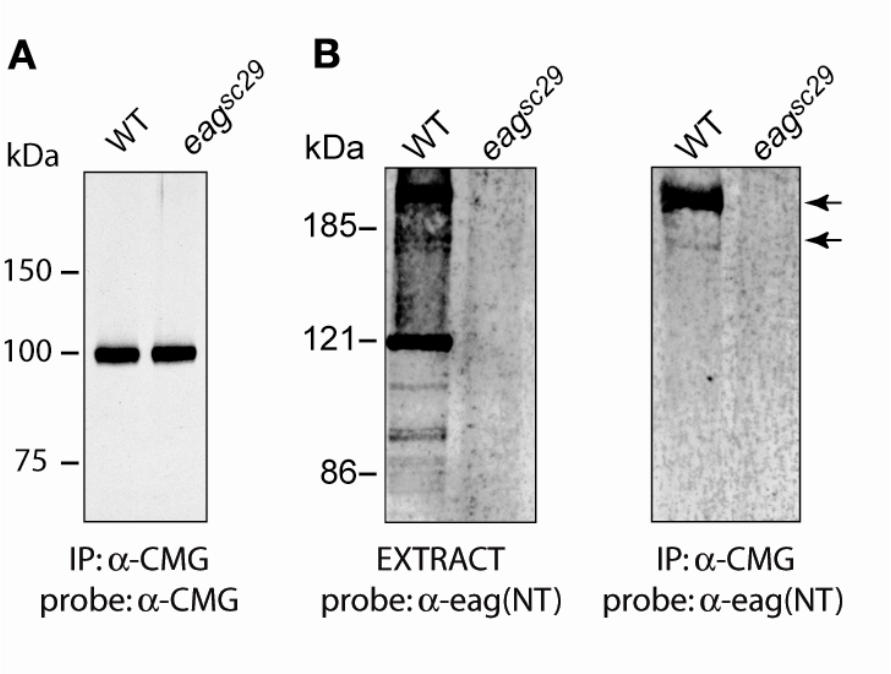

Figure A.4: Native EAG and CMG coimmunoprecipitate from *Drosophila* extracts. Protein extracts were prepared from the nervous system, imaginal discs, and body muscle fibers of third instar larvae. CMG antisera were used to immunopreciptate CMG and associating proteins from extracts prepared from the indicated genotypes. Precipitated proteins were resolved by SDS-PAGE, transferred to nitrocellulose, and then probed with either CMG (A) or EAG (NT) antisera (B, *right*), followed by HRP-conjugated anti-guinea pig or anti-rabbit IgG, respectively. For comparison, input extract probed with EAG (NT) antisera is shown in the left panel of (b). Respective loads were 5, 10, and 20 µl for extracts, immunoprecipitated and coimmunoprecipitated proteins, respectively (see Materials and Methods). Similar results were obtained in five experiments. Bands were visualized using ECL. WT, Wild type; IP, Immunoprecipitation.

shown). The EAG-CMG complex also could be observed in immunoprecipitation reactions using membrane fractions prepared from adult fly heads (data not shown). In addition, reciprocal co-immunoprecipitation of CMG using α-EAG(NT) antisera was possible, but only when CMG was overexpressed using the Gal4-UAS system coupled with the neuron-specific C155-elav driver; this is presumably because of an observed decrease in EAG precipitation efficiency when using α-EAG(NT) versus α-EAG(CT) antisera (data not shown). These results suggest that EAG and CMG are part of a protein complex *in vivo*; however, neither these results nor our electrophysiological experiments in oocytes address whether the interaction between EAG and CMG is direct.

C.7. In vitro binding assays identify a direct interaction between EAG and CMG

A direct association of EAG and CMG was suggested by *in vitro* binding assays (Fig A.5). In these assays, GST-tagged CMG or CMG domains were immobilized on glutathione sepharose beads and the ability to "pull-down" 6H-tagged EAG fragments assessed in Western blots using antibody directed against the MRSG-6H tag. The EAG and CMG fragments used to map the respective EAG- and CMG-binding sites are shown in Figure A.5, A and B, together with a rating of their relative binding. As shown in Figure A.5C for the EAG fragment 6H-EAG$_{869\text{-}1107}$, nearly all of the EAG available associated with GST-CMG (compare lanes 1 and 3). There was minimal background binding to the bead-immobilized GST tag, indicating that the association of EAG with CMG was not a result of a nonspecific effect.

Figure A.5: A direct interaction between EAG and CMG adaptor protein in *in vitro* binding assays. (A) Schematic representation and respective binding for the EAG protein constructs used in mapping experiments. For comparison, full length EAG is shown at the top with the primary domains as indicated, including the six putative transmembrane domains, pore (P), and the region with homology to cyclic nucleotide binding domains (CNBD). The amino acid residues contained in each EAG construct are noted by the subscripted numbers on the left and the relative binding of each construct to full length CMG is indicated on the right. Note that the EAG C-terminal cytoplasmic domain contains six SH3 binding motifs as defined by the PxxP consensus sequence. The locations of these potential binding sites are indicated by asterisks. **(B)** Schematic representation and respective binding for the CMG constructs used in mapping experiments as described for (a). Binding to 6H-$EAG_{869\text{-}1107}$ is shown in C-F. This fragment was chosen for display because there was minimal degradation during purification. **(C)** 6H-$EAG_{869\text{-}1107}$ binding to full length CMG and CMG domains. GST-tagged CMG fragments immobilized on glutathione Sepharose beads were assayed for their ability to pull-down 6H-$EAG_{869\text{-}1107}$ as described in Materials and Methods. *Top*, western blot probed with MRGS-6H antibody to detect interacting EAG fragments. *Bottom*, bound 6H-$EAG_{869\text{-}1107}$ quantified by densitometry; data are presented as the mean ± SEM; n = 3. **(D)** 6H-$EAG_{869\text{-}1107}$ binding to GST-SH3 domain fusion proteins. *Top*, the ability of purified GST-SH3 domains, derived from the proteins indicated above each lane, to pull-down 6H-$EAG_{869\text{-}1107}$ was in immunoblots by comparing the relative amount of associating 6H-$EAG_{869\text{-}1107}$ to the amount available during the interaction experiment (*left lane*). As shown in lanes 2 and 3, there was little or no background binding to either glutathione Sepharose or immobilized GST tag. *Bottom*, bound 6H-$EAG_{869\text{-}1107}$ quantified by densitometry; data are presented as the mean ± SEM; n = 3. **(E)** Dose-response curves comparing the binding of CMG and the CMG SH3 domains to 6H-$EAG_{869\text{-}1107}$. Wells were coated overnight with 6H-$EAG_{869\text{-}1107}$, washed, and then incubated with the indicated concentrations of GST fusion protein. Bound protein was detected using anti-GST antibody, followed by alkaline phosphatase-conjugated secondary antibody and treatment with p-nitrophenylphosphate. Binding was determined by colorimetric reaction at 405 nm. Each concentration was assayed in quadruplicate. Data are presented as the mean ± SEM; n = 4. O.D., Optical Density. **(F)** Effect of salt concentration on the 6H-$EAG_{869\text{-}1107}$-CMG complex. Experiments examining the binding to GST-CMG were performed as described in Materials and Methods, with the exception that PBS buffer was modified to include the indicated NaCl concentrations. Complex formation was relatively unaffected in up to 1000 mM salt. *Bottom*, bound 6H-$EAG_{869\text{-}1107}$ quantified by densitometry; data are presented as the mean ± SEM; n = 3.

FIGURE A.5

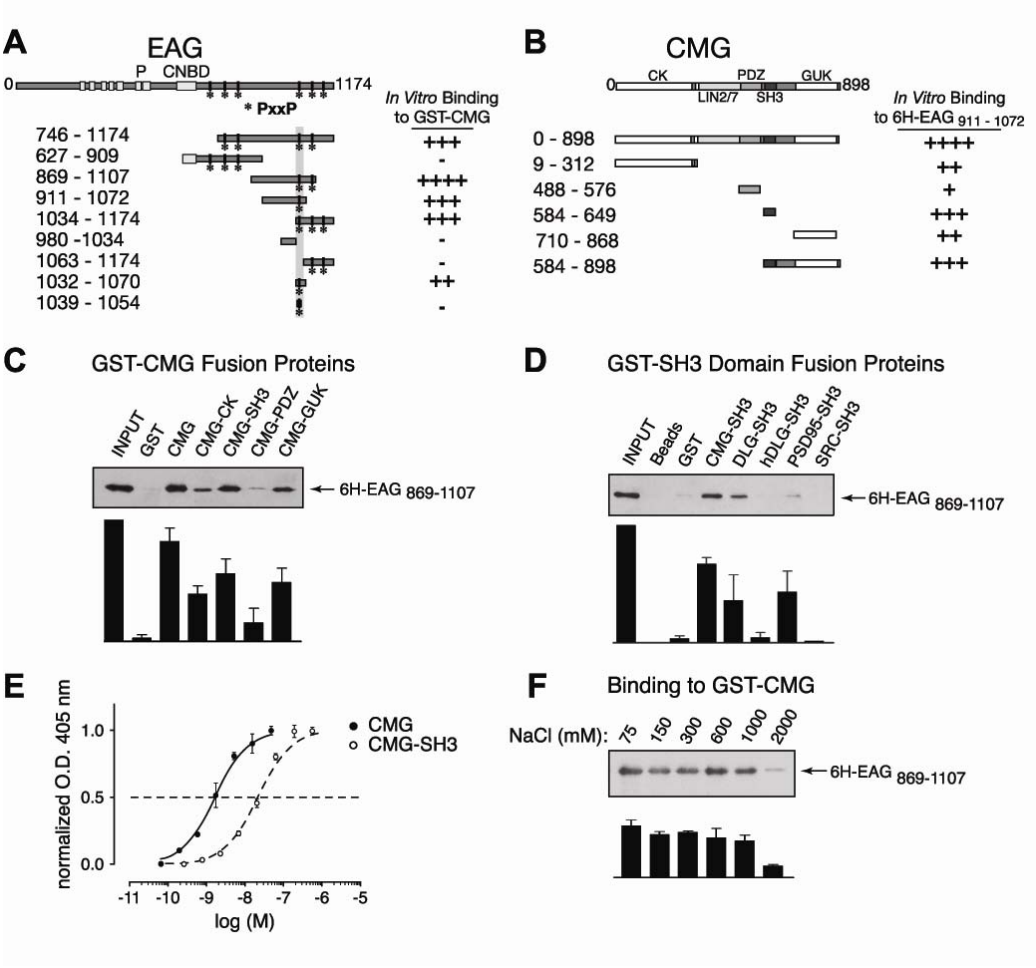
A
EAG
P CNBD
0
1174
* PxxP
In Vitro Binding to GST-CMG
746 - 1174 +++
627 - 909 -
869 - 1107 ++++
911 - 1072 +++
1034 - 1174 +++
980 -1034 -
1063 - 1174 -
1032 - 1070 ++
1039 - 1054 -
B
CMG
CK
PDZ
GUK
LIN2/7
SH3
0
898
In Vitro Binding to 6H-EAG 911 - 1072
0 - 898 ++++
9 - 312 ++
488 - 576 +
584 - 649 +++
710 - 868 ++
584 - 898 +++
C
GST-CMG Fusion Proteins
INPUT
GST
CMG
CMG-CK
CMG-SH3
CMG-PDZ
CMG-GUK
6H-EAG 869-1107
D
GST-SH3 Domain Fusion Proteins
INPUT
Beads
GST
CMG-SH3
DLG-SH3
hDLG-SH3
PSD95-SH3
SRC-SH3
6H-EAG 869-1107
E
normalized O.D. 405 nm
1.0
0.5
0.0
-11 -10 -9 -8 -7 -6 -5
log (M)
CMG
CMG-SH3
F
Binding to GST-CMG
NaCl (mM): 75 150 300 600 1000 2000
6H-EAG 869-1107

EAG C-terminal fragments associating with full length CMG associated most robustly with the SH3 and guanylate kinase (GUK) domains of CMG (Fig A.5C). Although interactions with the GST-tagged CaMKII-like and PDZ [postsynaptic density-95 (PSD-95)/ DLG/zona-occludens-1] domains of CMG were also observed, the SH3 and GUK domains came closest to approximating the binding observed to the full length CMG protein. Recent structural studies have suggested that the SH3 domain of PSD-95, another MAGUK protein, requires the GUK domain for proper orientation of the SH3 domain-binding pocket (McGee et al., 2001). However, in our experiments, there was no additional increase in the association of EAG when using a larger CMG fragment including both the SH3 and GUK domains (Fig A.5B, GST-$CMG_{584-898}$).

Additional experiments further characterized the interaction of EAG with CMG in regard to its specificity, affinity and mechanism. Figure A.5D shows *in vitro* pull-down assays examining the binding of 6H-$EAG_{869-1107}$ to a selection of SH3 domains fusion proteins immobilized on glutathione Sepharose beads. The association of EAG with the CMG SH3 domain was specific because there was minimal binding to the SH3 domains of src and the human DLG ortholog (Fig A.5D). Although EAG also bound to the SH3 domain of DLG, coexpression of EAG with DLG in oocytes failed to produce an increase in current (data not shown). In ELISAs (Fig A.5E), full length CMG bound 6H-$EAG_{869-1107}$ with a K_d of 1-2 nM, whereas the CMG SH3 domain displayed a K_d of ~ 20 nM. Thus, interactions with other domains of CMG likely contribute to the affinity of the interaction. Finally, as shown in Figure A.5F, the interaction between EAG and CMG was resistant to increases in salt concentration. Binding to CMG only decreased when

the salt concentration was increased to above 1 M, suggesting that binding is not solely mediated by electrostatic interactions.

C.8. Mapping the EAG interaction site identifies a noncanonical SH3 binding motif

Additional *in vitro* binding experiments were performed with the aim of mapping the primary interaction site in EAG. The C-terminal cytoplasmic domain of EAG contains six putative SH3 domain binding sites, as identified by the presence of a PxxP consensus sequence (Sparks et al., 1998). Indeed, as indicated on the right of Figure A.5A, any EAG C-terminal fragment that contained the fourth putative SH3 binding motif directly associated with GST-tagged CMG. To determine whether this region was sufficient for the interaction, 38 amino acids spanning spanning the fourth SH3 motif (residues 1032 – 1070) were attached to a DHFR tag. Because DHFR-$EAG_{1032-1070}$ associated with CMG (Fig A.5A), the fourth SH3 motif appears necessary and sufficient for the interaction.

Two strategies were employed to definitively establish the fourth SH3 binding motif as the site of the interaction with CMG. First, a peptide containing the fourth PxxP motif together with additional flanking amino acids ($EAG_{1039-1054}$) was synthesized, cross-linked to beads, and then examined for its ability to pull-down CMG SH3 domain that had been cleaved from the GST tag using thrombin. No association was observed even though a 16 amino acid peptide that has been used to investigate the specificity of binding to the Src SH3 domain (src peptide) (Sparks et al., 1998) associated with the Src SH3 domain under the same experimental conditions (data not shown). Second, rationalizing that the peptide may not have contained a sufficient number of flanking amino acids, we generated a point mutation in the first proline of the fourth SH3 binding

motif in the 6H-EAG$_{869-1107}$ fragment (P1045A). Little or no decrease in the association of this fragment with full length CMG was observed (Fig A.6B, compare lanes 1 and 4).

Recent work has established that some SH3 domains interact with a noncanonical binding motif characterized by an RxxK consensus sequence (Harkiolaki et al., 2003; Liu et al., 2003). As shown in Figure A.6A, this sequence also is present in EAG just four amino acids upstream of the fourth PxxP motif. Indeed, binding to CMG was substantially reduced when leucine was substituted for arginine at residue 1037 (Fig A.6B, lane 2, R1037L$_{869-1107}$). Binding to the SH3 domain was eliminated when the other basic residue in this motif, lysine at position 1040, was replaced by methionine (Fig A.6B, lane 3, K1040M).

To determine whether the above mutations were sufficient to disrupt the effect of CMG on EAG current, we returned to the oocyte expression system. As shown in Figure A.6C, which compares scaled representative traces for wild type and EAG-R1037L/ K1040M channels, channel function was largely unaffected by mutations in the SH3 domain binding site. Figure A.6D shows the result of coexpressing CMG with either wild type EAG, EAG-R1037L, EAG-K1040M, or the double mutant, EAG-R1037L/K1040M. As observed in our earlier experiments, CMG produced a more than twofold increase in the whole-cell conductance of wild type channels. The CMG-mediated increase was drastically reduced for EAG-R1037L and eliminated in EAG-K1040M and the double mutant. Finally, the SH3 binding motif also was required for the effect of EAG on CMG localization in COS-7 cells. As shown in Figure 6E, although wild type EAG produced the same changes in CMG localization observed in the experiments of Figure 3 (CTE-labeled panels), EAG-R1037L/K1040M failed to compete

Figure A.6: A noncanonical SH3 binding motif in EAG mediates the EAG-CMG interaction. (A) Comparison of the amino acid sequence surrounding the fourth putative SH3-binding motif to the amino acid sequence of the noncanonical SH3-binding site in SLP-76, the Src homology 2 (SH2) domain containing a leukocyte protein of 76 kDa. Note that both proteins also contain prolines in the nearby sequence. **(B)** *In vitro* binding assays comparing the association of 6H-$EAG_{869\text{-}1107}$ and mutant EAG fragments (R1037L, K1040M, and R1037L/K1040M EAG) to GST-CMG, as indicated. *Top*, immunoblotting with MRGS-6H antibody to detect interacting EAG fragments. *Middle and Bottom*, Coomassie-stained gels showing the relative amounts of GST-CMG and EAG fragments present in each interaction experiment. **(C)** Scaled representative traces obtained for wild type and EAG-R1037L/K1049M channels. Currents were elicited by a 400 ms test pulse to +40 mV from a holding potential of -80 mV. Peak current amplitudes were 2.2 and 5.0 μA for EAG and EAG-R1037L/K1040M, respectively. **(D)** Mutations in the EAG binding site inhibit the effect of CMG on EAG conductance. Fold-increase in the whole-cell conductance as a function of CMG coexpression for oocytes expressing wild type, R1037L, K1040M, and R1037L/K1040M EAG channels. Conductances were determined as described in Figure 1G in response to a test pulse to 60 mV (holding potential, -80 mV). To normalize for normal variations in expression across different batches of oocytes, the mean conductance in the presence of CMG was normalized to the mean conductance obtained for oocytes expressing only EAG or the indicated EAG mutants. The SE and number of oocytes examined for each condition is indicated above each bar. The effect of CMG was statistically analyzed using a two way ANOVA with oocyte batch and CMG as variables (*** $p < 0.001$; N.S., not significant). WT, Wild type. **(E)** Disruption of the CMG binding site also disrupts the ability to compete with Tbr-1 and recruit CMG out of the nucleus of COS-7 cells. *Top*, Background subtracted images for three expression conditions: CMG and Tbr-1 (CT), CMG, Tbr-1, and EAG (CTE), and CMG, Tbr-1, and EAG-RL/KM (CTR). Arrowheads indicate the segments used for the line scans presented in the middle panels. Scale bar, 10 μm. *Middle*, Representative line scans obtained as described in Figure 3C. *Bottom,* Averaged, normalized line scan data from three separate experiments examining the distribution of CMG to the cytoplasm, nucleus and membrane for the three expression conditions. One-way ANOVA comparisons of fluorescence intensity between CT versus CTE and CTE versus CTR conditions were significant (*** $p < 0.001$). In contrast, there was no significant difference (N.S.) between the CT and CTR conditions. Error bars represent SEM.

FIGURE A.6

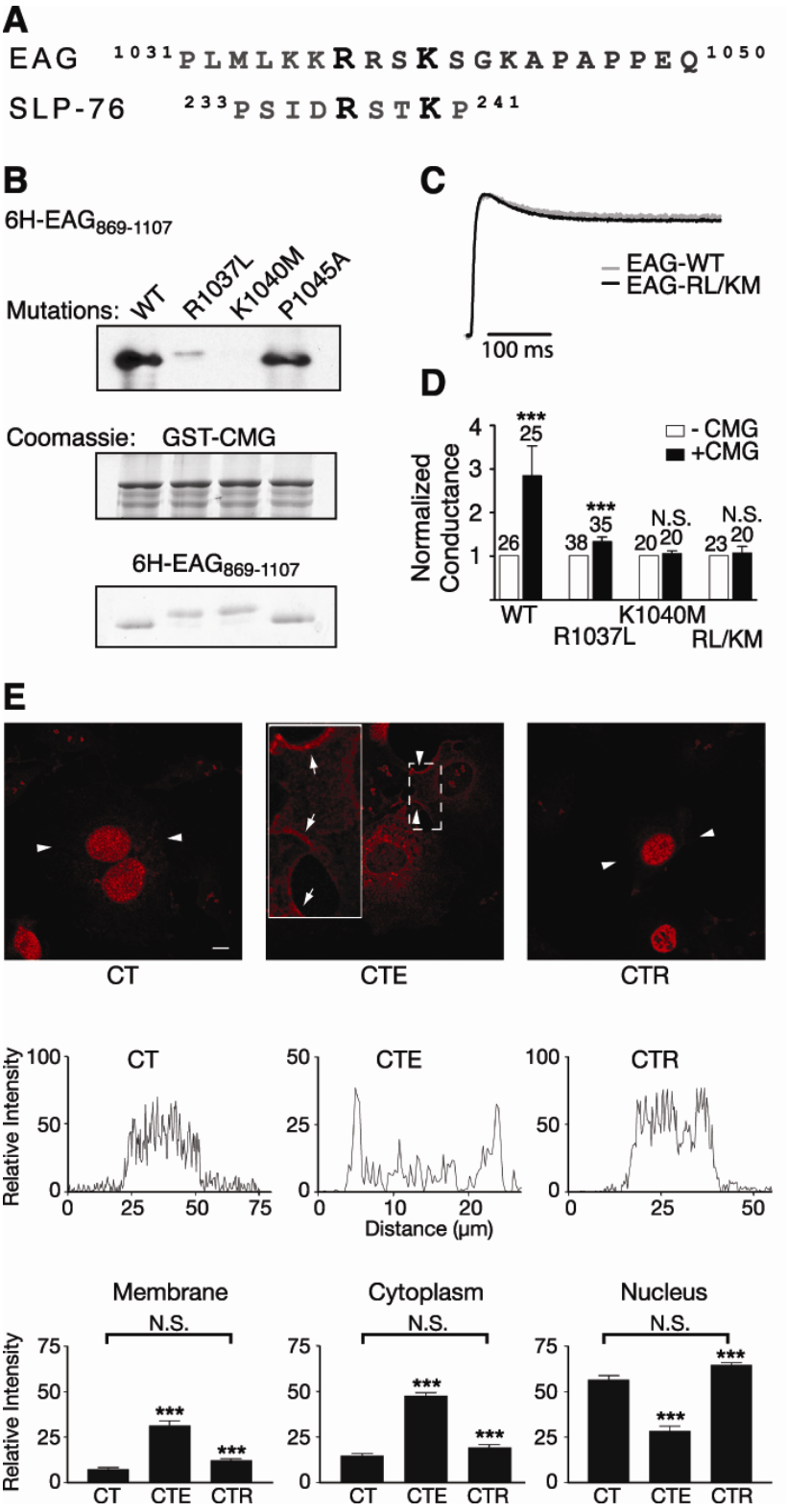
A
EAG 1031 P L M L K K R R S K S G K A P A P P E Q 1050
SLP-76 233 P S I D R S T K P 241
B
6H-EAG869-1107
Mutations: WT R1037L K1040M P1045A
Coomassie: GST-CMG
6H-EAG869-1107
C
EAG-WT
EAG-RL/KM
100 ms
D
Normalized Conductance
- CMG
+CMG
***
N.S.
WT
R1037L
K1040M
RL/KM
E
CT
CTE
CTR
Relative Intensity
Distance (μm)
Membrane
Cytoplasm
Nucleus

with Tbr-1 (CTR-labeled panels). When statistically analyzed using a one-way ANOVA, there was no significant difference in the distribution of CMG to the membrane, cytoplasm, or nucleus when comparing averaged line scan data for the CMG and Tbr-1 (CT) and CMG, Tbr-1, and EAG-R1037L/K1040M (CTR) conditions. Together, these results indicate that a direct interaction between EAG and CMG is required for the effect EAG on the localization of CMG, as well as the effect of CMG on EAG current.

D. DISCUSSION

Our findings indicate that EAG is functionally regulated by an association with the CMG adaptor protein. The primary effect of CMG is to increase EAG current and whole-cell conductance, and this increase depends on a direct association between proteins, because mutations of the CMG binding motif in EAG prevent the effect. In addition, EAG successfully competes with another CMG/CASK-interacting protein to alter the localization of CMG. Thus, another distinct function of the EAG-CMG complex may be to localize CMG to the plasma membrane.

The mechanism primarily responsible for the increase in current appears to be an increase in the surface expression of EAG. Intriguingly, effects opposite those produced by CMG, namely decreased EAG current, decreased surface expression of EAG, and decreased inactivation, are observed when phosphorylation of EAG-T787 is prevented either by mutation of the phosphorylation site or by inhibition of CaMKII (Wang et al., 2002c). These findings suggest that the effect of CMG is produced by an increase in the phosphorylation of EAG-T787. In agreement, CMG increased the phosphorylation of EAG-T787, and mutation of this site prevented the CMG-mediated increase in EAG

current without disrupting formation of the EAG-CMG complex. These results suggest that the mechanism underlying the effect of CMG is indirect and point to a change in the localization or activity of either a kinase or phosphatase in the vicinity of the channel. In addition, however, the possibility that CMG also directly affects the surface expression of phosphorylated EAG has not been ruled out. Direct and indirect effects of CMG may additively affect the membrane association of EAG channels.

At present, the enzyme most likely responsible for mediating the effect of CMG is CaMKII. EAG-T787 has previously been shown to be phosphorylated by CaMKII, inhibition of CaMKII has been shown to decrease EAG current, and CaMKII directly associates with CMG (Lu et al., 2003; Wang et al., 2002c). However, it is not known whether other kinases such as protein kinase A can also phosphorylate T787, nor has the phosphatase responsible for dephosphorylating T787 been identified. Our results do not rule out the possibility that CMG may change the localization, activity or efficiency of another kinase or a protein phosphatase. Nonetheless, given that CMG interacts with CaMKII (Lu et al., 2003) and given that no interaction between CMG (or its orthologs) and other kinases or phosphatases has been identified, the most likely model accounting for the CMG effect on EAG is one in which a common association with CMG colocalizes EAG with CaMKII and increases the efficiency of phosphorylation.

Intriguingly, after decreases in Ca^{2+}, the association with CMG promotes phosphorylation of T306 of CaMKII, rendering the kinase inactive and then releasing it (Lu et al., 2003). CaMKII cannot be activated by subsequent increases in Ca^{2+} as long as phosphorylation of T306 persists. The creation of a pool of inactive kinase predicts that CMG should have produced a decrease in EAG current, rather than the observed increase

at basal Ca^{2+} levels. These observations can be reconciled, however, if the cytoplasm and the local membrane are considered as separate compartments. Because CMG only associates with active kinase, CMG, in addition to globally increasing the pool of inactive kinase, may ensure that only active kinase is in the vicinity of the channel. Alternatively, EAG may directly or indirectly change the effect of CMG on CaMKII. Assuming that the majority of EAG is normally localized at the membrane, either alternative would result in an increase in active kinase at the membrane versus the cytoplasm. The stability of the CMG/CaMKII complex may also be regulated by the activity history of the synapse. Ca^{2+} influx can cause T287 phosphorylation, which, in addition to making the kinase activity Ca^{2+}-independent, can decrease the off-rate of CaM by four orders of magnitude (Putkey and Waxham, 1996). CaMKII with "trapped" CaM would be resistant to deactivation by CMG even at low intracellular Ca^{2+}. EAG that was localized at a synapse that had been previously active then would be expected to be susceptible to CMG regulation.

The common association of CMG with EAG and CaMKII suggests that CMG acts as the central scaffold for the complex. However, EAG also directly associates with activated CaMKII (Sun et al., 2004), suggesting that EAG and CMG play equally important roles. The association between EAG and CaMKII constitutively activates the kinase and CaMKII remains associated with EAG even once Ca^{2+} returns to resting levels (Sun et al., 2004). Thus, the presence of EAG in the complex may alter the net effect of CMG on CaMKII activity. Finally, although phosphorylation of EAG-T787 is likely to occur via the constitutively active kinase, this constitutive activity is considerably lower than that of the fully activated kinase (Sun et al., 2004). Indeed, in our experiments, the

association with CMG further increased EAG currents and phosphorylation of the channel above and beyond the levels achieved by the CaMKII endogenous to oocytes. CMG may localize and then transfer CaMKII to EAG, or CaMKII holoenzyme, which has 12 subunits, may be able to bind to both EAG and CMG simultaneously. In addition, CMG may increase the number of CaMKII molecules in the vicinity of the channel, and interlocking all three proteins may further stabilize an EAG-CMG-CaMKII complex.

The clearest demonstration of the physiological importance of CMG/CASK/LIN-2, to date, has been obtained in *Caenorhabditis elegans*, in which a complex of proteins including LIN-2, LIN-7 and LIN-10 localizes the receptor tyrosine kinase LET-23 to the basolateral surface of vulval precursor cells. The absence of LIN-2, LIN-7 or LIN-10 results in mislocalization of LET-23 receptors, causing a vulvaless phenotype (Kaech et al., 1998). The LIN-2--LIN-7--LIN-10 complex appears evolutionarily conserved because a similar complex, consisting of CASK, Velis and the munc18-1 interacting protein Mint1, homologs of LIN-2, LIN-7 and LIN-10, respectively, has been observed in the mammalian central nervous system (Butz et al., 1998). These authors suggest that CASK is a scaffold for proteins involved in synaptic vesicle exocytosis and cell adhesion. The presynaptic complex may include not only Velis and Mint1, but also N-type Ca^{2+} channels and neurexins (Hata et al., 1996; Maximov et al., 1999). When combined with the previously demonstrated presynaptic localization of EAG, CMG and CaMKII (Lu et al., 2003; Sun et al., 2004; Wang et al., 2002c), our findings provide additional support for a role of CMG/CASK in presynaptic function *in vivo*.

E. MATERIALS AND METHODS

E.1. Plasmids and construction

For protein purification, plasmids containing DNA fragments spanning the indicated amino acids were generated by PCR using primers containing restriction sites and bases to maintain reading frame during subcloning. Glutathione S-transferase (GST) and 6Histidine (6H) fusion constructs were generated using the pGEX-4T1 or pGEX-KG vectors (Amersham Biosciences, Piscataway NJ) (Guan and Dixon, 1991) or the pQE30 vector series (Qiagen, Valencia CA), respectively. Where indicated, sequence encoding dihydrofolate reductase (DHFR) was subcloned into the pQE-*eag* construct to aid in the purification and identification of the small EAG fragment. PQE32-$eag_{869-1107}$ was a gift from B. Ganetzky (University of Wisconsin, Madision, WI). With the exception of the SH3 domains of CMG and *Drosophila* discs large (DLG), GST-SH3 domain fusion proteins were a gift from Brian Kay (Argonne National Laboratory, Argonne IL). Site-directed mutagenesis was performed using the PCR-based QuikChange mutagenesis kit (Stratagene, La Jolla CA).

For expression of EAG mutant constructs in *Xenopus* oocytes, *Sph* I and *Nae* I sites flanking the EAG SH3 domain binding site were used to subclone single site mutations from pQE-*eag* constructs into pGH19-*eag* (Wilson et al., 1998). A Kozak sequence was added to pGEX-*cmg* using PCR, and *cmg*, together with the Kozak sequence, was shuttled into pBluescript-KSM (a gift from W. Joiner and L.K. Kaczmarek, Yale University, New Haven, CT), which had been modified to contain the untranslated regions of the *Xenopus* β-globin gene and a more flexible cloning site. All constructs were verified by sequencing.

E.2. Protein purification

GST-fusion proteins were purified according to manufacturer protocols (Amersham Biosciences). BL21 cells were freshly transformed with the construct of interest. Large-scale (1 L) cultures were grown in Luria Broth (LB) with ampicillin for 6 hrs and then induced for 6-12 hrs with isopropyl-β-D-thiogalactopyranoside. Bacteria were harvested by centrifugation, lysed, and cellular protein solubilized in buffer containing 150 mM NaCl, 20 mM Tris (pH 7.4) and 1% Triton X-100 in the presence of protease inhibitors (0.5 mM phenylmethanesulfonyl fluoride and 0.004 mg/ml each of aprotonin, pepstatin A, and leupeptin). In some cases GST-CMG was purified by incubation with 0.8 % N-lauroylsarcosine prior to solubilization and then neutralized with twice the concentration of Triton X-100. This increased the yield of CMG protein without affecting binding activity. Protein suspensions were centrifuged to remove insoluble material, and the supernatant incubated for 60-90 min with Glutathione-Sepharose 4B beads (Amersham Biosciences). Bead-immobilized proteins were extensively washed with 150 mM NaCl, 20 mM Tris (pH 7.4) and stored as a 50% slurry at 4 °C until use. 6H fusion proteins were purified similarly using nickel-nitrilotriacetic acid beads (Qiagen, Valencia CA) and a solubilization buffer containing 500 mM NaCl, 20 mM Hepes (pH 7.8) and 1% Triton X-100 in the presence of protease inhibitors. 6H fusion proteins were fractionally eluted from beads using successively increasing concentrations of imidazole ranging from 8 to 400 mM. Eluted fractions were checked for the presence of the desired protein using SDS-PAGE, and fractions containing the protein were pooled and dialyzed overnight in PBS (consisting of the following, in mM: 136 NaCl, 2.7 KCl, 10 Na_2HPO_4, 1.8 KH_2PO_4, pH 7.4). Dialyzed protein was stored at 4°C or frozen at -20°C prior to use. Protein

concentrations were determined by comparison to known concentrations of bovine serum albumin (BSA).

E.3. Peptides and antibodies

Peptides used for binding studies and immunization were synthesized by Open Biosystems (Huntsville, AL). An N-terminal peptide corresponding to amino acids 161-179 of the EAG sequence and a purified C-terminal (CT) fragment (6H-$EAG_{1034-1174}$) were used for immunization of rabbits according to standard procedures (Open Biosystems). Sera were screened against the antigens in ELISAs and in Western blots of purified N- or C-terminal EAG fragments as appropriate. Purified GST-$CMG_{152-897}$ was used for the immunization of guinea pigs as previously described (Dimitratos et al., 1997). Phosphospecific anti-EAG antibody was a gift from Leslie Griffith (Brandeis University, Waltham, MA).

E.4. *In vitro* binding assays

GST fusion proteins immobilized on Sepharose beads were mixed with 6H fusion proteins in PBS containing 0.5% Triton X-100 and protease inhibitors (EDTA-free Complete tablets; F. Hoffmann-LaRoche, Basel, Switzerland) and incubated with shaking for 2-3 hrs at 4 °C. Except where indicated otherwise, the protein concentrations used were 1-2 and 0.5-1 μM, respectively, in 100 μl buffer containing a constant 10 μl bead bed volume. The beads were collected by centrifugation and then washed three times with PBS containing 0.1% Triton X-100, followed by three washes with 50 mM Tris, pH 8.0, 140 mM NaCl, 0.1% Triton X-100, and a final wash with 50 mM Tris, pH 8.0. The

pellets, including beads and associated proteins, were resuspended in sample buffer and analyzed by SDS-PAGE and Western blotting. Blots were probed with MRGS-6H antibody (Qiagen) followed by horseradish peroxidase (HRP)-conjugated anti-mouse secondary and then visualized with ECL (Amersham Biosciences).

E.5. ELISAs

ELISAs were performed as described previously (Garcia et al., 1998; Muller et al., 1996) with minor modifications. GST-CMG fusion proteins were eluted from glutathione Sepharose according to manufacturer protocols (Amersham Biosciences). 6H-$EAG_{869-1107}$, at a concentration of 0.16 μg/ml in BBS (125 mM borate, 75 mM NaCl pH 8.5), was bound to the wells of Costar (Cambridge, MA) 96-well assay plates by overnight incubation (4°C). Plates were then washed extensively with BBS and blocked with BBS containing 1% bovine serum albumin (BBS-BSA) prior to addition of serially diluted CMG protein at the indicated concentrations (50 μl/well). Each concentration was assayed in quadruplicate. After overnight incubation (4°C), plates were washed four times and then incubated with anti-GST antibody (1:1000 in BBS-BSA). Plates were washed again and incubated with alkaline phosphatase-conjugated anti-rabbit IgG (1:1000 in BBS-BSA). After a final set of washes, binding to 6H-$EAG_{869-1107}$ was determined by treating wells with FAST p-Nitrophenylphosphate (Sigma-Aldrich, St. Louis MO) and measuring the colorometric reaction at 405 nm.

E.6. Immunocytochemistry

COS-7 cells were maintained at a subconfluent density at 37°C and 5% CO_2 in DMEM supplemented with 10% fetal bovine serum (FBS). Twenty-four hours before transfection, cells were plated and grown to 80% confluence on 12 mm poly-L-lysine coated glass coverslips (Becton-Dickinson, Franklin Lakes NJ). For transient transfection, each coverslip was washed twice with Opti-MEM (Invitrogen, Carlsbad CA) and incubated for 10 hrs in 350 µl Opti-MEM containing 0.4 µg of each of the indicated cDNAs and 1.5 µl LipofectAMINE reagent (Invitrogen, Carlsbad CA), followed by incubation in 1 ml of DMEM with 10% FBS for 12 hrs. Coverslips were washed with PBS and fixed with a 3:7 mixture of 50 mM glycine (pH 2.0) and absolute ethanol for 1 hr at room temperature (RT). After washing three times, cells were permeabilized with 0.1% Triton-X 100 in PBS for 20 min (RT) and blocked for 30 min in a blocking buffer consisting of 10 % horse serum and 0.1% BSA in distilled deionized water. Cells were then incubated with a 1:500 dilution of CMG antisera in blocking buffer for 1 hr at RT, washed with PBS, and incubated with a cyanine 2- or rhodamine-conjugated secondary antibody (Jackson ImmunoResearch, West Grove, PA) for 30 min at 37 °C. Coverslips were mounted on glass slides with Gelmount medium (Biomeda, Foster City, CA). Results were viewed with a Zeiss (Oberkochen, Germany) LSM 510 confocal microscope, and images were prepared for publication with Adobe Photoshop (version 7.0; Adobe Systems, San Jose, CA).

E.7. Immunoprecipitations

Body-wall muscle fibers and CNS tissue from third-instar larvae of the indicated genotypes were homogenized in radioimmunoprecipitation assay buffer (150 mM NaCl, 50 mM Tris pH 8.0, 0.1% SDS, 1% IGEPAL CA-630, 0.5% sodium deoxycholate) containing Complete protease inhibitor on ice and solubilized for 20 min. Cellular debris was removed by centrifugation (3000 x g, 5 min, 4 ^{o}C).

Fly head tissue was obtained from 15 ml of adult flies frozen in liquid nitrogen. Heads were collected by sieving and homogenized in ice cold HM buffer (1 mM EDTA, 5 mM HEPES, pH 7.4, and Complete protease inhibitor). Cell debris was removed by centrifugation, and supernatant was further centrifuged to separate membranes (15000 x g, 15 min). The heavy membrane pellet was solubilized in ice-cold buffer (HM buffer plus 100 mM NaCl and 1 % Triton X-100) for 20 min and supernatant was precleared with protein-A/G agarose beads (Santa Cruz Biotechnology, Santa Cruz CA).

For immunoprecipitations from *Xenopus* oocytes, 30 oocytes for each condition were homogenized in 1.5 ml 100 mM NaCl, 1 mM DTT, 0.5% Triton X-100, 20 mM Tris pH 7.4 and Complete protease inhibitor, and then solubilized on ice for 15 min. Homogenate was centrifuged 20000 x g, 4 ^{o}C, for 10 min and the supernatant collected.

Protein concentrations of homogenates were determined using Bradford assay (Bio-Rad, Hercules CA) and equilibrated across conditions by diluting homogenates to a concentration of 2 mg/ml. A volume of 600 µl of diluted extract was used for each immunoprecipitation reaction. CMG and EAG (NT) antisera were added to protein samples and incubated for 16 hrs at 4 ^{o}C. Immunocomplexes were precipitated with protein-A/G beads for 2 hrs at 4 ^{o}C and then washed 3 times in solubilization buffer and

boiled for 10 min in sample loading buffer (250 mM Tris pH 6.8, 12.5% glycerol, 0.125% bromophenol blue, 1% SDS, 3% β-mercaptoethanol). After addition of sample buffer, 5, 10, and 20 μl were loaded in each lane for extracts, immunoprecipitated and co-immunoprecipitated proteins, respectively.

Immunoprecipitations and cellular extracts were resolved via SDS-PAGE (8% acrylamide, 250 mM Tris pH 6.8, 2.5% SDS) and transferred to polyvinylidene difluoride (PVDF) membrane for Western blotting. Blots were blocked (5% dry milk in TBS) and washed, probed with either CMG or EAG (CT) sera (1:1000 and 1:2000, respectively) followed by HRP-conjugated secondary antibody (1:2000) and visualized by ECL (Amersham Biosciences).

For experiments biotinylating surface membrane proteins, oocytes were washed in cold PBS then incubated for 30 min in 2 mM Sulfo-NHS-LC-Biotin (Pierce, Rockford, IL) in PBS. The labeling reaction was quenched with 3 washes of 100 mM glycine in PBS. Fifty oocytes were homogenized in 1 ml of Buffer H (100 mM NaCl, 0.5% Triton X-100, 20 mM Tris, pH 7.4) supplemented with Complete protease inhibitor, 1 mM orthovanadate, 1 mM benzamidine, 1% phosphatase inhibitor cocktail 1 (Sigma), 2 μM microcystin LR and 5 mM 2-glycerol-phosphate.

Volume intensities of protein bands were quantified using Quantity One software (Bio-Rad). Experimental values ($n \geq 3$) were corrected for background by subtracting values obtained for uninjected lanes, and then were normalized to the value obtained for immunoprecipitated wild type EAG in the absence of CMG.

E.8. Electrophysiology

For expression in *Xenopus* oocytes, plasmids were linearized and RNA transcribed using the appropriate RNA polymerase according to manufacturer instructions (Message Machine; Ambion, Austin TX). RNA concentrations were quantified with spectrophotometric readings using an average reading for three or four dilutions of RNA.

The follicular membrane of stage V-VI oocytes was removed by incubation in Ca^{2+}-free OR2 solution (containing the following, in mM: 82.5 NaCl, 2.5 KCl, 1 $MgCl_2$, 5 Hepes, pH to 7.6 with NaOH) containing collagenase (2 mg/ml; Type 1A Sigma) for ~2 h at RT with gentle agitation. Oocytes were injected with premixed stocks of *eag* and *cmg* RNA. Individual oocytes were injected with 0.1-0.2 ng *eag* RNA and an excess of *cmg* RNA. In some oocyte batches (oocytes from the same frog), the capacity of oocytes to translate the *eag* constructs was verified by performing parallel injections of a larger volume of the same RNA mix and observing a linear increase in EAG current amplitude. After RNA injections, oocytes were maintained in L-15 media (containing the following: 50% L-15, 15 mM Hepes, 50 mg/ml gentamycin, and 5 mg/ml BSA, pH to 7.4 with NaOH) at 18 ^{O}C for 3-5 days. Recordings were performed using a Turbo TEC-10C amplifier (NPI Electronics, Tamm, Germany) and pCLAMP8 software (Molecular Devices, Union City, CA). The extracellular recording solution contained the following (in mM): 140 NaCl, 2 KCl, 1 $MgCl_2$, 10 Hepes, pH 7.1 with NaOH. Pipettes were filled with 2 M KCl and had resistances of 0.3 - 0.6 MΩ. Experiments were performed at RT.

Amplitude measurements refer to the peak currents observed during test pulses to the indicated voltages. Activation and inactivation time constants were determined by fitting traces (excluding capacitative transients) with two exponentials and a steady state.

Unless otherwise noted, measurements were statistically compared using a two-way ANOVA. Data are presented as the mean ± SEM.

BIBLIOGRAPHY

Abdul, M., and Hoosein, N. (2002a). Expression and activity of potassium ion channels in human prostate cancer. Cancer Lett *186*, 99-105.

Abdul, M., and Hoosein, N. (2002b). Voltage-gated sodium ion channels in prostate cancer: expression and activity. Anticancer Res *22*, 1727-1730.

Abdul, M., Santo, A., and Hoosein, N. (2003). Activity of potassium channel-blockers in breast cancer. Anticancer Res *23*, 3347-3351.

Accili, E. A., Proenza, C., Baruscotti, M., and DiFrancesco, D. (2002). From funny current to HCN channels: 20 years of excitation. News Physiol Sci *17*, 32-37.

Allen, D. H., Lepple-Wienhues, A., and Cahalan, M. D. (1997). Ion channel phenotype of melanoma cell lines. J Membr Biol *155*, 27-34.

Ambrosino, C., and Nebreda, A. R. (2001). Cell cycle regulation by p38 MAP kinases. Biol Cell *93*, 47-51.

Amigorena, S., Choquet, D., Teillaud, J. L., Korn, H., and Fridman, W. H. (1990). Ion channel blockers inhibit B cell activation at a precise stage of the G1 phase of the cell cycle. Possible involvement of K+ channels. J Immunol *144*, 2038-2045.

An, W. F., Bowlby, M. R., Betty, M., Cao, J., Ling, H. P., Mendoza, G., Hinson, J. W., Mattsson, K. I., Strassle, B. W., Trimmer, J. S., and Rhodes, K. J. (2000). Modulation of A-type potassium channels by a family of calcium sensors. Nature *403*, 553-556.

Arcangeli, A., Bianchi, L., Becchetti, A., Faravelli, L., Coronnello, M., Mini, E., Olivotto, M., and Wanke, E. (1995). A novel inward-rectifying K+ current with a cell-cycle dependence governs the resting potential of mammalian neuroblastoma cells. J Physiol *489 (Pt 2)*, 455-471.

Artym, V. V., and Petty, H. R. (2002). Molecular proximity of Kv1.3 voltage-gated potassium channels and beta(1)-integrins on the plasma membrane of melanoma cells: effects of cell adherence and channel blockers. J Gen Physiol *120*, 29-37.

Ayali, A., and Harris-Warrick, R. M. (1999). Monoamine control of the pacemaker kernel and cycle frequency in the lobster pyloric network. J Neurosci *19*, 6712-6722.

Bauer, C. K., and Schwarz, J. R. (2001). Physiology of EAG K+ channels. J Membr Biol *182*, 1-15.

Beaumont, V., Zhong, N., Froemke, R. C., Ball, R. W., and Zucker, R. S. (2002). Temporal synaptic tagging by I(h) activation and actin: involvement in long-term facilitation and cAMP-induced synaptic enhancement. Neuron *33*, 601-613.

Beaumont, V., and Zucker, R. S. (2000). Enhancement of synaptic transmission by cyclic AMP modulation of presynaptic Ih channels. Nat Neurosci *3*, 133-141.

Berchtold, M. W., Brinkmeier, H., and Muntener, M. (2000). Calcium ion in skeletal muscle: its crucial role for muscle function, plasticity, and disease. Physiol Rev *80*, 1215-1265.

Bernal, J., and Ehrlich, B. E. (1993). Guanine nucleotides modulate calcium currents in a marine Paramecium. J Exp Biol *176*, 117-133.

Bernstein, J. (1902). Untersuchungen zur Thermodynamik der bioelektrischen Strome. Erster Theil. Pflugers Arch *92*, 521-562.

Bhunia, A. K., Piontek, K., Boletta, A., Liu, L., Qian, F., Xu, P. N., Germino, F. J., and Germino, G. G. (2002). PKD1 induces p21(waf1) and regulation of the cell cycle via direct activation of the JAK-STAT signaling pathway in a process requiring PKD2. Cell *109*, 157-168.

Bianchi, L., Kwok, S. M., Driscoll, M., and Sesti, F. (2003). A potassium channel-MiRP complex controls neurosensory function in Caenorhabditis elegans. J Biol Chem *278*, 12415-12424.

Bianchi, L., Wible, B., Arcangeli, A., Taglialatela, M., Morra, F., Castaldo, P., Crociani, O., Rosati, B., Faravelli, L., Olivotto, M., and Wanke, E. (1998). herg encodes a K+ current highly conserved in tumors of different histogenesis: a selective advantage for cancer cells? Cancer Res *58*, 815-822.

Bildl, W., Strassmaier, T., Thurm, H., Andersen, J., Eble, S., Oliver, D., Knipper, M., Mann, M., Schulte, U., Adelman, J. P., and Fakler, B. (2004). Protein kinase CK2 is coassembled with small conductance Ca(2+)-activated K+ channels and regulates channel gating. Neuron *43*, 847-858.

Bolshakov, V. Y., Carboni, L., Cobb, M. H., Siegelbaum, S. A., and Belardetti, F. (2000). Dual MAP kinase pathways mediate opposing forms of long-term plasticity at CA3-CA1 synapses. Nat Neurosci *3*, 1107-1112.

Bortner, C. D., Hughes, F. M., Jr., and Cidlowski, J. A. (1997). A primary role for K+ and Na+ efflux in the activation of apoptosis. J Biol Chem *272*, 32436-32442.

Brackenbury, W. J., and Djamgoz, M. B. (2006). Activity-dependent regulation of voltage-gated Na+ channel expression in Mat-LyLu rat prostate cancer cell line. J Physiol *573*, 343-356.

Braun, A. P., and Schulman, H. (1995). The multifunctional calcium/calmodulin-dependent protein kinase: from form to function. Annu Rev Physiol *57*, 417-445.

Bruggemann, A., Stuhmer, W., and Pardo, L. A. (1997). Mitosis-promoting factor-mediated suppression of a cloned delayed rectifier potassium channel expressed in Xenopus oocytes. Proc Natl Acad Sci U S A *94*, 537-542.

Butz, S., Okamoto, M., and Sudhof, T. C. (1998). A tripartite protein complex with the potential to couple synaptic vesicle exocytosis to cell adhesion in brain. Cell *94*, 773-782.

Buxbaum, J. D. (2004). A role for calsenilin and related proteins in multiple aspects of neuronal function. Biochem Biophys Res Commun *322*, 1140-1144.

Buxbaum, J. D., Choi, E. K., Luo, Y., Lilliehook, C., Crowley, A. C., Merriam, D. E., and Wasco, W. (1998). Calsenilin: a calcium-binding protein that interacts with the presenilins and regulates the levels of a presenilin fragment. Nat Med *4*, 1177-1181.

Cahalan, M. D., Wulff, H., and Chandy, K. G. (2001). Molecular properties and physiological roles of ion channels in the immune system. J Clin Immunol *21*, 235-252.

Cai, S. Q., Hernandez, L., Wang, Y., Park, K. H., and Sesti, F. (2005). MPS-1 is a K+ channel beta-subunit and a serine/threonine kinase. Nat Neurosci *8*, 1503-1509.

Camacho, J., Sanchez, A., Stuhmer, W., and Pardo, L. A. (2000). Cytoskeletal interactions determine the electrophysiological properties of human EAG potassium channels. Pflugers Arch *441*, 167-174.

Carrion, A. M., Link, W. A., Ledo, F., Mellstrom, B., and Naranjo, J. R. (1999). DREAM is a Ca2+-regulated transcriptional repressor. Nature *398*, 80-84.

Catterall, W. A. (2000). Structure and regulation of voltage-gated Ca2+ channels. Annu Rev Cell Dev Biol *16*, 521-555.

Cayabyab, F. S., and Schlichter, L. C. (2002). Regulation of an ERG K+ current by Src tyrosine kinase. J Biol Chem *277*, 13673-13681.

Chandy, G. K., Wulff, H., Beeton, C., Pennington, M., Gutman, G. A., and Cahalan, M. D. (2004). K+ channels as targets for specific immunomodulation. Trends Pharmacol Sci *25*, 280-289.

Chandy, K. G., DeCoursey, T. E., Cahalan, M. D., McLaughlin, C., and Gupta, S. (1984). Voltage-gated potassium channels are required for human T lymphocyte activation. J Exp Med *160*, 369-385.

Chang, L., and Karin, M. (2001). Mammalian MAP kinase signalling cascades. Nature *410*, 37-40.

Chauvet, V., Tian, X., Husson, H., Grimm, D. H., Wang, T., Hiesberger, T., Igarashi, P., Bennett, A. M., Ibraghimov-Beskrovnaya, O., Somlo, S., and Caplan, M. J. (2004). Mechanical stimuli induce cleavage and nuclear translocation of the polycystin-1 C terminus. J Clin Invest *114*, 1433-1443.

Chen, C., Corbley, M. J., Roberts, T. M., and Hess, P. (1988). Voltage-sensitive calcium channels in normal and transformed 3T3 fibroblasts. Science *239*, 1024-1026.

Cheng, H. Y., Pitcher, G. M., Laviolette, S. R., Whishaw, I. Q., Tong, K. I., Kockeritz, L. K., Wada, T., Joza, N. A., Crackower, M., Goncalves, J., *et al.* (2002). DREAM is a critical transcriptional repressor for pain modulation. Cell *108*, 31-43.

Cherubini, A., Taddei, G. L., Crociani, O., Paglierani, M., Buccoliero, A. M., Fontana, L., Noci, I., Borri, P., Borrani, E., Giachi, M., *et al.* (2000). HERG potassium channels are more frequently expressed in human endometrial cancer as compared to non-cancerous endometrium. Br J Cancer *83*, 1722-1729.

Chouinard, S. W., Wilson, G. F., Schlimgen, A. K., and Ganetzky, B. (1995). A potassium channel beta subunit related to the aldo-keto reductase superfamily is encoded by the Drosophila hyperkinetic locus. Proc Natl Acad Sci U S A *92*, 6763-6767.

Chung, S. K., Reinhart, P. H., Martin, B. L., Brautigan, D., and Levitan, I. B. (1991). Protein kinase activity closely associated with a reconstituted calcium-activated potassium channel. Science *253*, 560-562.

Cohen, B. E., Pralle, A., Yao, X., Swaminath, G., Gandhi, C. S., Jan, Y. N., Kobilka, B. K., Isacoff, E. Y., and Jan, L. Y. (2005). A fluorescent probe designed for studying protein conformational change. Proc Natl Acad Sci U S A *102*, 965-970.

Cole, K. S., and Curtis, H. J. (1939). Electrical impedance of the squid giant axon during activity. J Gen Physiol *22*, 37-64.

Cole, K. S., and Moore, J. W. (1960). Potassium ion current in the squid giant axon: dynamic characteristic. Biophys J *1*, 1-14.

Cosens, D. J., and Manning, A. (1969). Abnormal electroretinogram from a Drosophila mutant. Nature *224*, 285-287.

Crawley, J. B., Rawlinson, L., Lali, F. V., Page, T. H., Saklatvala, J., and Foxwell, B. M. (1997). T cell proliferation in response to interleukins 2 and 7 requires p38MAP kinase activation. J Biol Chem *272*, 15023-15027.

Crews, S. T., and Fan, C. M. (1999). Remembrance of things PAS: regulation of development by bHLH-PAS proteins. Curr Opin Genet Dev *9*, 580-587.

Crociani, O., Guasti, L., Balzi, M., Becchetti, A., Wanke, E., Olivotto, M., Wymore, R. S., and Arcangeli, A. (2003). Cell cycle-dependent expression of HERG1 and HERG1B isoforms in tumor cells. J Biol Chem *278*, 2947-2955.

Cuello, L. G., Cortes, D. M., and Perozo, E. (2004). Molecular architecture of the KvAP voltage-dependent K+ channel in a lipid bilayer. Science *306*, 491-495.

Curran, M. E., Splawski, I., Timothy, K. W., Vincent, G. M., Green, E. D., and Keating, M. T. (1995). A molecular basis for cardiac arrhythmia: HERG mutations cause long QT syndrome. Cell *80*, 795-803.

Curtis, H. J., and Cole, K. S. (1942). Membrane resting and action potentials from the squid giant axon. J Cell Comp Physiol *19*, 135-144.

Davis, T. H., Chen, C., and Isom, L. L. (2004). Sodium channel beta1 subunits promote neurite outgrowth in cerebellar granule neurons. J Biol Chem *279*, 51424-51432.

DeCoursey, T. E., Chandy, K. G., Gupta, S., and Cahalan, M. D. (1984). Voltage-gated K+ channels in human T lymphocytes: a role in mitogenesis? Nature *307*, 465-468.

Deisseroth, K., Heist, E. K., and Tsien, R. W. (1998). Translocation of calmodulin to the nucleus supports CREB phosphorylation in hippocampal neurons. Nature *392*, 198-202.

Dimitratos, S. D., Woods, D. F., and Bryant, P. J. (1997). Camguk, Lin-2, and CASK: novel membrane-associated guanylate kinase homologs that also contain CaM kinase domains. Mechanisms of Development *63*, 127-130.

Dineley, K. T., Weeber, E. J., Atkins, C., Adams, J. P., Anderson, A. E., and Sweatt, J. D. (2001). Leitmotifs in the biochemistry of LTP induction: amplification, integration and coordination. J Neurochem *77*, 961-971.

Dolmetsch, R. E., Pajvani, U., Fife, K., Spotts, J. M., and Greenberg, M. E. (2001). Signaling to the nucleus by an L-type calcium channel-calmodulin complex through the MAP kinase pathway. Science *294*, 333-339.

Doyle, D. A., Morais Cabral, J., Pfuetzner, R. A., Kuo, A., Gulbis, J. M., Cohen, S. L., Chait, B. T., and MacKinnon, R. (1998). The structure of the potassium channel: molecular basis of K+ conduction and selectivity. Science *280*, 69-77.

Drysdale, R., Warmke, J., Kreber, R., and Ganetzky, B. (1991). Molecular characterization of eag: a gene affecting potassium channels in Drosophila melanogaster. Genetics *127*, 497-505.

Dubin, A. E., Liles, M. M., and Harris, G. L. (1998). The K+ channel gene ether a go-go is required for the transduction of a subset of odorants in adult Drosophila melanogaster. J Neurosci *18*, 5603-5613.

Duncan, L. M., Deeds, J., Hunter, J., Shao, J., Holmgren, L. M., Woolf, E. A., Tepper, R. I., and Shyjan, A. W. (1998). Down-regulation of the novel gene melastatin correlates with potential for melanoma metastasis. Cancer Res *58*, 1515-1520.

Engel, J. E., and Wu, C. F. (1998). Genetic dissection of functional contributions of specific potassium channel subunits in habituation of an escape circuit in Drosophila. J Neurosci *18*, 2254-2267.

Engeland, B., Neu, A., Ludwig, J., Roeper, J., and Pongs, O. (1998). Cloning and functional expression of rat ether-a-go-go-like K+ channel genes. J Physiol *513 (Pt 3)*, 647-654.

Fadool, D. A., Tucker, K., Perkins, R., Fasciani, G., Thompson, R. N., Parsons, A. D., Overton, J. M., Koni, P. A., Flavell, R. A., and Kaczmarek, L. K. (2004). Kv1.3 channel gene-targeted deletion produces "Super-Smeller Mice" with altered glomeruli, interacting scaffolding proteins, and biophysics. Neuron *41*, 389-404.

Fanger, C. M., Ghanshani, S., Logsdon, N. J., Rauer, H., Kalman, K., Zhou, J., Beckingham, K., Chandy, K. G., Cahalan, M. D., and Aiyar, J. (1999). Calmodulin mediates calcium-dependent activation of the intermediate conductance KCa channel, IKCa1. J Biol Chem *274*, 5746-5754.

Farias, L. M., Ocana, D. B., Diaz, L., Larrea, F., Avila-Chavez, E., Cadena, A., Hinojosa, L. M., Lara, G., Villanueva, L. A., Vargas, C., *et al.* (2004). Ether a go-go potassium channels as human cervical cancer markers. Cancer Res *64*, 6996-7001.

Fatt, P., and Katz, B. (1953a). The effect of inhibitory nerve impulses on a crustacean muscle fibre. J Physiol *121*, 374-389.

Fatt, P., and Katz, B. (1953b). The electrical properties of crustacean muscle fibres. J Physiol *120*, 171-204.

Fixemer, T., Wissenbach, U., Flockerzi, V., and Bonkhoff, H. (2003). Expression of the Ca2+-selective cation channel TRPV6 in human prostate cancer: a novel prognostic marker for tumor progression. Oncogene *22*, 7858-7861.

Flucher, B. E., and Franzini-Armstrong, C. (1996). Formation of junctions involved in excitation-contraction coupling in skeletal and cardiac muscle. Proc Natl Acad Sci U S A *93*, 8101-8106.

Fordyce, C. B., Jagasia, R., Zhu, X., and Schlichter, L. C. (2005). Microglia Kv1.3 channels contribute to their ability to kill neurons. J Neurosci *25*, 7139-7149.

Fraser, S. P., Diss, J. K., Chioni, A. M., Mycielska, M. E., Pan, H., Yamaci, R. F., Pani, F., Siwy, Z., Krasowska, M., Grzywna, Z., *et al.* (2005). Voltage-gated sodium channel expression and potentiation of human breast cancer metastasis. Clin Cancer Res *11*, 5381-5389.

Fraser, S. P., Diss, J. K., Lloyd, L. J., Pani, F., Chioni, A. M., George, A. J., and Djamgoz, M. B. (2004). T-lymphocyte invasiveness: control by voltage-gated Na+ channel activity. FEBS Lett *569*, 191-194.

Fraser, S. P., Salvador, V., Manning, E. A., Mizal, J., Altun, S., Raza, M., Berridge, R. J., and Djamgoz, M. B. (2003). Contribution of functional voltage-gated Na+ channel expression to cell behaviors involved in the metastatic cascade in rat prostate cancer: I. Lateral motility. J Cell Physiol *195*, 479-487.

Freedman, B. D., Price, M. A., and Deutsch, C. J. (1992). Evidence for voltage modulation of IL-2 production in mitogen-stimulated human peripheral blood lymphocytes. J Immunol *149*, 3784-3794.

Frings, S., Brull, N., Dzeja, C., Angele, A., Hagen, V., Kaupp, U. B., and Baumann, A. (1998). Characterization of ether-a-go-go channels present in photoreceptors reveals similarity to IKx, a K+ current in rod inner segments. J Gen Physiol *111*, 583-599.

Fu, H., Xia, K., Pallas, D. C., Cui, C., Conroy, K., Narsimhan, R. P., Mamon, H., Collier, R. J., and Roberts, T. M. (1994). Interaction of the protein kinase Raf-1 with 14-3-3 proteins. Science *266*, 126-129.

Gandhi, C. S., Clark, E., Loots, E., Pralle, A., and Isacoff, E. Y. (2003). The orientation and molecular movement of a k(+) channel voltage-sensing domain. Neuron *40*, 515-525.

Gandhi, C. S., and Isacoff, E. Y. (2002). Molecular models of voltage sensing. J Gen Physiol *120*, 455-463.

Ganetzky, B., Robertson, G. A., Wilson, G. F., Trudeau, M. C., and Titus, S. A. (1999). The eag family of K+ channels in Drosophila and mammals. Ann N Y Acad Sci *868*, 356-369.

Ganetzky, B., and Wu, C. F. (1983). Neurogenetic analysis of potassium currents in Drosophila: synergistic effects on neuromuscular transmission in double mutants. J Neurogenet *1*, 17-28.

Ganetzky, B., and Wu, C. F. (1985). Genes and membrane excitability in *Drosophila*. Trends Neurosci *8*, 322-326.

Garcia, E. P., Mehta, S., Blair, L. A., Wells, D. G., Shang, J., Fukushima, T., Fallon, J. R., Garner, C. C., and Marshall, J. (1998). SAP90 binds and clusters kainate receptors causing incomplete desensitization. Neuron *21*, 727-739.

Garcia-Ferreiro, R. E., Kerschensteiner, D., Major, F., Monje, F., Stuhmer, W., and Pardo, L. A. (2004). Mechanism of block of hEag1 K+ channels by imipramine and astemizole. J Gen Physiol *124*, 301-317.

Garrido, J. J., Giraud, P., Carlier, E., Fernandes, F., Moussif, A., Fache, M. P., Debanne, D., and Dargent, B. (2003). A targeting motif involved in sodium channel clustering at the axonal initial segment. Science *300*, 2091-2094.

Goldstein, S. A., Bockenhauer, D., O'Kelly, I., and Zilberberg, N. (2001). Potassium leak channels and the KCNK family of two-P-domain subunits. Nat Rev Neurosci *2*, 175-184.

Gomez-Ospina, N., Tsuruta, F., Barreto-Chang, O., Hu, L., and Dolmetsch, R. (2006). The C terminus of the L-type voltage-gated calcium channel Ca(V)1.2 encodes a transcription factor. Cell *127*, 591-606.

Grabner, M., Dirksen, R. T., Suda, N., and Beam, K. G. (1999). The II-III loop of the skeletal muscle dihydropyridine receptor is responsible for the Bi-directional coupling with the ryanodine receptor. J Biol Chem *274*, 21913-21919.

Graves, L. M., Guy, H. I., Kozlowski, P., Huang, M., Lazarowski, E., Pope, R. M., Collins, M. A., Dahlstrand, E. N., Earp, H. S., 3rd, and Evans, D. R. (2000). Regulation of carbamoyl phosphate synthetase by MAP kinase. Nature *403*, 328-332.

Griffith, L. C., Verselis, L. M., Aitken, K. M., Kyriacou, C. P., Danho, W., and Greenspan, R. J. (1993). Inhibition of calcium/calmodulin-dependent protein kinase in Drosophila disrupts behavioral plasticity. Neuron *10*, 501-509.

Griffith, L. C., Wang, J., Zhong, Y., Wu, C. F., and Greenspan, R. J. (1994). Calcium/calmodulin-dependent protein kinase II and potassium channel subunit eag similarly affect plasticity in Drosophila. Proc Natl Acad Sci U S A *91*, 10044-10048.

Grimm, D. H., Karihaloo, A., Cai, Y., Somlo, S., Cantley, L. G., and Caplan, M. J. (2006). Polycystin-2 regulates proliferation and branching morphogenesis in kidney epithelial cells. J Biol Chem *281*, 137-144.

Guan, K. L., and Dixon, J. E. (1991). Eukaryotic proteins expressed in Escherichia coli: an improved thrombin cleavage and purification procedure of fusion proteins with glutathione S-transferase. Analytical Biochemistry *192*, 262-267.

Guan, Z., Kim, J. H., Lomvardas, S., Holick, K., Xu, S., Kandel, E. R., and Schwartz, J. H. (2003). p38 MAP kinase mediates both short-term and long-term synaptic depression in aplysia. J Neurosci *23*, 7317-7325.

Guillemin, K., and Krasnow, M. A. (1997). The hypoxic response: huffing and HIFing. Cell *89*, 9-12.

Gulbis, J. M., Mann, S., and MacKinnon, R. (1999). Structure of a voltage-dependent K+ channel beta subunit. Cell *97*, 943-952.

Gutman, G. A., Chandy, K. G., Adelman, J. P., Aiyar, J., Bayliss, D. A., Clapham, D. E., Covarriubias, M., Desir, G. V., Furuichi, K., Ganetzky, B., *et al.* (2003). International

Union of Pharmacology. XLI. Compendium of voltage-gated ion channels: potassium channels. Pharmacol Rev *55*, 583-586.

Guy, H. R., Durell, S. R., Warmke, J., Drysdale, R., and Ganetzky, B. (1991). Similarities in amino acid sequences of Drosophila eag and cyclic nucleotide-gated channels. Science *254*, 730.

Hanaoka, K., Qian, F., Boletta, A., Bhunia, A. K., Piontek, K., Tsiokas, L., Sukhatme, V. P., Guggino, W. B., and Germino, G. G. (2000). Co-assembly of polycystin-1 and -2 produces unique cation-permeable currents. Nature *408*, 990-994.

Hanks, S. K., Quinn, A. M., and Hunter, T. (1988). The protein kinase family: conserved features and deduced phylogeny of the catalytic domains. Science *241*, 42-52.

Hardingham, G. E., and Bading, H. (2003). The Yin and Yang of NMDA receptor signalling. Trends Neurosci *26*, 81-89.

Harkiolaki, M., Lewitzky, M., Gilbert, R. J., Jones, E. Y., Bourette, R. P., Mouchiroud, G., Sondermann, H., Moarefi, I., and Feller, S. M. (2003). Structural basis for SH3 domain-mediated high-affinity binding between Mona/Gads and SLP-76. EMBO Journal *22*, 2571-2582.

Hartshorne, R. P., and Catterall, W. A. (1984). The sodium channel from rat brain. Purification and subunit composition. J Biol Chem *259*, 1667-1675.

Hata, Y., Butz, S., and Sudhof, T. C. (1996). CASK: a novel dlg/PSD95 homolog with an N-terminal calmodulin-dependent protein kinase domain identified by interaction with neurexins. Journal of Neuroscience *16*, 2488-2494.

Heginbotham, L., Lu, Z., Abramson, T., and MacKinnon, R. (1994). Mutations in the K+ channel signature sequence. Biophys J *66*, 1061-1067.

Hegle, A. P., Marble, D. D., and Wilson, G. F. (2006). A voltage-driven switch for ion-independent signaling by ether-a-go-go K+ channels. Proc Natl Acad Sci U S A *103*, 2886-2891.

Hell, J. W., Westenbroek, R. E., Breeze, L. J., Wang, K. K., Chavkin, C., and Catterall, W. A. (1996). N-methyl-D-aspartate receptor-induced proteolytic conversion of postsynaptic class C L-type calcium channels in hippocampal neurons. Proc Natl Acad Sci U S A *93*, 3362-3367.

Hille, B. (2001). Ion channels of excitable membranes, 3rd edn (Sunderland, MA, Sinauer Associates).

Hodgkin, A. L., and Huxley, A. F. (1945). Resting and action potentials in single nerve fibres. J Physiol *104*, 176-195.

Hodgkin, A. L., and Huxley, A. F. (1952a). The components of membrane conductance in the giant axon of Loligo. J Physiol *116*, 473-496.

Hodgkin, A. L., and Huxley, A. F. (1952b). Currents carried by sodium and potassium ions through the membrane of the giant axon of Loligo. J Physiol *116*, 449-472.

Hodgkin, A. L., and Huxley, A. F. (1952c). The dual effect of membrane potential on sodium conductance in the giant axon of Loligo. J Physiol *116*, 497-506.

Hodgkin, A. L., and Huxley, A. F. (1952d). A quantitative description of membrane current and its application to conduction and excitation in nerve. J Physiol *117*, 500-544.

Hodgkin, A. L., Huxley, A. F., and Katz, B. (1952). Measurement of current-voltage relations in the membrane of the giant axon of Loligo. J Physiol *116*, 424-448.

Hodgkin, A. L., and Katz, B. (1949). The effect of sodium ions on the electrical activity of the giant axon of the squid. J Physiol *108*, 37-77.

Hoenderop, J. G., Nilius, B., and Bindels, R. J. (2005). Calcium absorption across epithelia. Physiol Rev *85*, 373-422.

Holmes, T. C., Berman, K., Swartz, J. E., Dagan, D., and Levitan, I. B. (1997). Expression of voltage-gated potassium channels decreases cellular protein tyrosine phosphorylation. J Neurosci *17*, 8964-8974.

Holmes, T. C., Fadool, D. A., Ren, R., and Levitan, I. B. (1996). Association of Src tyrosine kinase with a human potassium channel mediated by SH3 domain. Science *274*, 2089-2091.

Hoshi, T., Zagotta, W. N., and Aldrich, R. W. (1990). Biophysical and molecular mechanisms of Shaker potassium channel inactivation. Science *250*, 533-538.

Hoskins, R., Hajnal, A. F., Harp, S. A., and Kim, S. K. (1996). The C. elegans vulval induction gene lin-2 encodes a member of the MAGUK family of cell junction proteins. Development *122*, 97-111.

Hsueh, Y. P., Wang, T. F., Yang, F. C., and Sheng, M. (2000). Nuclear translocation and transcription regulation by the membrane-associated guanylate kinase CASK/LIN-2. Nature *404*, 298-302.

Huang, C. L. (2004). The transient receptor potential superfamily of ion channels. J Am Soc Nephrol *15*, 1690-1699.

Hulme, J. T., Ahn, M., Hauschka, S. D., Scheuer, T., and Catterall, W. A. (2002). A novel leucine zipper targets AKAP15 and cyclic AMP-dependent protein kinase to the C terminus of the skeletal muscle Ca2+ channel and modulates its function. J Biol Chem *277*, 4079-4087.

Hulme, J. T., Konoki, K., Lin, T. W., Gritsenko, M. A., Camp, D. G., 2nd, Bigelow, D. J., and Catterall, W. A. (2005). Sites of proteolytic processing and noncovalent association of the distal C-terminal domain of CaV1.1 channels in skeletal muscle. Proc Natl Acad Sci U S A *102*, 5274-5279.

Isom, L. L., De Jongh, K. S., and Catterall, W. A. (1994). Auxiliary subunits of voltage-gated ion channels. Neuron *12*, 1183-1194.

Jaramillo, A. M., Zheng, X., Zhou, Y., Amado, D. A., Sheldon, A., Sehgal, A., and Levitan, I. B. (2004). Pattern of distribution and cycling of SLOB, Slowpoke channel binding protein, in Drosophila. BMC Neurosci *5*, 3.

Jeng, C. J., Chang, C. C., and Tang, C. Y. (2005). Differential localization of rat Eag1 and Eag2 K+ channels in hippocampal neurons. Neuroreport *16*, 229-233.

Jiang, Y., Lee, A., Chen, J., Ruta, V., Cadene, M., Chait, B. T., and MacKinnon, R. (2003a). X-ray structure of a voltage-dependent K+ channel. Nature *423*, 33-41.

Jiang, Y., Ruta, V., Chen, J., Lee, A., and MacKinnon, R. (2003b). The principle of gating charge movement in a voltage-dependent K+ channel. Nature *423*, 42-48.

Joiner, W. J., Khanna, R., Schlichter, L. C., and Kaczmarek, L. K. (2001). Calmodulin regulates assembly and trafficking of SK4/IK1 Ca2+-activated K+ channels. J Biol Chem *276*, 37980-37985.

Kaczmarek, L. K. (2006). Non-conducting functions of voltage-gated ion channels. Nat Rev Neurosci *7*, 761-771.

Kaech, S. M., Whitfield, C. W., and Kim, S. K. (1998). The LIN-2/LIN-7/LIN-10 complex mediates basolateral membrane localization of the C. elegans EGF receptor LET-23 in vulval epithelial cells. Cell *94*, 761-771.

Kagan, A., Melman, Y. F., Krumerman, A., and McDonald, T. V. (2002). 14-3-3 amplifies and prolongs adrenergic stimulation of HERG K+ channel activity. Embo J *21*, 1889-1898.

Kaplan, W. D., and Trout, W. E., 3rd (1969). The behavior of four neurological mutants of Drosophila. Genetics *61*, 399-409.

Karim, F. D., and Rubin, G. M. (1998). Ectopic expression of activated Ras1 induces hyperplastic growth and increased cell death in Drosophila imaginal tissues. Development *125*, 1-9.

Keen, J. E., Khawaled, R., Farrens, D. L., Neelands, T., Rivard, A., Bond, C. T., Janowsky, A., Fakler, B., Adelman, J. P., and Maylie, J. (1999). Domains responsible for constitutive and Ca(2+)-dependent interactions between calmodulin and small conductance Ca(2+)-activated potassium channels. J Neurosci *19*, 8830-8838.

Kenworthy, A. K. (2001). Imaging protein-protein interactions using fluorescence resonance energy transfer microscopy. Methods *24*, 289-296.

Kim, D. Y., Carey, B. W., Wang, H., Ingano, L. A., Binshtok, A. M., Wertz, M. H., Pettingell, W. H., He, P., Lee, V. M., Woolf, C. J., and Kovacs, D. M. (2007). BACE1 regulates voltage-gated sodium channels and neuronal activity. Nat Cell Biol *9*, 755-764.

Kim, D. Y., Ingano, L. A., Carey, B. W., Pettingell, W. H., and Kovacs, D. M. (2005). Presenilin/gamma-secretase-mediated cleavage of the voltage-gated sodium channel beta2-subunit regulates cell adhesion and migration. J Biol Chem *280*, 23251-23261.

Kim, E., Niethammer, M., Rothschild, A., Jan, Y. N., and Sheng, M. (1995). Clustering of Shaker-type K+ channels by interaction with a family of membrane-associated guanylate kinases. Nature *378*, 85-88.

Krapivinsky, G., Medina, I., Krapivinsky, L., Gapon, S., and Clapham, D. E. (2004). SynGAP-MUPP1-CaMKII synaptic complexes regulate p38 MAP kinase activity and NMDA receptor-dependent synaptic AMPA receptor potentiation. Neuron *43*, 563-574.

Kurokawa, J., Motoike, H. K., Rao, J., and Kass, R. S. (2004). Regulatory actions of the A-kinase anchoring protein Yotiao on a heart potassium channel downstream of PKA phosphorylation. Proc Natl Acad Sci U S A *101*, 16374-16378.

Lastraioli, E., Guasti, L., Crociani, O., Polvani, S., Hofmann, G., Witchel, H., Bencini, L., Calistri, M., Messerini, L., Scatizzi, M., *et al.* (2004). herg1 gene and HERG1 protein are overexpressed in colorectal cancers and regulate cell invasion of tumor cells. Cancer Res *64*, 606-611.

Lecain, E., Sauvaget, E., Crisanti, P., Van Den Abbeele, T., and Huy, P. T. (1999). Potassium channel ether a go-go mRNA expression in the spiral ligament of the rat. Hear Res *133*, 133-138.

Levitan, I. B. (1999). It is calmodulin after all! Mediator of the calcium modulation of multiple ion channels. Neuron *22*, 645-648.

Levitan, I. B. (2006). Signaling protein complexes associated with neuronal ion channels. Nat Neurosci *9*, 305-310.

Lewis, R. S., and Cahalan, M. D. (1995). Potassium and calcium channels in lymphocytes. Annu Rev Immunol *13*, 623-653.

Liman, E. R., Hess, P., Weaver, F., and Koren, G. (1991). Voltage-sensing residues in the S4 region of a mammalian K+ channel. Nature *353*, 752-756.

Lin, C. S., Boltz, R. C., Blake, J. T., Nguyen, M., Talento, A., Fischer, P. A., Springer, M. S., Sigal, N. H., Slaughter, R. S., Garcia, M. L., and et al. (1993). Voltage-gated potassium channels regulate calcium-dependent pathways involved in human T lymphocyte activation. J Exp Med *177*, 637-645.

Liu, Q., Berry, D., Nash, P., Pawson, T., McGlade, C. J., and Li, S. S. (2003). Structural basis for specific binding of the Gads SH3 domain to an RxxK motif-containing SLP-76 peptide: a novel mode of peptide recognition. Molecular Cell *11*, 471-481.

Lu, C. S., Hodge, J. J., Mehren, J., Sun, X. X., and Griffith, L. C. (2003). Regulation of the Ca2+/CaM-responsive pool of CaMKII by scaffold-dependent autophosphorylation. Neuron *40*, 1185-1197.

Ludwig, J., Terlau, H., Wunder, F., Bruggemann, A., Pardo, L. A., Marquardt, A., Stuhmer, W., and Pongs, O. (1994). Functional expression of a rat homologue of the voltage gated either a go-go potassium channel reveals differences in selectivity and activation kinetics between the Drosophila channel and its mammalian counterpart. Embo J *13*, 4451-4458.

MacFarlane, S. N., and Sontheimer, H. (2000). Modulation of Kv1.5 currents by Src tyrosine phosphorylation: potential role in the differentiation of astrocytes. J Neurosci *20*, 5245-5253.

MacLean, J. N., Zhang, Y., Goeritz, M. L., Casey, R., Oliva, R., Guckenheimer, J., and Harris-Warrick, R. M. (2005). Activity-independent coregulation of IA and Ih in rhythmically active neurons. J Neurophysiol *94*, 3601-3617.

MacLean, J. N., Zhang, Y., Johnson, B. R., and Harris-Warrick, R. M. (2003). Activity-independent homeostasis in rhythmically active neurons. Neuron *37*, 109-120.

Malhotra, J. D., Kazen-Gillespie, K., Hortsch, M., and Isom, L. L. (2000). Sodium channel beta subunits mediate homophilic cell adhesion and recruit ankyrin to points of cell-cell contact. J Biol Chem *275*, 11383-11388.

Malhotra, J. D., Thyagarajan, V., Chen, C., and Isom, L. L. (2004). Tyrosine-phosphorylated and nonphosphorylated sodium channel beta1 subunits are differentially localized in cardiac myocytes. J Biol Chem *279*, 40748-40754.

Marble, D. D., Hegle, A. P., Snyder, E. D., 2nd, Dimitratos, S., Bryant, P. J., and Wilson, G. F. (2005). Camguk/CASK enhances Ether-a-go-go potassium current by a phosphorylation-dependent mechanism. J Neurosci *25*, 4898-4907.

Maximov, A., Sudhof, T. C., and Bezprozvanny, I. (1999). Association of neuronal calcium channels with modular adaptor proteins. Journal of Biological Chemistry *274*, 24453-24456.

Mayford, M., Bach, M. E., Huang, Y. Y., Wang, L., Hawkins, R. D., and Kandel, E. R. (1996). Control of memory formation through regulated expression of a CaMKII transgene. Science *274*, 1678-1683.

McEwen, D. P., and Isom, L. L. (2004). Heterophilic interactions of sodium channel beta1 subunits with axonal and glial cell adhesion molecules. J Biol Chem *279*, 52744-52752.

McGee, A. W., Dakoji, S. R., Olsen, O., Bredt, D. S., Lim, W. A., and Prehoda, K. E. (2001). Structure of the SH3-guanylate kinase module from PSD-95 suggests a mechanism for regulated assembly of MAGUK scaffolding proteins. Molecular Cell *8*, 1291-1301.

Meyer, R., and Heinemann, S. H. (1998). Characterization of an eag-like potassium channel in human neuroblastoma cells. J Physiol *508 (Pt 1)*, 49-56.

Meyer, R., Schonherr, R., Gavrilova-Ruch, O., Wohlrab, W., and Heinemann, S. H. (1999). Identification of ether a go-go and calcium-activated potassium channels in human melanoma cells. J Membr Biol *171*, 107-115.

Mochida, S., Yokoyama, C. T., Kim, D. K., Itoh, K., and Catterall, W. A. (1998). Evidence for a voltage-dependent enhancement of neurotransmitter release mediated via the synaptic protein interaction site of N-type Ca2+ channels. Proc Natl Acad Sci U S A *95*, 14523-14528.

Morais Cabral, J. H., Lee, A., Cohen, S. L., Chait, B. T., Li, M., and Mackinnon, R. (1998). Crystal structure and functional analysis of the HERG potassium channel N terminus: a eukaryotic PAS domain. Cell *95*, 649-655.

Morozov, A., Muzzio, I. A., Bourtchouladze, R., Van-Strien, N., Lapidus, K., Yin, D., Winder, D. G., Adams, J. P., Sweatt, J. D., and Kandel, E. R. (2003). Rap1 couples cAMP signaling to a distinct pool of p42/44MAPK regulating excitability, synaptic plasticity, learning, and memory. Neuron *39*, 309-325.

Mu, D., Chen, L., Zhang, X., See, L. H., Koch, C. M., Yen, C., Tong, J. J., Spiegel, L., Nguyen, K. C., Servoss, A., *et al.* (2003). Genomic amplification and oncogenic properties of the KCNK9 potassium channel gene. Cancer Cell *3*, 297-302.

Muller, B. M., Kistner, U., Kindler, S., Chung, W. J., Kuhlendahl, S., Fenster, S. D., Lau, L. F., Veh, R. W., Huganir, R. L., Gundelfinger, E. D., and Garner, C. C. (1996). SAP102, a novel postsynaptic protein that interacts with NMDA receptor complexes in vivo. Neuron *17*, 255-265.

Mumm, J. S., and Kopan, R. (2000). Notch signaling: from the outside in. Dev Biol *228*, 151-165.

Murata, H., Tajima, N., Nagashima, Y., Yao, M., Baba, M., Goto, M., Kawamoto, S., Yamamoto, I., Okuda, K., and Kanno, H. (2002). Von Hippel-Lindau tumor suppressor protein transforms human neuroblastoma cells into functional neuron-like cells. Cancer Res *62*, 7004-7011.

Murata, Y., Iwasaki, H., Sasaki, M., Inaba, K., and Okamura, Y. (2005). Phosphoinositide phosphatase activity coupled to an intrinsic voltage sensor. Nature *435*, 1239-1243.

Mycielska, M. E., Fraser, S. P., Szatkowski, M., and Djamgoz, M. B. (2003). Contribution of functional voltage-gated Na+ channel expression to cell behaviors involved in the metastatic cascade in rat prostate cancer: II. Secretory membrane activity. J Cell Physiol *195*, 461-469.

Nakai, J., Dirksen, R. T., Nguyen, H. T., Pessah, I. N., Beam, K. G., and Allen, P. D. (1996). Enhanced dihydropyridine receptor channel activity in the presence of ryanodine receptor. Nature *380*, 72-75.

Nakanishi, K., Zhang, F., Baxter, D. A., Eskin, A., and Byrne, J. H. (1997). Role of calcium-calmodulin-dependent protein kinase II in modulation of sensorimotor synapses in Aplysia. J Neurophysiol *78*, 409-416.

Occhiodoro, T., Bernheim, L., Liu, J. H., Bijlenga, P., Sinnreich, M., Bader, C. R., and Fischer-Lougheed, J. (1998). Cloning of a human ether-a-go-go potassium channel expressed in myoblasts at the onset of fusion. FEBS Lett *434*, 177-182.

Onganer, P. U., and Djamgoz, M. B. (2005). Small-cell lung cancer (human): potentiation of endocytic membrane activity by voltage-gated Na(+) channel expression in vitro. J Membr Biol *204*, 67-75.

Pal, S., Hartnett, K. A., Nerbonne, J. M., Levitan, E. S., and Aizenman, E. (2003). Mediation of neuronal apoptosis by Kv2.1-encoded potassium channels. J Neurosci *23*, 4798-4802.

Palmer, A., Gavin, A. C., and Nebreda, A. R. (1998). A link between MAP kinase and p34(cdc2)/cyclin B during oocyte maturation: p90(rsk) phosphorylates and inactivates the p34(cdc2) inhibitory kinase Myt1. Embo J *17*, 5037-5047.

Pan, Z., Kao, T., Horvath, Z., Lemos, J., Sul, J. Y., Cranstoun, S. D., Bennett, V., Scherer, S. S., and Cooper, E. C. (2006). A common ankyrin-G-based mechanism retains KCNQ and NaV channels at electrically active domains of the axon. J Neurosci *26*, 2599-2613.

Paolini, C., Fessenden, J. D., Pessah, I. N., and Franzini-Armstrong, C. (2004). Evidence for conformational coupling between two calcium channels. Proc Natl Acad Sci U S A *101*, 12748-12752.

Papazian, D. M., Timpe, L. C., Jan, Y. N., and Jan, L. Y. (1991). Alteration of voltage-dependence of Shaker potassium channel by mutations in the S4 sequence. Nature *349*, 305-310.

Pardo, L. A. (2004). Voltage-gated potassium channels in cell proliferation. Physiology (Bethesda) *19*, 285-292.

Pardo, L. A., Bruggemann, A., Camacho, J., and Stuhmer, W. (1998). Cell cycle-related changes in the conducting properties of r-eag K+ channels. J Cell Biol *143*, 767-775.

Pardo, L. A., Contreras-Jurado, C., Zientkowska, M., Alves, F., and Stuhmer, W. (2005). Role of voltage-gated potassium channels in cancer. J Membr Biol *205*, 115-124.

Pardo, L. A., del Camino, D., Sanchez, A., Alves, F., Bruggemann, A., Beckh, S., and Stuhmer, W. (1999). Oncogenic potential of EAG K(+) channels. Embo J *18*, 5540-5547.

Patt, S., Preussat, K., Beetz, C., Kraft, R., Schrey, M., Kalff, R., Schonherr, K., and Heinemann, S. H. (2004). Expression of ether a go-go potassium channels in human gliomas. Neurosci Lett *368*, 249-253.

Pearson, G., Robinson, F., Beers Gibson, T., Xu, B. E., Karandikar, M., Berman, K., and Cobb, M. H. (2001). Mitogen-activated protein (MAP) kinase pathways: regulation and physiological functions. Endocrine Reviews *22*, 153-183.

Pei, L., Wiser, O., Slavin, A., Mu, D., Powers, S., Jan, L. Y., and Hoey, T. (2003). Oncogenic potential of TASK3 (Kcnk9) depends on K+ channel function. Proc Natl Acad Sci U S A *100*, 7803-7807.

Pemberton, K. E., Hill-Eubanks, L. J., and Jones, S. V. P. (2000). Modulation of low-threshold T-type calcium channels by the five muscarinic receptor subtypes in NIH 3T3 cells. Pflugers Archives -- European Journal of Physiology *440*, 452-461.

Perraud, A. L., Fleig, A., Dunn, C. A., Bagley, L. A., Launay, P., Schmitz, C., Stokes, A. J., Zhu, Q., Bessman, M. J., Penner, R., *et al.* (2001). ADP-ribose gating of the calcium-permeable LTRPC2 channel revealed by Nudix motif homology. Nature *411*, 595-599.

Peterson, B. Z., DeMaria, C. D., Adelman, J. P., and Yue, D. T. (1999). Calmodulin is the Ca2+ sensor for Ca2+ -dependent inactivation of L-type calcium channels. Neuron *22*, 549-558.

Phelps, C. B., and Brand, A. H. (1998). Ectopic gene expression in Drosophila using GAL4 system. Methods *14*, 367-379.

Pillozzi, S., Brizzi, M. F., Balzi, M., Crociani, O., Cherubini, A., Guasti, L., Bartolozzi, B., Becchetti, A., Wanke, E., Bernabei, P. A., *et al.* (2002). HERG potassium channels are constitutively expressed in primary human acute myeloid leukemias and regulate cell proliferation of normal and leukemic hemopoietic progenitors. Leukemia *16*, 1791-1798.

Pitt, G. S., Zuhlke, R. D., Hudmon, A., Schulman, H., Reuter, H., and Tsien, R. W. (2001). Molecular basis of calmodulin tethering and Ca2+-dependent inactivation of L-type Ca2+ channels. J Biol Chem *276*, 30794-30802.

Prakriya, M., Feske, S., Gwack, Y., Srikanth, S., Rao, A., and Hogan, P. G. (2006). Orai1 is an essential pore subunit of the CRAC channel. Nature *443*, 230-233.

Preisig-Muller, R., Schlichthorl, G., Goerge, T., Heinen, S., Bruggemann, A., Rajan, S., Derst, C., Veh, R. W., and Daut, J. (2002). Heteromerization of Kir2.x potassium

channels contributes to the phenotype of Andersen's syndrome. Proc Natl Acad Sci U S A *99*, 7774-7779.

Preussat, K., Beetz, C., Schrey, M., Kraft, R., Wolfl, S., Kalff, R., and Patt, S. (2003). Expression of voltage-gated potassium channels Kv1.3 and Kv1.5 in human gliomas. Neurosci Lett *346*, 33-36.

Price, M., Lee, S. C., and Deutsch, C. (1989). Charybdotoxin inhibits proliferation and interleukin 2 production in human peripheral blood lymphocytes. Proc Natl Acad Sci U S A *86*, 10171-10175.

Putkey, J. A., and Waxham, M. N. (1996). A peptide model for calmodulin trapping by calcium/calmodulin-dependent protein kinase II. Journal of Biological Chemistry *271*, 29619-29623.

Qin, N., Olcese, R., Bransby, M., Lin, T., and Birnbaumer, L. (1999). Ca2+-induced inhibition of the cardiac Ca2+ channel depends on calmodulin. Proc Natl Acad Sci U S A *96*, 2435-2438.

Ramsey, I. S., Moran, M. M., Chong, J. A., and Clapham, D. E. (2006). A voltage-gated proton-selective channel lacking the pore domain. Nature *440*, 1213-1216.

Ratcliffe, C. F., Westenbroek, R. E., Curtis, R., and Catterall, W. A. (2001). Sodium channel beta1 and beta3 subunits associate with neurofascin through their extracellular immunoglobulin-like domain. J Cell Biol *154*, 427-434.

Reinhart, P. H., and Levitan, I. B. (1995). Kinase and phosphatase activities intimately associated with a reconstituted calcium-dependent potassium channel. J Neurosci *15*, 4572-4579.

Rettig, J., Heinemann, S. H., Wunder, F., Lorra, C., Parcej, D. N., Dolly, J. O., and Pongs, O. (1994). Inactivation properties of voltage-gated K+ channels altered by presence of beta-subunit. Nature *369*, 289-294.

Rettig, J., Sheng, Z. H., Kim, D. K., Hodson, C. D., Snutch, T. P., and Catterall, W. A. (1996). Isoform-specific interaction of the alpha1A subunits of brain Ca2+ channels with the presynaptic proteins syntaxin and SNAP-25. Proc Natl Acad Sci U S A *93*, 7363-7368.

Riazanova, L. V., Pavur, K. S., Petrov, A. N., Dorovkov, M. V., and Riazanov, A. G. (2001). [Novel type of signaling molecules: protein kinases covalently linked to ion channels]. Mol Biol (Mosk) *35*, 321-332.

Rios, E., and Brum, G. (1987). Involvement of dihydropyridine receptors in excitation-contraction coupling in skeletal muscle. Nature *325*, 717-720.

Rios, E., and Pizarro, G. (1991). Voltage sensor of excitation-contraction coupling in skeletal muscle. Physiol Rev *71*, 849-908.

Robertson, G. A., Warmke, J. M., and Ganetzky, B. (1996). Potassium currents expressed from Drosophila and mouse eag cDNAs in Xenopus oocytes. Neuropharmacology *35*, 841-850.

Rosen, L. B., Ginty, D. D., Weber, M. J., and Greenberg, M. E. (1994). Membrane depolarization and calcium influx stimulate MEK and MAP kinase via activation of Ras. Neuron *12*, 1207-1221.

Rouzaire-Dubois, B., and Dubois, J. M. (1998). K+ channel block-induced mammalian neuroblastoma cell swelling: a possible mechanism to influence proliferation. J Physiol *510 (Pt 1)*, 93-102.

Runnels, L. W., Yue, L., and Clapham, D. E. (2001). TRP-PLIK, a bifunctional protein with kinase and ion channel activities. Science *291*, 1043-1047.

Ryazanova, L. V., Dorovkov, M. V., Ansari, A., and Ryazanov, A. G. (2004). Characterization of the protein kinase activity of TRPM7/ChaK1, a protein kinase fused to the transient receptor potential ion channel. J Biol Chem *279*, 3708-3716.

Saganich, M. J., Machado, E., and Rudy, B. (2001). Differential expression of genes encoding subthreshold-operating voltage-gated K+ channels in brain. J Neurosci *21*, 4609-4624.

Saimi, Y., and Kung, C. (2002). Calmodulin as an ion channel subunit. Annu Rev Physiol *64*, 289-311.

Sano, Y., Inamura, K., Miyake, A., Mochizuki, S., Yokoi, H., Matsushime, H., and Furuichi, K. (2001). Immunocyte Ca2+ influx system mediated by LTRPC2. Science *293*, 1327-1330.

Sasaki, M., Takagi, M., and Okamura, Y. (2006). A voltage sensor-domain protein is a voltage-gated proton channel. Science *312*, 589-592.

Savignac, M., Pintado, B., Gutierrez-Adan, A., Palczewska, M., Mellstrom, B., and Naranjo, J. R. (2005). Transcriptional repressor DREAM regulates T-lymphocyte proliferation and cytokine gene expression. Embo J *24*, 3555-3564.

Schlingmann, K. P., Weber, S., Peters, M., Niemann Nejsum, L., Vitzthum, H., Klingel, K., Kratz, M., Haddad, E., Ristoff, E., Dinour, D., *et al.* (2002). Hypomagnesemia with secondary hypocalcemia is caused by mutations in TRPM6, a new member of the TRPM gene family. Nat Genet *31*, 166-170.

Schmitz, C., Dorovkov, M. V., Zhao, X., Davenport, B. J., Ryazanov, A. G., and Perraud, A. L. (2005). The channel kinases TRPM6 and TRPM7 are functionally nonredundant. J Biol Chem *280*, 37763-37771.

Schmitz, C., Perraud, A. L., Fleig, A., and Scharenberg, A. M. (2004). Dual-function ion channel/protein kinases: novel components of vertebrate magnesium regulatory mechanisms. Pediatr Res *55*, 734-737.

Schmitz, C., Perraud, A. L., Johnson, C. O., Inabe, K., Smith, M. K., Penner, R., Kurosaki, T., Fleig, A., and Scharenberg, A. M. (2003). Regulation of vertebrate cellular Mg2+ homeostasis by TRPM7. Cell *114*, 191-200.

Schneider, M. F. (1981). Membrane charge movement and depolarization-contraction coupling. Annu Rev Physiol *43*, 507-517.

Schneider, M. F., and Chandler, W. K. (1973). Voltage dependent charge movement of skeletal muscle: a possible step in excitation-contraction coupling. Nature *242*, 244-246.

Schonherr, R., and Heinemann, S. H. (1996). Molecular determinants for activation and inactivation of HERG, a human inward rectifier potassium channel. J Physiol *493 (Pt 3)*, 635-642.

Schonherr, R., Lober, K., and Heinemann, S. H. (2000). Inhibition of human ether a go-go potassium channels by Ca(2+)/calmodulin. Embo J *19*, 3263-3271.

Schonherr, R., Mannuzzu, L. M., Isacoff, E. Y., and Heinemann, S. H. (2002). Conformational switch between slow and fast gating modes: allosteric regulation of voltage sensor mobility in the EAG K+ channel. Neuron *35*, 935-949.

Schopperle, W. M., Holmqvist, M. H., Zhou, Y., Wang, J., Wang, Z., Griffith, L. C., Keselman, I., Kusinitz, F., Dagan, D., and Levitan, I. B. (1998). Slob, a novel protein that interacts with the Slowpoke calcium-dependent potassium channel. Neuron *20*, 565-573.

Schultz, J. E., Klumpp, S., Benz, R., Schurhoff-Goeters, W. J., and Schmid, A. (1992). Regulation of adenylyl cyclase from Paramecium by an intrinsic potassium conductance. Science *255*, 600-603.

Schwarz, E. C., Wissenbach, U., Niemeyer, B. A., Strauss, B., Philipp, S. E., Flockerzi, V., and Hoth, M. (2006). TRPV6 potentiates calcium-dependent cell proliferation. Cell Calcium *39*, 163-173.

Scully, A. L., and Kay, S. A. (2000). Time flies for Drosophila. Cell *100*, 297-300.

Selverston, A. I., and Moulins, M. (1985). Oscillatory neural networks. Annu Rev Physiol *47*, 29-48.

Selvin, P. R. (1995). Fluorescence resonance energy transfer. Methods Enzymol *246*, 300-334.

Sheng, M., McFadden, G., and Greenberg, M. E. (1990). Membrane depolarization and calcium induce c-fos transcription via phosphorylation of transcription factor CREB. Neuron *4*, 571-582.

Sheng, Z. H., Yokoyama, C. T., and Catterall, W. A. (1997). Interaction of the synprint site of N-type Ca2+ channels with the C2B domain of synaptotagmin I. Proc Natl Acad Sci U S A *94*, 5405-5410.

Shieh, C. C., Coghlan, M., Sullivan, J. P., and Gopalakrishnan, M. (2000). Potassium channels: molecular defects, diseases, and therapeutic opportunities. Pharmacol Rev *52*, 557-594.

Sidell, N., and Schlichter, L. (1986). Retinoic acid blocks potassium channels in human lymphocytes. Biochem Biophys Res Commun *138*, 560-567.

Silva, A. J., Paylor, R., Wehner, J. M., and Tonegawa, S. (1992a). Impaired spatial learning in alpha-calcium-calmodulin kinase II mutant mice. Science *257*, 206-211.

Silva, A. J., Stevens, C. F., Tonegawa, S., and Wang, Y. (1992b). Deficient hippocampal long-term potentiation in alpha-calcium-calmodulin kinase II mutant mice. Science *257*, 201-206.

Silverman, W. R., Roux, B., and Papazian, D. M. (2003). Structural basis of two-stage voltage-dependent activation in K+ channels. Proc Natl Acad Sci U S A *100*, 2935-2940.

Smith, P. L., and Yellen, G. (2002). Fast and slow voltage sensor movements in HERG potassium channels. J Gen Physiol *119*, 275-293.

Soroceanu, L., Manning, T. J., Jr., and Sontheimer, H. (1999). Modulation of glioma cell migration and invasion using Cl(-) and K(+) ion channel blockers. J Neurosci *19*, 5942-5954.

Sparks, A. B., Rider, J. E., Kay, B. K., Curriculum in, G., and Molecular Biology, U. o. N. C. a. C. H. U. S. A. (1998). Mapping the specificity of SH3 domains with phage-displayed random-peptide libraries. Methods in molecular biology (Clifton, NJ) *84*.

Srinivasan, J., Schachner, M., and Catterall, W. A. (1998). Interaction of voltage-gated sodium channels with the extracellular matrix molecules tenascin-C and tenascin-R. Proc Natl Acad Sci U S A *95*, 15753-15757.

Stansfeld, C. E., Roper, J., Ludwig, J., Weseloh, R. M., Marsh, S. J., Brown, D. A., and Pongs, O. (1996). Elevation of intracellular calcium by muscarinic receptor activation induces a block of voltage-activated rat ether-a-go-go channels in a stably transfected cell line. Proc Natl Acad Sci U S A *93*, 9910-9914.

Storey, N. M., Gomez-Angelats, M., Bortner, C. D., Armstrong, D. L., and Cidlowski, J. A. (2003). Stimulation of Kv1.3 potassium channels by death receptors during apoptosis in Jurkat T lymphocytes. J Biol Chem *278*, 33319-33326.

Sun, X. X., Hodge, J. J., Zhou, Y., Nguyen, M., and Griffith, L. C. (2004). The eag potassium channel binds and locally activates calcium/calmodulin-dependent protein kinase II. J Biol Chem *279*, 10206-10214.

Sutton, K. G., McRory, J. E., Guthrie, H., Murphy, T. H., and Snutch, T. P. (1999). P/Q-type calcium channels mediate the activity-dependent feedback of syntaxin-1A. Nature *401*, 800-804.

Sweatt, J. D. (2004). Mitogen-activated protein kinases in synaptic plasticity and memory. Curr Opin Neurobiol *14*, 311-317.

Takeda, K., Matsuzawa, A., Nishitoh, H., Tobiume, K., Kishida, S., Ninomiya-Tsuji, J., Matsumoto, K., and Ichijo, H. (2004). Involvement of ASK1 in Ca2+-induced p38 MAP kinase activation. EMBO Rep *5*, 161-166.

Tanabe, T., Beam, K. G., Powell, J. A., and Numa, S. (1988). Restoration of excitation-contraction coupling and slow calcium current in dysgenic muscle by dihydropyridine receptor complementary DNA. Nature *336*, 134-139.

Tang, C. Y., Bezanilla, F., and Papazian, D. M. (2000). Extracellular Mg(2+) modulates slow gating transitions and the opening of Drosophila ether-a-Go-Go potassium channels. J Gen Physiol *115*, 319-338.

Taylor, B. L., and Zhulin, I. B. (1999). PAS domains: internal sensors of oxygen, redox potential, and light. Microbiol Mol Biol Rev *63*, 479-506.

Terlau, H., Ludwig, J., Steffan, R., Pongs, O., Stuhmer, W., and Heinemann, S. H. (1996). Extracellular Mg2+ regulates activation of rat eag potassium channel. Pflugers Arch *432*, 301-312.

Thomas, G. M., and Huganir, R. L. (2004). MAPK cascade signalling and synaptic plasticity. Nat Rev Neurosci *5*, 173-183.

Treisman, R. (1996). Regulation of transcription by MAP kinase cascades. Curr Opin Cell Biol *8*, 205-215.

Trimarchi, J. R., Liu, L., Smith, P. J., and Keefe, D. L. (2002). Apoptosis recruits two-pore domain potassium channels used for homeostatic volume regulation. Am J Physiol Cell Physiol *282*, C588-594.

Trudeau, M. C., Titus, S. A., Branchaw, J. L., Ganetzky, B., and Robertson, G. A. (1999). Functional analysis of a mouse brain Elk-type K+ channel. J Neurosci *19*, 2906-2918.

Trudeau, M. C., Warmke, J. W., Ganetzky, B., and Robertson, G. A. (1995). HERG, a human inward rectifier in the voltage-gated potassium channel family. Science *269*, 92-95.

Vautier, F., Belachew, S., Chittajallu, R., and Gallo, V. (2004). Shaker-type potassium channel subunits differentially control oligodendrocyte progenitor proliferation. Glia *48*, 337-345.

Vianna, M. R., Alonso, M., Viola, H., Quevedo, J., de Paris, F., Furman, M., de Stein, M. L., Medina, J. H., and Izquierdo, I. (2000). Role of hippocampal signaling pathways in long-term memory formation of a nonassociative learning task in the rat. Learn Mem *7*, 333-340.

Wang, H., Zhang, Y., Cao, L., Han, H., Wang, J., Yang, B., Nattel, S., and Wang, Z. (2002a). HERG K+ channel, a regulator of tumor cell apoptosis and proliferation. Cancer Res *62*, 4843-4848.

Wang, J., Zhou, Y., Wen, H., and Levitan, I. B. (1999). Simultaneous binding of two protein kinases to a calcium-dependent potassium channel. J Neurosci *19*, RC4.

Wang, J. W., Soll, D. R., and Wu, C. F. (2002b). Morphometric description of the wandering behavior in Drosophila larvae: a phenotypic analysis of K+ channel mutants. J Neurogenet *16*, 45-63.

Wang, Z., Wilson, G. F., and Griffith, L. C. (2002c). Calcium/calmodulin-dependent protein kinase II phosphorylates and regulates the Drosophila eag potassium channel. J Biol Chem *277*, 24022-24029.

Warmke, J., Drysdale, R., and Ganetzky, B. (1991). A distinct potassium channel polypeptide encoded by the Drosophila eag locus. Science *252*, 1560-1562.

Warmke, J. W., and Ganetzky, B. (1994). A family of potassium channel genes related to eag in Drosophila and mammals. Proc Natl Acad Sci U S A *91*, 3438-3442.

Wei, X., Neely, A., Lacerda, A. E., Olcese, R., Stefani, E., Perez-Reyes, E., and Birnbaumer, L. (1994). Modification of Ca2+ channel activity by deletions at the carboxyl terminus of the cardiac alpha 1 subunit. J Biol Chem *269*, 1635-1640.

Weng, J., Cao, Y., Moss, N., and Zhou, M. (2006). Modulation of voltage-dependent Shaker family potassium channels by an aldo-keto reductase. J Biol Chem *281*, 15194-15200.

Wilson, G. F., and Chiu, S. Y. (1993). Mitogenic factors regulate ion channels in Schwann cells cultured from newborn rat sciatic nerve. J Physiol *470*, 501-520.

Wilson, G. F., Wang, Z., Chouinard, S. W., Griffith, L. C., and Ganetzky, B. (1998). Interaction of the K channel beta subunit, Hyperkinetic, with eag family members. J Biol Chem *273*, 6389-6394.

Wilson, P. D., and Falkenstein, D. (1995). The pathology of human renal cystic disease. Curr Top Pathol *88*, 1-50.

Wonderlin, W. F., and Strobl, J. S. (1996). Potassium channels, proliferation and G1 progression. J Membr Biol *154*, 91-107.

Wong, H. K., Sakurai, T., Oyama, F., Kaneko, K., Wada, K., Miyazaki, H., Kurosawa, M., De Strooper, B., Saftig, P., and Nukina, N. (2005). beta Subunits of voltage-gated sodium channels are novel substrates of beta-site amyloid precursor protein-cleaving enzyme (BACE1) and gamma-secretase. J Biol Chem *280*, 23009-23017.

Wong, W., and Scott, J. D. (2004). AKAP signalling complexes: focal points in space and time. Nat Rev Mol Cell Biol *5*, 959-970.

Woodfork, K. A., Wonderlin, W. F., Peterson, V. A., and Strobl, J. S. (1995). Inhibition of ATP-sensitive potassium channels causes reversible cell-cycle arrest of human breast cancer cells in tissue culture. J Cell Physiol *162*, 163-171.

Wu, C. F., Ganetzky, B., Haugland, F. N., and Liu, A. X. (1983). Potassium currents in Drosophila: different components affected by mutations of two genes. Science *220*, 1076-1078.

Xia, X., Hirschberg, B., Smolik, S., Forte, M., and Adelman, J. P. (1998a). dSLo interacting protein 1, a novel protein that interacts with large-conductance calcium-activated potassium channels. J Neurosci *18*, 2360-2369.

Xia, X. M., Fakler, B., Rivard, A., Wayman, G., Johnson-Pais, T., Keen, J. E., Ishii, T., Hirschberg, B., Bond, C. T., Lutsenko, S.*, et al.* (1998b). Mechanism of calcium gating in small-conductance calcium-activated potassium channels. Nature *395*, 503-507.

Xiao, Z. C., Ragsdale, D. S., Malhotra, J. D., Mattei, L. N., Braun, P. E., Schachner, M., and Isom, L. L. (1999). Tenascin-R is a functional modulator of sodium channel beta subunits. J Biol Chem *274*, 26511-26517.

Yao, X., and Kwan, H. Y. (1999). Activity of voltage-gated K+ channels is associated with cell proliferation and Ca2+ influx in carcinoma cells of colon cancer. Life Sci *65*, 55-62.

Yeromin, A. V., Zhang, S. L., Jiang, W., Yu, Y., Safrina, O., and Cahalan, M. D. (2006). Molecular identification of the CRAC channel by altered ion selectivity in a mutant of Orai. Nature *443*, 226-229.

Yokoyama, C. T., Sheng, Z. H., and Catterall, W. A. (1997). Phosphorylation of the synaptic protein interaction site on N-type calcium channels inhibits interactions with SNARE proteins. J Neurosci *17*, 6929-6938.

Yoshimura, Y., Aoi, C., and Yamauchi, T. (2000). Investigation of protein substrates of Ca(2+)/calmodulin-dependent protein kinase II translocated to the postsynaptic density. Brain Res Mol Brain Res *81*, 118-128.

Yu, F. H., and Catterall, W. A. (2004). The VGL-chanome: a protein superfamily specialized for electrical signaling and ionic homeostasis. Sci STKE *2004*, re15.

Yu, S. P., Yeh, C. H., Sensi, S. L., Gwag, B. J., Canzoniero, L. M., Farhangrazi, Z. S., Ying, H. S., Tian, M., Dugan, L. L., and Choi, D. W. (1997). Mediation of neuronal apoptosis by enhancement of outward potassium current. Science *278*, 114-117.

Zeng, H., Fei, H., and Levitan, I. B. (2004). The slowpoke channel binding protein Slob from Drosophila melanogaster exhibits regulatable protein kinase activity. Neurosci Lett *365*, 33-38.

Zhang, C., and Zhou, Z. (2002). Ca(2+)-independent but voltage-dependent secretion in mammalian dorsal root ganglion neurons. Nat Neurosci *5*, 425-430.

Zhang, W., Hirschler-Laszkiewicz, I., Tong, Q., Conrad, K., Sun, S. C., Penn, L., Barber, D. L., Stahl, R., Carey, D. J., Cheung, J. Y., and Miller, B. A. (2006). TRPM2 is an ion channel that modulates hematopoietic cell death through activation of caspases and PARP cleavage. Am J Physiol Cell Physiol *290*, C1146-1159.

Zhang, Y., Oliva, R., Gisselmann, G., Hatt, H., Guckenheimer, J., and Harris-Warrick, R. M. (2003). Overexpression of a hyperpolarization-activated cation current (Ih) channel gene modifies the firing activity of identified motor neurons in a small neural network. J Neurosci *23*, 9059-9067.

Zhong, N., Beaumont, V., and Zucker, R. S. (2004). Calcium influx through HCN channels does not contribute to cAMP-enhanced transmission. J Neurophysiol *92*, 644-647.

Zhong, N., and Zucker, R. S. (2004). Roles of Ca2+, hyperpolarization and cyclic nucleotide-activated channel activation, and actin in temporal synaptic tagging. J Neurosci *24*, 4205-4212.

Zhou, Y., Schopperle, W. M., Murrey, H., Jaramillo, A., Dagan, D., Griffith, L. C., and Levitan, I. B. (1999). A dynamically regulated 14-3-3, Slob, and Slowpoke potassium channel complex in Drosophila presynaptic nerve terminals. Neuron *22*, 809-818.

Zhu, J. J., Qin, Y., Zhao, M., Van Aelst, L., and Malinow, R. (2002). Ras and Rap control AMPA receptor trafficking during synaptic plasticity. Cell *110*, 443-455.

Zou, A., Lin, Z., Humble, M., Creech, C. D., Wagoner, P. K., Krafte, D., Jegla, T. J., and Wickenden, A. D. (2003). Distribution and functional properties of human KCNH8 (Elk1) potassium channels. Am J Physiol Cell Physiol *285*, C1356-1366.

Zuhlke, R. D., Pitt, G. S., Deisseroth, K., Tsien, R. W., and Reuter, H. (1999). Calmodulin supports both inactivation and facilitation of L-type calcium channels. Nature *399*, 159-162.